POLSKA AKADEMIA NAUK
INSTYTUT FIZYKI
i
POLSKIE TOWARZYSTWO FIZYCZNE

ACTA PHYSICA POLONICA

MIESIĘCZNIK

Vol. XX — Fasc. 12

WARSZAWA 1961

PAŃSTWOWE WYDAWNICTWO NAUKOWE

PAŃSTWOWE WYDAWNICTWO NAUKOWE — Oddział w Krakowie
Kraków, ul. Smoleńsk 14

Nakład 938 + 122 egz.	*Podpisano do druku w grudniu 1961*
Ark. wyd. 5,5, ark. druk. 5 1/8	*Druk ukończono w grudniu 1961*
Papier druk. sat. 80 g, kl. III, 70 × 100 cm	*Zam. prod. 478/61.*
Do składania w lipcu 1961	*Cena zł 30.—*

DRUKARNIA NARODOWA W KRAKOWIE, ul. Manifestu Lipcowego 19

NUMERICAL VALUES OF TWO-CENTRE INTEGRALS FOR 3D ELECTRONS

By Maciej Suffczyński

Institute of Theoretical Physics, University of Warsaw, Warsaw

(Received May 15, 1961)

Nuclear attraction integrals and overlap integrals for 3*d* electrons in chromium, manganese, iron, cobalt, nickel, copper and zinc have been computed. The atomic wave functions have been approximated by analytical expression with two exponentials.

Calculations based on the tight-binding approximation may be of some use in the study of 3*d* electrons in transition metals. The computation of the necessary integrals in the two-centre approximation has been suggested by Fletcher and Wohlfarth (1951). The calculation of nuclear attraction integrals in crystals is different from the case of the free molecules. To simulate the crystal potential one calculates the nuclear attraction integrals with the atomic sphere excised (Fletcher 1952). The radius of the sphere is always taken equal to half the distance between the neighbours, for simplicity.

We report here a numerical study of the two-centre integrals, both nuclear attraction and overlap, for 3*d* electrons in chromium, manganese, iron, cobalt, nickel, copper and zinc (see Suffczyński 1959). The numerical computations were done on Ferranti Mercury Computer.

The atomic potential seen by a 3*d* electron was approximated by $U(r) = Z_p(r)/r$, with $Z_p(r) = 1 + (Z - 1)\, e^{-\gamma r}$. Here Z is the atomic number of the atom, and γ for all the considered elements was taken equal 3. This was a simplification dictated by a lack of better knowledge of the actual potential for the 3*d* electron.

The radial part of the atomic 3*d* wave function has been approximated by analytical expression with two exponentials only.

$$P_A(r) = r^3(B_1 e^{-b_1 r} + B_2 e^{-b_2 r}) \tag{1}$$

The coefficient B_1 by the smaller exponent b_1 was chosen so as to fit the tail of the numerical wave function. The choice of b_2 affects the tail usually slightly, (see Suffczyński 1955). A b_2 was chosen rather arbitrarily. Then the machine calculated B_2 so as to get an exact normalization of the radial wave function according to eq. (3) of the author's reference (1956 c).

The use of the two exponentials only in eq. (1) is the most obvious drawback of the present calculation. Different choices have been tried for the exponents, resulting in analytical functions which fit in different ranges of r the numerical wave functions given in the literature. The use which can be made of the numerical results reported here requires first of all to decide which analytical wave function to choose for a problem at hand. At the time when this work was being done the report of Watson (1959) was not yet accessible.

In the present calculation of the nuclear attraction integrals (E) the exact formulae for the two-centre energy integrals in the crystal have been used, as published by the author (1956 a, c). In the notation of ref. (1956c) all the terms $\nu = 0, 1, 2, 3, 4, 5, 6, 7$ have been computed and summed here. Concerning the formulae of ref. (1956c) it should be noted here that the $(dd\pi)$ energy integral will have the proper + sign if the coordinate systems for the two centres will both be made right-handed. Further a misprint in the formula (21) of ref. (1956c) should be corrected at the present occasion: the term $270/\alpha^5$ should read $2700/\alpha^5$ (see Suffczyński 1959).

The formulae for the overlap integrals for $3d$ electrons are published by Kotani *et al.* (1955) and by Jaffe (1953) and Roberts and Jaffe (1957). The overlap integrals (S) have to reduce to unity for zero distance between the two centres as we use normalized wave functions.

The lattice constants quoted in different sources are slightly different. For that reason the two-centre integrals have been calculated for different distances distinguished by subscripts. The order of the neighbour is denoted by a roman numeral. The half-distance between a neighbour and the central atom is denoted here by R and expressed in Bohr units. The atomic constants have been taken from the tables of Cohen and DuMond (1955).

1 Bohr unit of length $= 0.529172 \times 10^{-8}$ cm
1 atomic unit of energy $= 27.20976$ electron-volts.

The energy integrals (E) are expressed in electron-volts using this atomic unit of energy.

In the tabulation of the results the necessary letters describing the integrals are written once for each metal and are omitted in subsequent numerical cases. The values of the two-centre integrals are written in the floating point form, $x.xxx, \pm y$, where the number behind the comma is the power of ten by which the number before the comma should be multiplied. In the tabulation only the absolute values of the integrals are given, in other words, we list in each case

$$\begin{array}{lll} -E(3d3d\sigma) & E(3d3d\pi) & -E(3d3d\delta) \\ S(3d3d\sigma) & -S(3d3d\pi) & S(3d3d\delta) \end{array}$$

Chromium, $Z=24$

The selfconsistent calculation of the atomic functions of Cr^{++} without exchange has been published by Mooney (1939). The $3d$ radial function can be approximated with the two exponents $b_1 = 2$, $b_2 = 5$ (see Suffczyński 1955. An error in B's given there for chromium is corrected below). It was tried also to approximate the $3d$ function of chromium by

an expression similar to the one approximating $3d$ function calculated with exchange for Mn^{++} by Hartree (1955). This led to the exponents $b_1=2.3$, $b_2=5$.

The lattice constants in the body-centered cubic chromium is quoted as $a_1=2.879\times$ $\times 10^{-8}$ cm. The corresponding half-distances of the three consecutive neighbours are in Bohr units,

$$\begin{aligned} a_1\sqrt{3}/4 &= R(I_1) &= 2.355838 \\ a_1/2 &= R(II_1) &= 2.7202875 \\ a_1/\sqrt{2} &= R(III_1) &= 3.847067 \end{aligned}$$

The lattice constant of the b. c. c. chromium is also quoted as $a_2=2.8845\times 10^{-8}$ cm. The corresponding half-distances of the neighbours are then, in Bohr units,

$$\begin{aligned} a_2\sqrt{3}/4 &= R(I_2) &= 2.3603387 \\ a_2/2 &= R(II_2) &= 2.7254843 \\ a_2/\sqrt{2} &= R(III_2) &= 3.854417 \end{aligned}$$

The two-centre integrals have been computed for both lattice constants and they are listed here to show the variation with interatomic distance.

$b_1 = 2$ $\quad b_2 = 5$
$B_1 = 3.448$ $\quad B_2 = 49.7046$

		$(3d3d\sigma)$	$(3d3d\pi)$	$(3d3d\delta)$
I_1	E	7.750,−1	4.853,−1	8.107,−2
	S	6.863,−2	4.840,−2	8.897,−3
II_1	E	3.624,−1	1.817,−1	2.516,−2
	S	4.042,−2	2.173,−2	3.211,−3
III_1	E	2.222,−2	6.697,−3	5.956,−4
	S	3.955,−3	1.204,−3	1.093,−4
I_2	E	7.682,−1	4.796,−1	7.992,−2
	S	6.825,−2	4.795,−2	8.788,−3
II_2	E	3.582,−1	1.791,−1	2.474,−2
	S	4.008,−2	2.147,−2	3.164,−3
III_2	E	2.178,−2	6.547,−3	5.809,−4
	S	3.886,−3	1.179,−3	1.068,−4

$b_1 = 2$ $\quad b_2 = 5$
$B_1 = 3.558$ $\quad B_2 = 46.39986$

I_1	E	8.097,−1	5.103,−1	8.554,−2
	S	7.249,−2	5.129,−2	9.442,−3
II_1	E	3.806,−1	1.917,−1	2.660,−2
	S	4.283,−2	2.306,−2	3.411,−3

III_1	E	2.352,−2	7.100,−3	6.320,−4
	S	4.205,−3	1.280,−3	1.162,−4
I_2	E	8.027,−1	5.043,−1	8.433,−2
	S	7.209,−2	5.081,−2	9.326,−3
II_2	E	3.763,−1	1.890,−1	2.616,−2
	S	4.247,−2	2.279,−2	3.361,−3
III_2	E	2.306,−2	6.941,−3	6.164,−4
	S	4.132,−3	1.254,−3	1.136,−4

$b_1 = 2$ $b_2 = 5$
$B_1 = 4.4$ $B_2 = 16.76491$

I_1	E	1.079, 0	7.144,−1	1.228,−1
	S	1.048,−1	7.583,−2	1.411,−2
II_1	E	5.279,−1	2.746,−1	3.877,−2
	S	6.333,−2	3.450,−2	5.136,−3
III_1	E	3.456,−2	1.054,−2	9.441,−4
	S	6.369,−3	1.944,−3	1.767,−4
I_2	E	1.070, 0	7.063,−1	1.210,−1
	S	1.043,−1	7.514,−2	1.394,−2
II_2	E	5.222,−1	2.707,−1	3.813,−2
	S	6.280,−2	3.409,−2	5.060,−3
III_2	E	3.389,−2	1.031,−2	9.210,−4
	S	6.259,−3	1.904,−3	1.727,−4

$b_1 = 2.3$ $b_2 = 5$
$B_1 = 4.64$ $B_2 = 61.50236$

I_1	E	3.601,−1	1.714,−1	2.303,−2
	S	3.029 −2	1.601 −2	2.348,−3
II_1	E	1.295,−1	5.051,−2	5.692,−3
	S	1.374,−2	5.721,−3	6.846,−4
III_1	E	3.755,−3	9.169,−4	6.778,−5
	S	6.469,−4	1.599,−4	1.204,−5
I_2	E	3.558,−1	1.689,−1	2.264,−2
	S	3.002,−2	1.582,−2	2.313,−3
II_2	E	1.276,−1	4.962,−2	5.578,−3
	S	1.358,−2	5.635,−3	6.725,−4
III_2	E	3.664,−3	8.924,−4	6.582,−5
	S	6.327,−4	1.559,−4	1.172,−5

Manganese, $Z=25$

The atomic functions for Mn^{++} have been calculated with exchange by Hartree (1955). The $3d$ radial function was approximated with two exponents $b_1 = 2.3$, $b_2 = 5$.

Manganese has a complicated crystal structure. In the calculation of the two-centre integrals the distance between the nearest neighbours was taken $d = 2.24 \times 10^{-8}$ cm. The corresponding half-distance is, in Bohr units, $d/2 = R(I) = 2.1165141$.

$b_1 = 2.3$ $\quad b_2 = 5$
$B_1 = 4.64$ $\quad B_2 = 61.50236$

		$(3d3d\sigma)$	$(3d3d\pi)$	$(3d3d\delta)$
I	E	6.829, −1	3.762, −1	5.756, −2
	S	4.699, −2	2.999, −2	5.141, −3

Iron, $Z=26$

For iron the wave functions calculated by J. H. Wood (1955) have been used. Wood was taking the exchange effects into account by using an average exchange potential proposed by Slater (1951). The $3d1$ (spin up) wave function computed by Wood was approximated by several analytical expressions with one exponent near 2 and the second near 5.

In the b. c. c. iron the lattice constants $a_1 = 2.8663$ kX and $d_1 = 2.4823$ kX were measured by Basinski, Hume-Rothery and Sutton (1955). Taking 1 kX $= 1.002063 \times 10^{-8}$ cm we get the corresponding half-distances of the first order and second order neighbours, in Bohr units, (Du Mond and Cohen 1953)

$$d_1/2 = R(I_1) = 2.345471$$
$$a_1/2 = R(II_1) = 2.7082937$$

The lattice constant for the b. c. c. iron is usually quoted as $a_2 = 2.86645 \times 10^{-8}$ cm. The corresponding half-distances of the three consecutive neighbours, are, in Bohr units, (Cohen and DuMond 1955)

$$a_2\sqrt{3}/4 = R(I_2) = 2.345569$$
$$a_2/2 = R(II_2) = 2.708429$$
$$a_2/\sqrt{2} = R(III_2) = 3.830297$$

$b_1 = 2.1$ $\quad b_2 = 5.1$
$B_1 = 2.815$ $\quad B_2 = 81.97726$

		$(3d3d\sigma)$	$(3d3d\pi)$	$(3d3d\delta)$
I_1	E	4.119, −1	2.214, −1	3.328, −2
	S	3.133, −2	1.954, −2	3.289, −3
II_1	E	1.688, −1	7.456, −2	9.410, −3
	S	1.654, −2	8.051, −3	1.102, −3

I_2	E	4.118,−1	2.214,−1	3.327,−2
	S	3.133,−2	1.953,−2	3.288,−3
II_2	E	1.687,−1	7.453,−2	9.406,−3
	S	1.654,−2	8.049,−3	1.101,−3
III_2	E	7.549,−3	2.090,−3	1.733,−4
	S	1.251,−3	3.548,−4	3.026,−5

$b_1 = 2.2$ $b_2 = 5.1$
$B_1 = 3.19$ $B_2 = 82.55929$

I_1	S	2.503,−2	1.423,−2	2.225,−3
II_1	S	1.215,−2	5.443,−3	6.948,−4
I_2	E	3.308,−1	1.638,−1	2.299,−2
	S	2.502,−2	1.423,−2	2.225,−3
II_2	E	1.249,−1	5.107,−2	6.034,−3
	S	1.215,−2	5.441,−3	6.945,−4
III_2	E	4.394,−3	1.136,−3	8.868,−5
	S	7.230,−4	1.913,−4	1.534,−5

$b_1 = 2.2$ $b_2 = 5.1$
$B_1 = 3.459$ $B_2 = 77.80095$

I_1	E	3.709,−1	1.860,−1	2.630,−2
	S	2.877,−2	1.648,−2	2.588,−3
II_1	E	1.416,−1	5.842,−2	6.944,−3
	S	1.408,−2	6.334,−3	8.107,−4
I_2	E	3.708,−1	1.859,−1	2.629,−2
	S	2.877,−2	1.648,−2	2.587,−3
II_2	E	1.416,−1	5.840,−2	6.941,−3
	S	1.408,−2	6.332,−3	8.103,−4

$b_1 = 2.25$ $b_2 = 5.1$
$B_1 = 3.597$ $B_2 = 79.44393$

I_2	E	3.210,−1	1.543,−1	2.107,−2
	S	2.466,−2	1.350,−2	2.044,−3
II_2	E	1.174,−1	4.654,−2	5.351,−3
	S	1.155,−2	4.990,−3	6.174,−4
III_2	E	3.713,−3	9.321,−4	7.079,−5
	S	6.146,−4	1.575,−4	1.226,−5

$b_1 = 2.3$ $b_2 = 5$
$B_1 = 4.2$ $B_2 = 68.22085$

I_2	E	3.292,−1	1.543,−1	2.058,−2
	S	2.604,−2	1.375,−2	2.018,−3

II_2	E	1.169,−1	4.517,−2	5.067,−3
	S	1.179,−2	4.916,−3	5.900,−4

$b_1 = 2.3$ $b_2 = 5.1$
$B_1 = 4.09$ $B_2 = 75.52839$

I_2	S	2.464,−2	1.301,−2	1.911,−3
II_2	S	1.116,−2	4.654,−3	5.588,−4

Cobalt, $Z=27$

The $3d$ wave function for cobalt was taken the same as for iron. The lattice constants for hexagonal cobalt are $a = 2.5074 \times 10^{-8}$ cm and $c = 4.0699 \times 10^{-8}$ cm. The resulting half-distances of the first order neighbours are, in Bohr units

$$\begin{aligned} \tfrac{1}{2}c(3/8)^{1/2} &= R(I_1) = 2.3549 \\ \tfrac{1}{2}(a^2/3 + c^2/4)^{1/2} &= R(I_2) = 2.359667 \\ a/2 &= R(I_3) = 2.369173 \\ c/2 &= R(I_4) = 3.845536 \end{aligned}$$

The half-distances for the second and third order neighbours are in Bohr units,

$$\begin{aligned} a/\sqrt{2} &= R(II) = 3.3505165 \\ a\sqrt{3}/2 &= R(III) = 4.1035279 \end{aligned}$$

In the face-centered cubic cobalt with the lattice constant $a_f = 3.5442 \times 10^{-8}$ cm the half-distances of the first and second order neighbours are

$$\begin{aligned} \tfrac{1}{2}a_f/\sqrt{2} &= R(I_f) = 2.367971 \\ a_f/2 &= R(II_f) = 3.348817 \end{aligned}$$

$b_1 = 2.1$ $b_2 = 5.1$
$B_1 = 2.815$ $B_2 = 81.97726$

		$(3d3d\sigma)$	$(3d3d\pi)$	$(3d3d\delta)$
I_1	E	4.081,−1	2.174,−1	3.244,−2
	S	3.087,−2	1.911,−2	3.198,−3
I_2	E	4.035,−1	2.144,−1	3.191,−2
	S	3.064,−2	1.890,−2	3.154,−3
I_3	E	3.945,−1	2.084,−1	3.088,−2
	S	3.018,−2	1.848,−2	3.066,−3
I_4	E	7.251,−3	1.995,−3	1.645,−4
	S	1.203,−3	3.390,−4	2.876,−5
II	E	3.028,−2	1.001,−2	9.755,−4
	S	4.127,−3	1.429,−3	1.457,−4

I_f	E	3.956,−1	2.092,−1	3.101,−2
	S	3.023,−2	1.853,−2	3.077,−3
II_f	E	3.042,−2	1.007,−2	9.814,−4
	S	4.144,−3	1.436,−3	1.465,−4

$b_1 = 2.2$ $b_2 = 5.1$
$B_1 = 3.459$ $B_2 = 77.80095$

I_1	E	3.667,−1	1.822,−1	2.559,−2
	S	2.829,−2	1.609,−2	2.512,−3
I_2	E	3.622,−1	1.795,−1	2.515,−2
	S	2.805,−2	1.590,−2	2.475,−3
I_3	E	3.535,−1	1.742,−1	2.429,−2
	S	2.757,−2	1.552,−2	2.402,−3
I_4	E	4.860,−3	1.254,−3	9.756,−5
	S	8.108,−4	2.135,−4	1.704,−5
II	E	2.239,−2	6.931,−3	6.366,−4
	S	3.078,−3	9.922,−4	9.493,−5
I_f	E	3.545,−1	1.749,−1	2.440,−2
	S	2.763,−2	1.557,−2	2.411,−3
II_f	E	2.250,−2	6.972,−3	6.407,−4
	S	3.092,−3	9.973,−4	9.549,−5

$b_1 = 2.2$ $b_2 = 5.1$
$B_1 = 3.19$ $B_2 = 82.55929$

I_1	E	3.272,−1	1.606,−1	2.239,−2
	S	2.460,−2	1.389,−2	2.160,−3
I_2	E	3.232,−1	1.582,−1	2.200,−2
	S	2.439,−2	1.373,−2	2.128,−3
I_3	E	3.153,−1	1.535,−1	2.124,−2
	S	2.397,−2	1.340,−2	2.065,−3
I_4	E	4.208,−3	1.081,−3	8.393,−5
	S	6.927,−4	1.822,−4	1.453,−5
II	E	1.951,−2	6.007,−3	5.497,−4
	S	2.637,−3	8.484,−4	8.108,−5
III	E	1.842,−3	4.350,−4	3.124,−5
	S	3.309,−4	7.942,−5	5.827,−6
I_f	E	3.163,−1	1.541,−1	2.134,−2
	S	2.402,−2	1.344,−2	2.073,−3
II_f	E	1.961,−2	6.042,−3	5.532,−4
	S	2.648,−3	8.528,−2	8.156,−5

$b_1 = 2.3$	$b_2 = 5$			
$B_1 = 4.2$	$B_2 = 68.22085$			
I_1	E	3.248,−1	1.510,−1	1.200,−2
	S	2.556,−2	1.340,−2	1.957,−3
I_2	E	3.206,−1	1.486,−1	1.964,−2
	S	2.531,−2	1.323,−2	1.926,−3
I_3	E	3.122,−1	1.439,−1	1.893,−2
	S	2.483,−2	1.289,−2	1.866,−3
I_4	E	3.198,−3	7.758,−4	5.711,−5
	S	5.355,−4	1.323,−4	9.959,−6
II	E	1.627,−2	4.728,−3	4.104,−4
	S	2.252,−3	6.781,−4	6.108,−5
III	E	1.332,−3	2.971,−4	2.024,−5
	S	2.428,−4	5.479,−5	3.798,−6
I_f	E	3.133,−1	1.445,−1	1.902,−2
	S	2.489,−2	1.293,−2	1.873,−3
II_f	E	1.636,−2	4.757,−3	4.131,−4
	S	2.262,−3	6.818,−4	6.146,−5
$b_1 = 2.3$	$b_2 = 5.1$			
$B_1 = 4.09$	$B_2 = 75.52839$			
I_1	S	2.418,−2	1.268,−2	1.852,−3
I_2	S	2.395,−2	1.252,−2	1.823,−3
I_3	S	2.349,−2	1.220,−2	1.766,−3
I_4	S	5.074,−4	1.253,−4	9.440,−6
II_f	S	2.132,−3	6.423,−4	5.788,−5
I_f	S	2.355,−2	1.224,−2	1.773,−3
II_f	S	2.143,−3	6.459,−4	5.823,−5

Nickel, $Z = 28$

For the $3d$ function in nickel the approximation assumed by Fletcher (1952) has been used.

The lattice constant of the f. c. c. nickel is quoted as $a_1 = 3.52394 \times 10^{-8}$ cm. The corresponding half-distances for the first and second order neighbours are, in Bohr units,

$$\tfrac{1}{2}\, a_1/\sqrt{2} = R(I_1) = 2.35443$$
$$a_1/2 = R(II_1) = 3.3296735$$

If the lattice constant were taken as $a_2 = 3.608 \times 10^{-8}$ cm the half-distances would be

$$\tfrac{1}{2}\, a_2/\sqrt{2} = R(I_2) = 2.41$$
$$a_2/2 = R(II_2) = 3.408254675$$

$R(I_2)$ is the half-distance used in the original calculation of Fletcher (1952).

$b_1 = 2$ $\quad b_2 = 5$
$B_1 = 1.979$ $\quad B_2 = 85.86026$

		$(3d3d\sigma)$	$(3d3d\pi)$	$(3d3d\delta)$
I_1	E	3.787, −1	2.112, −1	3.302, −2
	S	2.651, −2	1.765, −2	3.151, −3
II_1	E	3.424, −2	1.208, −2	1.250, −3
	S	4.400, −3	1.654, −3	1.813, −4
I_2	E	3.339, −1	1.805, −1	2.745, −2
II_2	E	2.780, −2	9.511, −3	9.573, −4

The appoximation of Fletcher consists in taking only the terms with $r = 0, 1, 2, 3$ in the integration over all space and only the term with $r = 0$ in the integration over the atomic sphere, in the energy integrals (see Suffczyński 1956c). This approximation gives in the present case the values

I_2	E	3.3316, −1	1.8006, −1	2.7392, −2

which are very close to the values obtained from the full expressions with $r = 0, 1, \ldots 7$. Thus the approximation of Fletcher, that is omitting the integrals with unequal exponents over the atomic sphere, has been found, in the course of the present computation, to be very satisfactory indeed.

Copper, $Z = 29$

The wave functions for atomic Cu^+ have been calculated with exchange by Hartree (1936). It has been approximated by Fletcher (1952) and the same, essentially, approximation was used here.

The lattice constant of copper is $a = 3.608 \times 10^{-8}$ cm. The corresponding distances of the first and second order neighbours are, in Bohr units,

$$\tfrac{1}{2}a/\sqrt{2} = R(I) = 2.41$$
$$a/2 = R(II) = 3.40825$$

$b_1 = 2$ $\quad b_2 = 5$
$B_1 = 1.979$ $\quad B_2 = 85.86026$

		$(3d3d\sigma)$	$(3d3d\pi)$	$(3d3d\delta)$
I	E	3.383, −1	1.823, −1	2.766, −2
	S	2.443, −2	1.562, −2	2.695, −3
II	E	2.800, −2	9.562, −3	9.614, −4
	S	3.705, −3	1.343, −3	1.427, −4

Zinc, $Z = 30$

The wave function for $3d$ electrons in zinc has been taken the same as in copper. The lattice constants for hexagonal zinc are $a = 2.659 \times 10^{-8}$ cm and $c = 4.935 \times 10^{-8}$ cm.

The resulting half-distances for the first order neighbours are, in Bohr units,

$$a/2 = R(I_1) = 2.5124156$$
$$\tfrac{1}{2}(a^2/3 + c^2/4)^{\frac{1}{2}} = R(I_2) = 2.7459173$$

$b_1 = 2$ $\quad b_2 = 5$

$B_1 = 1.979$ $\quad B_2 = 85.86026$

		$(3d3d\sigma)$	$(3d3d\pi)$	$(3d3d\delta)$
I_1	E	2.702, −1	1.374, −1	1.981, −2
	S	2.085, −2	1.241, −2	2.017, −3
I_2	E	1.544, −1	6.986, −2	9.067, −3
	S	1.404, −2	7.192, −3	1.030, −3

In the present calculations the numerical values of Fletcher (1952) and of the author (1956b) have been satisfactorily confirmed. This gives confidence in the accuracy of the former and in the programme of the present numerical work.

My thanks are due to Mr. S. Michaelson for introducing me to Ferranti Autocode programming and to Miss R. Fenn for her effective help in checking the programmes. The work was done in 1959 in the Department of Mathematics, Imperial College, London. The access to the Ferranti Mercury Computer of the London University Computing Unit is gratefully acknowledged.

REFERENCES

Basiński, Z. S., Hume-Rothery, W., and Sutton, A. L., *Proc. Roy. Soc.* A, **229,** 459 (1955),
Cohen, E. R., Du Mond, J. W. M., Layton, T. W. and Rollett, J. S., *Rev. mod. Phys.*, **27,** 363 (1955).
Du Mond, J. W. M. and Cohen, E. R., *Rev. mod. Phys.*, **25,** 691 (1953).
Fletcher, G. C., *Proc. Phys. Soc.* A **65,** 192 (1952).
Fletcher, G. C., and Wohlfarth, E. P., *Phil. Mag.*, **42,** 106 (1951).
Hartree, D. R., *Proc. Camb. Phil. Soc.*, **51**, 126 (1955).
Hartree, D. R. and Hartree, W., *Proc. Roy. Soc.* A **157,** 490 (1936).
Jaffé, H. H., *J. chem. Phys.*, **21,** 258 (1953).
Kotani, M. *et al., Tables of Molecular Integrals,* Maruzen Co., Tokyo (1955).
Mooney, R. L., *Phys. Rev.*, **55,** 557 (1939).
Roberts, J. L. and Jaffé, H. H., *J. chem. Phys.*, **27,** 883 (1957).
Slater, J. C., *Phys. Rev.*, **81,** 385 (1951).
Suffczyński, M., *Acta phys. Polon.*, **14,** 493 (1955). *Acta phys. Polon.*, **15,** 111 (1956b). *Bull. Acad. Polon. Sci.* Cl. III, **4,** 273 (1956a). *Acta phys. Polon.*, **15,** 287 (1956c). *Bull. Acad. Polon. Sci.* Cl. III, **7,** 285 (1959).
Watson, R. E., *Solid State and Molecular Theory Group Technical Report No.* 12, MIT (1959).
Wood, J. H., *privately distributed tables.*

THE SPINOR SPACE AS AN EUCLIDEAN COMPLEX SPACE

By Jerzy Lukierski

Institute of Theoretical Physics, University of Wrocław, Wrocław

(Received May 23, 1961)

The equivalence between Rzewuski's spinor space and 4-dimensional Euclidean complex space is proved. The free field equation in spinor space is solved by the procedure of analytical continuation. The field equation with sources is investigated, using the complex distribution $\delta(z)$.

Introduction

In a series of papers Rzewuski (1958a, b, 1959, 1960a, b) investigated the spinor space as geometrical basis for the theory of elementary particles. The full group of transformations in spinor space is a direct product of two 6-parametric unimodular groups $\boldsymbol{C}\times\boldsymbol{C}'$ and a phase factor group a. The simplest faithful representation $z_{\alpha;\beta}$ ($\alpha, \beta = 1, 2$) of the 12-parametric group $\boldsymbol{C}\times\boldsymbol{C}'$ was used as the complex coordinate of spinor space.

Recently, Mozrzymas and Rzewuski (1961) proposed an interesting method of solving a second order differential equation in spinor space. This equation, in the paper by Mozrzymas and Rzewuski, is treated as an analytical continuation of the Klein-Gordon equation, and its solution in spinor space can be obtained from any solution of the Klein-Gordon equation by the procedure of analytical continuation. In the present paper, this method of solution is shown to be intimately related to the isomorphism between the spinor space and Euclidean four-dimensional complex space.

The equivalence between spinor and vector spaces was investigated by Rzewuski (1958b) and, independently, by Roman (1960). Rzewuski introduced an eight-dimensional real vector space with two real metric forms, isomorphic to the original spinor space. In this paper, we consider complex vector spaces. It is shown that the interpretation of spinor space as an Euclidean complex vector space admits of explaining certain results, hitherto calculated explicitly, as simple consequences of this property of Rzewuski's space-time theory.

1. *Isomorphism Between the Spinor Space and the Euclidean Complex Space*

Let us introduce a complex four-dimensional space with Euclidean metric:

$$z_\mu^2 = z^2 = \text{inv.} \tag{1.1}$$

The linear transformations

$$z'_\mu = a_{\mu\nu} z_\nu \quad (\mu,\nu = 1, 2, 3, 4) \tag{1.2}$$

are limited by virtue of (1.1) as follows:

$$a_{\mu\nu}a_{\mu\varrho} = \delta_{\nu\varrho} \quad (a_{\mu\nu} - \text{complex}). \tag{1.3}$$

For Rzewuski's spinor space $z_{\alpha;\beta}$ we have

$$\tfrac{1}{2} z_{\alpha;\beta}z^{\alpha;\beta} = u^2 = \text{inv} \quad (\alpha, \beta, \gamma, \delta = 1,2) \tag{1.4}$$

where

$$z^{1;1} = z_{2;2} \quad z^{1;2} = -z_{2;1} \quad z^{2;1} = -z_{1;2} \quad z^{2;2} = z_{1;1}$$

If

$$z'_{\alpha;\beta} = S^{\gamma;}_{\alpha} z_{\gamma;\delta} S'^{T;\delta}_{\beta} \tag{1.5}$$

we have, by (1.4),

$$|S^{\gamma;}_{\alpha}| = |S'^{;\delta}_{\beta}| = 1 \tag{1.6}$$

The space with the invariant forms (1.1) and (1.4) are connected as follows:

$$z_{\mu} = \tfrac{1}{2}\, \sigma_{\mu\alpha;\beta} z^{\alpha;\beta} \tag{1.7a}$$

or

$$z_{\alpha;\beta} = \sigma_{\mu\alpha;\beta} z_{\mu} \tag{1.7b}$$

where the $\sigma_{i\alpha;\beta}$ are the elements of the well-known Pauli matrices, $\sigma_{4\alpha;\beta} = i\delta_{\alpha\beta}$. The justification of (1.7) results from (1.1), (1.4). After substitution of (1.7a) in (1.1) or (1.7b) in (1.4), we have

$$u^2 = z^2 \tag{1.8}$$

The isomorphism between the spinor and complex Euclidean spaces may be stated for infinitesimal transformations. From (1.2), we have

$$\delta z_{\mu} = \delta a_{\mu\nu} z_{\nu} \tag{1.9}$$

and, from (1.5),

$$\delta z_{\alpha;\beta} = \delta S^{\gamma;}_{\alpha} z_{\gamma;\beta} + z_{\alpha;\delta} \delta S'^{T;\delta}_{\beta} \tag{1.10}$$

The relations (1.3) and (1.6) imply

$$\delta a_{\mu\nu} = -\delta a_{\nu\mu} \tag{1.11}$$

and

$$\delta S^{1;}_{1} = -\delta S^{2;}_{2} \quad \delta S'^{;1}_{1} = -\delta S'^{;2}_{2} \tag{1.12}$$

By (1.7b), we have

$$\delta z_{\alpha;\beta} = \sigma_{\mu\alpha;\beta} \delta z_{\mu} \tag{1.13}$$

Using the properties of σ_{μ}-matrices, we obtain directly from (1.9-10) and (1.13) that

$$\delta a_{\mu\nu} = \tfrac{1}{2} (\delta S^{\gamma;}_{\alpha} \sigma_{\nu\gamma;\varrho} \sigma^{\alpha;\varrho}_{\mu} + \sigma^{\alpha;\varrho}_{\mu} \sigma_{\nu\alpha;\delta} \delta S'^{T;\delta}_{\varrho}) \tag{1.14}$$

We see that the infinitesimal parameters of transformations in spinor and complex Euclidean spaces are connected linearly.

On assuming

$$\delta a_{\mu\nu} = (\delta a_{\mu\nu})^*, \tag{1.15}$$

we obtain an Euclidean space with complex vector components and real transformation coefficients. From (1.14-15), we obtain

$$\delta S = -\delta S^+ \qquad \delta S' = -\delta S'^+ \tag{1.16a}$$

where δS, $\delta S'$ are infinitesimal 2×2 matrices (see (1.10)) which implies for finite

$$SS^+ = 1 \qquad S'S'^+ = 1 \tag{1.16b}$$

The Minkowski case (complex vectors, six-parametric group of Lorentz rotations) is determined by the choice

$$\delta a_{ij} = (\delta a_{ij})^* \qquad \delta a_{i4} = -(\delta a_{i4})^* \tag{1.17}$$

Using (1.14) and (1.17), it is readily shown that

$$\delta S = \delta S'^+ \tag{1.18a}$$

which is fulfilled only if

$$S = S'^+ \tag{1.18b}$$

The cases for which $\delta S = 0$ or $\delta S' = 0$ were investigated by Rzewuski (1958b). Stating the results of Rzewuski's paper in our notation, we have

$$\delta S' = 0: \quad \delta a_{ij} = e_{ijk}\ \delta a_{k4} \tag{1.19a}$$

$$\delta S = 0: \quad \delta a_{ij} = -e_{ijk}\,\delta a_{k4} \tag{1.19b}$$

Thus it is shown that the Euclidean complex space includes spinors in $\boldsymbol{C}$ (and scalars in $\boldsymbol{C}'$) as well as spinors in $\boldsymbol{C}'$ (and scalars in $\boldsymbol{C}$). By a special choice of the infinitesimal transformations in spinor space we can obtain the result that the spinor coordinates $z_{\alpha;\beta}$ describe the components of the complex Euclidean or Minkowski vectors.

2. *Solution of the Free Field Equation in Spinor Space*

Let us investigate only second order differential equations in spinor space. We have the following two second order differential operators, invariant with respect to the group $\boldsymbol{C}\times\boldsymbol{C}'$:

$$\hat{D} = \frac{\partial^2}{\partial z_{\alpha;\beta}\partial z_{\alpha;\beta}} \qquad \hat{D}^* = \frac{\partial^2}{\partial z^*_{\alpha;\beta}\partial z^{\alpha;\beta *}} \tag{2.1}$$

There are two points of view on the theory of interaction in spinor space (Rzewuski 1960a):

1) The free field equation (together with the initial conditions) determines the free field uniquely.

In this conventional case, the differential equation includes $\hat{D}$ as well as $\hat{D}^*$. An example of this type can be provided by the following equation, justified by the symmetry properties:

$$\{F(\hat{D}, \hat{D}^*) + F(\hat{D}^*, \hat{D})\} f(z_{\alpha;\beta} z^*_{\alpha;\beta}) = 0 \tag{2.2}$$

where F is a polynomial in $\hat{D}$, $\hat{D}^*$.

2) The free field equation admits the degrees of freedom describing interaction.

E.g. the equation investigated by Rzewuski and Mozrzymas (Mozrzymas 1961, Rzewuski 1959, Rzewuski 1960a, Mozrzymas and Rzewuski 1961)

$$(D - \epsilon^2_{;\mu} \varkappa^2 z^*_{\alpha;\beta} z^{\alpha;\beta^*}) f(z_{\alpha;\beta}, z^*_{\alpha;\beta}) = 0 \tag{2.3}$$

admits of arbitrariness in the dependence of $f\ (z_{\alpha;\beta}, z^*_{\alpha;\beta})$ on $z^*_{\alpha;\beta}$

In this paper will be continued the latter treatment of the free field, which represents a new approach to the problem of interaction. We assume the following free field equation:

$$\{D - \varkappa^2 M^2 (z^*_{\alpha;\beta} z^{\alpha;\beta^*})\}\ F(z_{\alpha;\beta}, z^*_{\alpha;\beta}) \tag{2.4}$$

where M^2 is an arbitrary scalar constructed from $z^*_{\alpha;\beta}$.

By (1.7a) we have, instead of (2.4),

$$\left\{\frac{\partial^2}{\partial z^2_\mu} - \varkappa^2 M^2(z^{*2}_\mu)\right\} F(z_\mu, z^*_\mu) = 0 \tag{2.5}$$

The substitution

$$Z_\mu = M(z^{*2}_\mu) z_\mu \tag{2.6}$$

implies

$$\left\{\frac{\partial^2}{\partial Z^2_\mu} - \varkappa^2\right\} F(Z_\mu, Z^*_\mu) = 0 \tag{2.7}$$

if Z^2_μ is complex.

In the case of

$$M^2(z^{*2}_\mu) = A z^{*2}_\mu \tag{2.8}$$

as realized in eq. (2.3) $(A = \epsilon^2_{;\mu})$ we have

$$Z^2_\mu = Z^{*2}_\mu \tag{2.9}$$

and it is necessary to introduce a new real variable α

$$e^{i2\alpha} = \frac{z^2_\mu}{z^{*2}_\mu} \tag{2.10}$$

as investigated by Rzewuski (1959). Because of

$$\frac{\partial}{\partial z_\mu} = \frac{\partial Z_\mu}{\partial z_\mu} \frac{\partial}{\partial Z_\mu} \tag{2.11}$$

where

$$\frac{\partial Z_\mu}{\partial z_\mu} = M(z_\mu^{*2}) \frac{\partial \alpha}{\partial z_\mu} = -i \frac{z_\mu}{z_\varrho^2} \tag{2.12}$$

we have using (2.6)

$$\frac{\partial}{\partial z_\mu} = M(z_\mu^{*2}) \left\{ \frac{\partial}{\partial Z_\mu} - i \frac{Z_\mu}{Z_\sigma^2} \frac{\partial}{\partial \alpha} \right\} \tag{2.13}$$

and eq. (2.5) can be rewritten as follows:

$$\left\{ \left(\frac{\partial}{\partial Z_\mu} - i \frac{Z_\mu}{Z_\sigma^2} \frac{\partial}{\partial \alpha} \right)^2 - \varkappa^2 \right\} F(Z_{\mu,\alpha}) = 0 \tag{2.14}$$

where Z_μ describes only seven degrees of freedom (see (2.9)) and the remaining degree is described by the angular variable α.

The case described by the equality (2.8) (where $A = \epsilon_{;\mu}^2$) was investigated recently. From our considerations it is easy to deduce the method of solving the equation presented in the paper by Mozrzymas and Rzewuski (1961).

Let us introduce the following vector components y_μ

$$y_\mu = \tfrac{1}{2} \sigma_\mu^{\alpha;\beta} z_{\alpha;\beta} \tag{2.15}$$

where

$$z_{\alpha;\beta} = z_{\beta;\alpha}^* \tag{2.16}$$

It is readily shown that

$$y_i = y_i^* \qquad y_4 = -y_4^* \tag{2.17}$$

The condition (2.16) is invariant under the transformations in spinor space satisfying the relation (1.18b). Assuming (1.18b), we see from (2.17) and Sect. 1 that the y_μ are usual Minkowski vectors.

We now write the Klein-Gordon equation in the variables y_μ:

$$\left\{ \frac{\partial^2}{\partial y_\mu^2} - \varkappa^2 \right\} F(y_\mu) = 0 \tag{2.18}$$

The general solution of eq. (2.4) with the value of M determined by (2.8) can be obtained from (2.18) by means of the following two steps:

$$1) \quad \frac{\partial}{\partial y_\mu} \to \frac{\partial}{\partial y_\mu} - i \frac{y_\mu}{y_\sigma^2} \frac{\partial}{\partial_\alpha} \qquad \alpha - \text{real} \tag{2.19a}$$

$$2) \quad y_\mu \to Z_\mu \qquad Z_\mu \text{ complex, } Z_\sigma^2 \text{ real} \tag{2.19b}$$

The first step can be interpreted as the introduction of a certain interaction (Rzewuski 1960a, b). The general solution of the Klein-Gordon equation after the interchange 1) was already obtained in Rzewuski's paper (1959). The second step consists in the analytical continuation of the coordinates. Using (2.6), (2.8) and (2.10), we obtain the solution as a function of $z_{\alpha;\beta}$.

The first step is connected only with the form (2.8) of M^2. If M^2 is not bilinear in the length of z_μ^*, the general solution can be obtained by the procedure of analytical continuation

$$y_\mu \to Z_\mu \qquad Z_\mu \text{ complex}, \quad Z_\sigma^2 \text{ complex}. \tag{2.20}$$

3. *Curved Orthogonal Basis in Spinor Space*

Let us consider the Euclidean complex vector space z_μ (with real or complex z_σ^2). The transformations (1.2) can be generalized as follows:

$$a_{\mu\nu} \to A_{\mu\nu}(z_\lambda^*) \tag{3.1}$$

wherein

$$A_{\mu\nu}(z_\lambda^*)\, A_{\mu\varrho}(z_\lambda^*) = \delta_{\nu\varrho} \tag{3.2}$$

As the dependence of $A_{\mu\nu}$ on z_λ^* is not, in general, determined by a function of invariant from z_σ^{2*}, the transformation properties of u_μ;

$$u_\mu = A_{\mu\nu}(z_\lambda^*)\, z_\nu \tag{3.3}$$

differ from the transformation properties of z_μ. The two most interesting cases are these: 1) u_μ is a scalar with respect to $\boldsymbol{C}'$ and a vector component with respect to $\boldsymbol{C}$, and inversely 2) u_μ describes a scalar with respect to $\boldsymbol{C}$ and a vector component with respect to $\boldsymbol{C}'$. Assuming that

$$A_{\mu\nu}(z_\varrho^*) = \frac{1}{2}\, \sigma_\mu^{\alpha\dot\beta;}\, \sigma_\tau^{;\gamma\dot\delta}\, \sigma_{\varrho\dot\beta;\dot\delta}\, \sigma_{\nu\alpha;\gamma}\, \epsilon_{;\tau}\, \frac{z_\varrho^*}{\sqrt{\epsilon_{;\lambda}^2 z_\lambda^{*2}}} \tag{3.4}$$

where $\epsilon_{;\tau}$ is a unit vector in space, described by $\boldsymbol{C}'$ or

$$A'_{\mu\nu}(z_\varrho^*) = \frac{1}{2}\, \sigma_\tau^{\alpha\dot\beta;}\, \sigma_\mu^{;\gamma\dot\delta}\, \sigma_{\nu\alpha;\gamma}\, \sigma_{\varrho\dot\beta;\dot\delta}\, e_{\tau;}\, \frac{z_\varrho^*}{\sqrt{e_{\lambda;}^2 z_\lambda^{*2}}} \tag{3.5}$$

where $e_{\tau;}$ is a unit vector in space-time, we obtain these two cases, respectively. Indeed, using the properties of σ_μ—matrices, the transformation properties of $A_{\mu\nu}$ and $A'_{\mu\nu}$ are readily determined. We can also prove that the relation (3.2) is satisfied for (3.4) and (3.5).

The vectors z_μ are defined by means of the formula (1.7a). Let us insert in (3.3) the vectors Z_μ defined by (2.6). It is easily proved that

$$U_\mu = A_{\mu\nu}(z_\varrho^*)\, Z_\nu \tag{3.6}$$

and

$$U'_\mu = A'_{\mu\nu}(z_\varrho^*)\, Z_\nu \tag{3.7}$$

satisfy the relations

$$\begin{aligned} U_i &= U_i^* \qquad U_4 = -\,U_4^* \\ U'_i &= U_i'^* \qquad U'_4 = -\,U_4'^* \end{aligned} \tag{3.8}$$

Comparing the bilinear formula of Rzewuski (1958a, 1959) for the position four-vector in space-time

$$X_{\mu;} = \tfrac{1}{2}\,\sigma_{\mu}^{\alpha\dot{\beta}_;} z_{\alpha;\gamma} z_{\beta;\delta} z^{*}_{\beta;\delta} \sigma_{\tau}^{\dot{\gamma}\dot{\delta}} \epsilon_{\tau;} \tag{3.9}$$

with eq. (3.6), and on using (1.7), we obtain the result that the vectors $X_{\mu;}$ and U_{μ} are identical. As the formula (3.6) defines four real variables, and Z_{μ} describes seven degrees of freedom (assuming (2.8)), we can in addition to (3.6) define three more variables α_i independent of $X_{\mu;}$ The orthogonal character of the transformation (3.6) implies

$$\frac{\partial^2}{\partial Z_{\mu}^2} = \frac{\partial^2}{\partial X_{\mu;}^2} + \hat{D}'\left(X_{\mu;},\ \alpha_l,\ \frac{\partial}{\partial X_{\mu;}},\ \frac{\partial}{\partial \alpha_i}\right) \tag{3.10}$$

and, if the dependence of the field function on Z_{μ} can be expressed by means of X_{μ} or if

$$\frac{\partial F}{\partial \alpha_i} = 0, \tag{3.11}$$

we have

$$\hat{D}'F = 0. \tag{3.12}$$

The equality (3.10) is a consequence of the result that the variables (3.9) present a special case of the variables (3.3). Finally, we obtain the interpretation of X_{μ} as coordinates in a certain orthogonal curvilinear coordinate system defined in a real four-dimensional subspace of the full complex four-dimensional Euclidean space z_{μ} (with eight real degrees of freedom).

4. *Remarks on the Equation with Sources in Spinor Space*

Eq. (2.4) may be written with the delta-function on the right hand side:

$$\left\{\frac{\partial^2}{\partial z_{\mu}^2} - \varkappa^2 M^2(z_{\mu}^{*2})\right\} \Delta\,(z_{\mu},\, z_{\mu}^{*}) = \delta(z_1)\,\delta(z_2)\,\delta(z_3)\,\delta(z_4) \tag{4.1}$$

The delta-function with complex argument z can be defined as

$$\delta(z) = \frac{1}{2\pi}\int_{L} e^{ipz}\,dp \tag{4.2}$$

where the path of integration $\mathcal{L}$ is chosen as follows:

$$\mathcal{L}\colon\quad p = \alpha z^{*} \qquad -\infty < \alpha < \infty \tag{4.3}$$

and the direction of the path is determined by the condition $\mathrm{Re}\,dp > 0$. Thus, we have

$$dp = \frac{\mathrm{Re}(z^{*})}{|\mathrm{Re}(z^{*})|}\,z^{*}\,d\alpha \tag{4.4}$$

if

$$d\alpha > 0.$$

From (4.2), we obtain

$$\delta(z) = \frac{\mathrm{Re}(z^*)}{|\mathrm{Re}(z^*)|} z^* \frac{1}{2\pi} \int_{-\infty}^{+\infty} e^{i\alpha|z|^2}\, d\alpha \tag{4.5}$$

and, finally,

$$\delta(z) = \frac{\mathrm{Re}(z^*)}{|\mathrm{Re}(z^*)|} z^* \delta(|z|^2)$$

It is easy to prove that, for an arbitrary path of integration K, we have

$$\int_K \delta(z - z_0) f(z)\, dz = \begin{cases} f(z_0) & \text{if } z_0 \text{ belongs to } K \\ 0 & \text{if } z_0 \text{ lies outside } K \end{cases} \tag{4.7}$$

and

$$\int_K \delta(z - z_0)\, dz = \begin{cases} 1 & \text{if } z_0 \text{ belongs to } K \\ 0 & \text{if } z_0 \text{ lies outside } K \end{cases}$$

Formula (4.6) can also be proved by help of the definition of the delta function depending on a complex argument, as introduced by Nakanishi (1958) (see Appendix).

The analytical continuation of the delta function can therefore be effected, as, for the real argument x we have

$$\delta(x) = \frac{x}{|x|} x\, \delta(x^2) \tag{4.8}$$

Formula (4.8) is a special case of (4.6), if $z = z^*$. We obtain the interchange $\delta(x) \to \delta(z)$ if, in the relation with real y, y'

$$\delta(y) = \frac{\mathrm{Re}\, y'}{|\mathrm{Re}\, y'|} y'\, \delta(y y'), \tag{4.9}$$

we put

$$x = y = y' \tag{4.10a}$$

Passing to complex arguments, as follows (see Fig. 1a, 1b):

$$y \to z \qquad y' \to z^*, \tag{4.10b}$$

we obtain from (4.8) the equality (4.6).

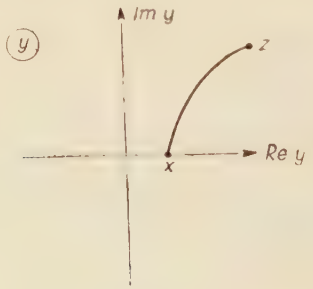

Fig. 1*a*

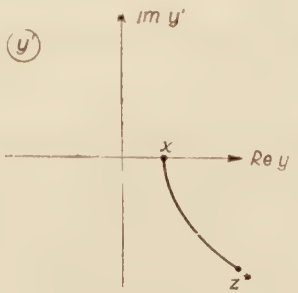

Fig. 1*b*

By (4.6), eq. (4.1) can be written in real variables, with delta functions of real arguments. Let us introduce, for each complex component z, the variables as follows:

$$z = r\, e^{i\varphi} \tag{4.11}$$

The differentiation operator $\dfrac{\partial}{\partial z}$ can be expressed thus:

$$\frac{\partial}{\partial z} = e^{-i\varphi}\left(\frac{\partial}{\partial r} - \frac{i}{r}\frac{\partial}{\partial \varphi}\right) \tag{4.12}$$

and the operator of second differentiation

$$\frac{\partial^2}{\partial z^2} = e^{-i2\varphi}\left(\frac{\partial^2}{\partial r^2} - \frac{2i}{r}\frac{\partial^2}{\partial \varphi \partial r} - \frac{1}{r^2}\frac{\partial^2}{\partial \varphi^2}\right) \tag{4.13}$$

The complex delta function (4.6) can be expressed as follows:

$$\delta(z) = \theta(\varphi)\, e^{-i\varphi}\delta(r) \tag{4.14}$$

where

$$\theta(\varphi) = \begin{cases} 1 \text{ if } 0 \leqslant \varphi \leqslant \dfrac{\pi}{2}, \dfrac{3}{2}\pi < \varphi < 2\pi \\ -1 \text{ if } \dfrac{\pi}{2} < \varphi \leqslant \dfrac{3}{2}\pi \end{cases} \tag{4.15}$$

The equation (4.1), written in the variables r_μ, φ_μ where[1]

$$z_\mu = r_\mu e^{i\varphi_\mu} \tag{4.16}$$

is of the form

$$\left\{\sum_{\mu=1}^{4} e^{i\Gamma_\mu}\left(\frac{\partial^2}{\partial r_\mu^2} - \frac{2i}{r_\mu}\frac{\partial^2}{\partial r_\mu \partial \varphi_\mu} - \frac{1}{r_\mu^2}\frac{\partial^2}{\partial \varphi_\mu^2}\right) - \right.$$

$$\left. - e^{\frac{i}{2}\sum_{\varrho=1}^{4}\Gamma_\varrho}\varkappa^2 M^2\right\} \Delta(r_\nu, \varphi_\nu; \varkappa^2) = \prod_{\mu=1}^{4}\theta(\alpha_\mu)\,\delta(r_\mu) \tag{4.17}$$

where

$$\Gamma_\mu = \sum_{\mu \neq \nu} \varphi_\nu - \varphi_\mu \tag{4.17a}$$

Eq. (4.1) or (4.17) defines Green's function for the equation with sources in the full Euclidean complex space z_μ, defined by X_μ (physical part of spinor space), and by α_l and α (isotopic part of spinor space).

---

[1] Einstein summation convention is not used.

We obtain the physical interpretation of the solution of the inhomogeneous equation in spinor space (for example (4.1)) in accordance with Rzewuski's prodecure (1960) on averaging over the four degrees of freedom α_i, α independent of X_μ. The second possibility of a physical interpretation can be related to the average over the four degrees of freedom φ_μ (see (4.16)). In this method, the solution of (4.17) can be interpreted physically after the following procedure:

$$\Delta(r_\mu;\varphi_\mu;\varkappa^2)\to\frac{1}{(2\pi)^4}\int_0^{2\pi}d\varphi_1\ldots\int_0^{2\pi}d\varphi_4\,\Delta(r_\mu,\varphi_\mu;\varkappa^2)=\Delta(r_\mu;\varkappa^2) \tag{4.18}$$

where r_i, ir_4 define four space-time degrees of freedom.

The interpretation in (4.18) implies that the 4-vector of position in space-time is invariant only with respect to the transformations of the 6-parameter subgroup $\boldsymbol{C}\times\boldsymbol{C}$ of $\boldsymbol{C}\times\boldsymbol{C}'$ (see (1.18b)). This property is easy to prove, taking into account the relations (2.15) and (4.16).

The author wishes to thank Professor Rzewuski and Mr Mozrzymas for their helpful and valuable discussions.

APPENDIX

Nakanishi (1958) introduced by means of the Cauchy formula the following definition of

$$\delta_K(z)=\frac{1}{2\pi i}\left(\frac{1}{z_+}-\frac{1}{z_-}\right) \tag{A.1}$$

where z_+ defines the path of integration K_+, and z_-—the path of integration K_- (see Fig. 2a, 2b, 2c).

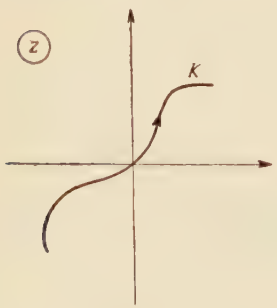

Fig. 2a

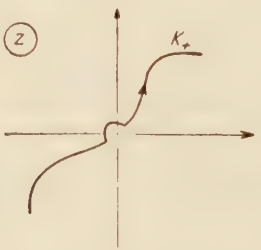

Fig. 2b

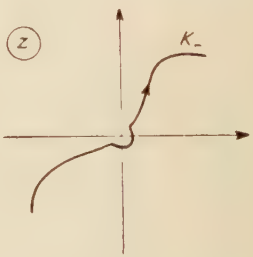

Fig. 2c

Since

$$f(z_0)=\frac{1}{2\pi i}\int_{C_\varepsilon}\frac{f(z)dz}{z-z_0} \tag{A.2}$$

where C_ε is an infinitesimal circle about the point $z=0$, satisfying the relation $C_\varepsilon=K_+-K_-$ the properties (4.7) of the complex delta function are satisfied.

Let us investigate only the straight lines K. If $z=0$ belongs to K, the argument for an arbitrary point of the path is equal to φ_0 or $\varphi_0+\pi$, where φ_0 determines K.

We have in this case:

$$\frac{1}{z_\pm} = e^{-i\varphi_0}\frac{1}{|z|\pm i\varepsilon} \quad \text{if } \frac{\pi}{2} < \varphi \leqslant \frac{\pi}{2}$$

$$\frac{1}{z_\pm} = e^{-i\varphi_0}\frac{1}{|z|\pm i\varepsilon} \quad \text{if } \frac{\pi}{2} < \varphi \leqslant \frac{3}{2}\pi \tag{A.3}$$

and

$$\delta(z) = \frac{\operatorname{Re} z}{|\operatorname{Re} z|}\, e^{-i\varphi_0}\frac{1}{2\pi i}\left(\frac{1}{|z|+i\varepsilon} - \frac{1}{|z|-i\varepsilon}\right) \tag{A.4}$$

Since

$$\delta(|z|) = \frac{1}{2\pi i}\left(\frac{1}{|z|+i\varepsilon} - \frac{1}{|z|-i\varepsilon}\right), \tag{A.5}$$

for the straight line $\varphi_0 = \text{const}$, $\varphi_0 + \pi = \text{const}$

we have

$$\delta(z) = \frac{\operatorname{Re}(z^*)}{|\operatorname{Re}(z^*)|}\, e^{-i\varphi_0}\delta(|z|) \tag{A.6}$$

Using

$$\delta(|z|) = |z| \cdot \delta(|z|^2)$$

we obtain from (A.6) that

$$\delta(z) = \frac{\operatorname{Re}(z^*)}{|\operatorname{Re}(z^*)|}\, z^*\delta(|z|^2) \tag{A.7}$$

Formula (A.7) is valid for an arbitrary path of integration with a continuous derivative in the point $z=0$. Indeed, from (A.7) we see that only for $z=0$ must the form of the curve K be taken into account. If in (A.6) we introduce the following interchange

$$\varphi_0 \to \varphi(0) \tag{A.8}$$

where the formula $z=|z|\, e^{i\varphi(0)}$ describes points of the path of integration K in the infinitesimal neighbourhood of the point $z=0$, the relations (A.6-7) are also satisfied.

REFERENCES

Mozrzymas, J., *Roczniki Naukowe Uniwersytetu Wrocławskiego* (1961), (in press).

Mozrzymas, J. and Rzewuski J., *Bull. Acad. Polon. Sci. Ser. Sci. math. astron. phys.* (1961), (in press).

Nakanishi, H., *Progr. theor. Phys.*, **19,** 607 (1958).

Roman, P., *Theory of Elementary Particles*, Amsterdam 1960.

Rzewuski, J. *Nuovo Cimento*, **9,** 942 (1958a).

Rzewuski, J., *Acta phys. Polon.*, **17,** 417 (1958b).

Rzewuski, J. *Acta phys. Polon.*, **18,** 549 (1959).

Rzewuski, J., *Bull. Acad. Polon. Sci. Ser. Sci. math. astron. phys.*, **8,** 777, 783 (1960a, b).

ZUR MÖGLICHKEIT DER ELEKTRONENHAFTSTELLENANALYSE MIT HILFE DER EXOELEKTRONENEMISSION

Von B. Sujak

Institut für Experimentalphysik der Universität, Wrocław

(Eingegangen am 29 Mai 1961)

Die Möglichkeit der Elektronenhaftstellenanalyse auf Grund der Erscheinungen von Exoelektronenemission wird besprochen.

Es werden besonders die Möglichkeiten einer Analyse mit Hilfe der Messungen von: 1) Postelektronenemission (Abklingkurven), 2) Photostimulierten Coelectronenemission und 3) Thermostimulierten Coelektronenemission (Glow-Kurven) zusammenfassend diskuttiert.

Die Untersuchungen der Exoelektronenemission sind vom Anfang an mit dem Ziele geführt worden, diese Erscheinung in der Zukunft zur Elektronenhaftstellenanalyse der dünnen Oberflächenschichten des Festkörpers auszunutzen.

Im Grunde genommen liegen bis jetzt drei Möglichkeiten vor, die Haftstellenanalyse einer Oberflächenshicht mit Hilfe der Exoelektronen durchzuführen, und zwar durch:

1) Eine Analyse der Abklingkurven (Postelektronenemission).

2) Eine Analyse des Emissionsstromes der Exoelektronen, der während einer Erwärmung der Probe mit konstanter Geschwindigkeit der Temperaturerhöhung gemessen wird (thermostimulierte Coelektronenemission, öfters Glow-Kurven Analyse genannt).

3) Eine Analyse der Abhängigkeit der Exoelektronenemissionsintensität von der Lichtwellenlänge des beleuchtenden Lichtes auf gleiche auffallende Lichtenergie (oder Quantenzahl) reduziert (photostimulierte Coelektronenemission).

Diese Grundmöglichkeiten werden auf den nachstehenden Seiten umrissen. Es werden auch von anderen Autoren abgeleitete Beziehungen angeführt. Auf die Ableitung selbst wird aber verzichtet und nur auf Originalarbeiten verwiesen.

Postelektronenemission

Nassenstein (1955) hat die Gleichungen der Theorie der Phosphoreszenz auf die Exoelektronenemission übertragen, um mit diesen, die mit der Zeit in Dunkelheit abklingende Emission von Exoelektronen beschreiben zu versuchen.

Bei der Voraussetzung, dass es sich um einen monomolekularen Prozess handelte, schrieb er:

a) für den Fall der einzelnen diskreten Haftstellenarten und bei der Annahme, dass jedes, nahe an der Oberfläche befreite Elektron den Kristall verlassen kann

$$I = \Omega n_0 s e^{-\frac{\varepsilon}{kT}} \cdot \exp\left[-ste^{-\frac{\varepsilon}{kT}}\right] \tag{1}$$

oder auch

$$I = I_0 \exp\left[-ste^{-\frac{\varepsilon}{kT}}\right] \tag{2}$$

b) für den Fall der gleichmässigen Verteilung der Haftstellen,

$$I = N_\varepsilon (kT/t)\,(1 - e^{-st}) \tag{3}$$

wobei für Zeiten $t > 10^{-7}$ sec (welche eingentlich in Betracht kommen) dieser Ausdruck praktisch in

$$I = N_\varepsilon kT \cdot t^{-1} \tag{4}$$

übergeht.

c) für den Fall einer Haftstellenverteilung, die einem Exponentialgesetz $N_\varepsilon = Ae^{-\alpha\varepsilon}$ folgt; wird der Emissionsstrom folgend beschrieben:

$$I = f(s, kT) \cdot Bt^{(\alpha kT+1)} \tag{5}$$

dass heisst, die Emission verläuft nach dem Gesetz:

$$I \sim t^{-a} \tag{6}$$

wobei

$$a = \alpha\, kT + 1 \tag{7}$$

Wenn die besetzten Elektronenhaftstellen in einem kleinen Energieintervall $(\varepsilon_1, \varepsilon_2)$ liegen und in diesem Energieintervall N_ε konstant ist, verläuft die Elektronenemissionsintesität wie folgt:

$$I = N_\varepsilon \frac{kT}{t}\left\| \exp\left[-ste^{-\frac{\varepsilon_2}{kT}}\right] - \exp\left[-ste^{-\frac{\varepsilon_1}{kT}}\right]\right\| \tag{8}$$

Die Bedeutung der Symbole bei den Abgeleiteten Abhängigkeiten ist folgend:

ε — energetische Tiefe der besetzen Haftstellen in eV (thermische Aktivierungsenergie),

T — absolute Temperatur,

t — Zeit in sec,

k — Boltzmann-Konstante $= 8{,}62 \cdot 10^{-5}$ eV/Grad

$s \cdot \exp\left[-\dfrac{\varepsilon}{kT}\right]$ — Wahrscheinlichkeit, dass ein Elektron bei der Temperatur T aus einer Haftstelle der Tiefe ε thermisch befreit wird,

s — etwa 10^8 sec^{-1},

Ω — eine Grösse die angibt wieviele der befreiten Elektronen den Kristall als Exoelektronenstrom verlassen können, bei (2) bis (8) gleich 1 gesetzt,

n_0 — Anzahl der Elektronen, die in den für die Emission wirksamen Haftstellen der

Tiefe ε zur Zeit t=0 gelagert waren,

B — Konstante.

Zur Illustration des vorgesagten wird eine theoretisch errechnete Abklingkurve der Exoelektronenemission für eine konstante Haftstellenverteilung (N_ε = konstant) in dem

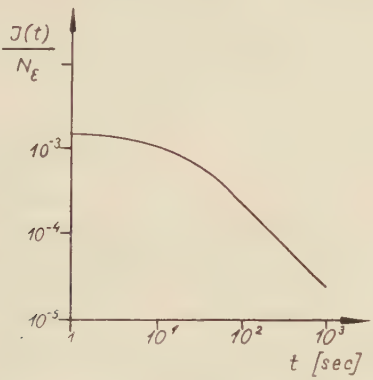

Fig. 1. Theoretisch errechnete Abklingkurve der Postelektronenemission für eine konstante Haftstellenverteilung (N_ε = konstant) im Energieintervall von (ε_1, ε_2) ε_1 = 0,55 eV bis ε_2 = 0,75 eV aber N_ε = 0 für $\varepsilon < \varepsilon_1$, $\varepsilon > \varepsilon_2$ und für T = 300°K (nach Nassenstein 1955).

Energieintervall ε_1 = 0,55 eV bis ε_2 = 0,75 eV und für T = 300°K nach Nassenstein (1955) in Fig. 1 wiedergegeben.

Thermostimulierte Coelektronenemission (Glow-Kurven)

Die Glow-Kurven-Methode beruht auf der Messung der Intensität der Exoelektronenemission während die emittierende Probe mit konstanter Geschwindigkeit erwärmt wird. Bei dieser Methode sind — je nach der Anzahl der Arten von mit Elektronen besetzten Haftstellen — bestimmte Maxima auf der Exoelektronen-Intensitätskurve zu finden. Wenn diese Maxima scharf voneinander getrennt zu finden sind, ist die Identifizierung und die Analyse der entsprechenden Haftstellen erleichtert, oft aber nur in diesem Falle möglich.

Die Haftstellenarten werden durch deren energetische Tiefe ε charakterisiert (Fig. 2). Durch diese wird im Falle der Glow-Kurven-Methode die thermische Energie gemeint, die zum Befreien des festhaftenden Elektrons aus der Haftstelle benötigt wird. Diese Energie wird oft als thermische Aktivierungsenergie bezeichnet.

Zur Bestimmung der energetischen Tiefe ε, der als Exoelektronen-Emissionszentren dienenden Haftstellen, wird eine annäherende Beziehung zwischen dieser und der Temperatur T_m, die der Temperaturlage des Maximum entspricht, verwendet. Diese Beziehung wurde zuerst vom Randall und Wilkins (1945a, b) zur Bestimmung der energetischen Tiefe der Lumineszenzzentren abgeleitet. Sie wurde aber zuerst vom Bohun (1954) auf die Exoelektronen Glow-Kurven übertragen (Fig. 2). Diese Beziehung lautet:

$$\varepsilon = 25\, kT_m \tag{9}$$

oder auch

$$\varepsilon = \frac{Tm}{500}\,[\mathrm{eV}] \tag{10}$$

Bohun und Dolejsi zeigten auch (1959), dass die an Alkalihaloiden erzielten Messergebnisse auf eine Monomolekularen Prozess hinweisen und dass die Austrittsarbeit nur einen sehr kleinen Einfluss auf die Temperatur T_m hat. Die Austrittsarbeit beeinflusst lediglich sehr stark nur die Intensität der Exoelektronenemission. Es scheint, dass die Be-

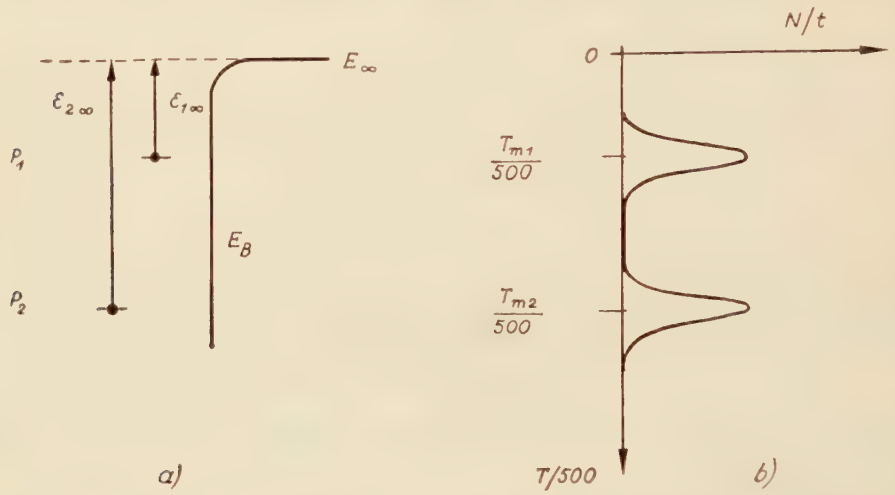

Fig. 2. a) Energetisches Schema von 2 Haftstellenarten bei der Oberfläche eines Festkörpers. P_1 und P_2 — zwei verschiedene (energetisch genommen) Haftstellen, E_∞ — gleich Null gesetztes Energieniveau des Elektrons im Unendlichen (wenn in Ruhezustand), E_B — Verlauf der Energiebarriere für das Elektron an der Oberfläche des Festkörpers, ε_1 und ε_2 — Aktivierungsenergie der Haftstellen P_1 und P_2. b) Glow-Kurven (schematisch) die dem Fall der Haftstellen P_1 und P_2 entspricht.

ziehung (9) oder (10) nur auf das Volumen einer Wirksamen Oberflächenschicht bezogen werden kann, wie die allerletzten Untersuchungsergebnise z. B. von Seidl deuten (1960).

Bei der Diskussion des Problemes führte Seidl (1960) zwei Interpretationsmechanisme ein. Einer von denen ist mehr als eine Oberflächenemission zu betrachten. Bei diesem Mechanismus ist das Entweichen der Elektronen aus den Haftstellen lediglich durch die Emission bedigt. Bei diesem Mechanismus wird ε einmal aus dem Anlaufteil des Maximum des Emissionsstromes

$$\frac{N}{t} = n_0 \nu \Omega \cdot e^{-\frac{\varepsilon}{kT}} \tag{11}$$

und das anderemal aus der Richardsonschen Gerade, auf die schon bereits Bohun hingewiesen hat,

$$\ln \frac{b}{T_m^2} = -\frac{\varepsilon}{kT_m} - \ln \frac{\nu \Omega k}{\varepsilon} \tag{12}$$

bestimmt. Dabei bedeuten:

$\frac{N}{t}$ — Impulsgeschwindigkeit (es wird angenommen, dass ein jedes emittierte Elektron registriert wird, was bis jetzt nicht nachgewiesen wurde, besonders bei den Messungen mit Hilfe des Luftspitzenzählers),

n_0 — Anfängliche Anzahl der lokalisierten Elektronen,

ν — Schwingungsfrequenz des Elektrons in der Potentialmulde des Haftstellenzentrums,

Ω — Geometrische Wahrscheinlichkeit der Emission,

k — Boltzmannsche Konstante,

T — Temperatur der Probe,

b — Geschwindigkeit der Temperaturerhöhung der Probe,

T_m — Temperatur, die der Lage des Maximum auf der Glow-Kurve entspricht.

Die Übereinstimmung der Werte ε, die aus (11) und (12) ermittelt werden, soll zugleich ein Kriterium für die Verwendbarkeit der gegebenen Interpretation sein, das heisst, dass das Entweichen der Elektronen aus den Haftstellen lediglich durch die Emission bedingt wird. In diesem Falle kann aber auch ε aus der folgenden Beziehung annäherend ermittelt werden:

$$\frac{T_m}{T_p} = 1 + 1{,}69\,\frac{kT_m}{\varepsilon} \tag{13}$$

wobei T_p die Temperatur ist, die der halben Höhe des Maximums auf der Seite der niedrigeren Temperatur entspricht.

Da die Lage des Maximums T_m auf der Glow-Kurve von der Geschwindigkeit der Temperaturerhöhung abhängt, wird sie von den Sachbearbeiter auf etwa 1 Grad/sec bis 2 Grad/sec bei allen Messreihen festgelegt und bei den Ergebnissen stets angegeben.

Der maximale Emissionstrom (bei der Temperatur T_m) ist nicht nur von der anfänglichen Anzahl der lokalisierten Elektronen n_0, sondern auch von der Geschwindigkeit der Temperaturerhöhung der Probe b auf folgende Weise abhängig:

$$\left(\frac{N}{t}\right)_{\max} = \frac{n_0\,\varepsilon b}{e\,kT_m^2} \tag{14}$$

Der zweite Fall, der vom Seidl diskuttiert wurde, ist mehr durch einen inneren Mechanismus gesteuert, wie z. B. eine Überführung des Elektrons aus der Haftstelle in das Leitungsband. Dabei kann die Austrittsarbeit fast keine Rolle spielen. In diesem Falle gelingt er wiederum zu der Formel (9):

$$\varepsilon_p = C \cdot kT_m \tag{15}$$

wobei nur dann $C \sim 1$ ist, wenn

$$1 \gg \frac{\nu\Omega_\infty}{b}\,\frac{kT_m^2}{\varepsilon_\infty}\left(1 + \frac{kT_m}{\varepsilon_\infty}\right) e^{-\frac{\varepsilon_\infty}{kT_m}} \tag{16}$$

Die neu eingeführten Symbole haben folgende Bedeutung:

ε_p — Aktivationsenergie des inneren Prozesses,

ε_∞ — Austrittsarbeit der Elektronen,

Ω_p — Geometrische Wahrscheinlichkeit des Überführens des Elektrons in das Leitfähigkeitsband,

Ω_∞ — Geometrische Wahrscheinlichkeit der Emission des Elektrons nach aussen.

Seidl bemerkt jedoch, dass die Ungleichheit (16) wahrscheinlich ziemlich häufig erfüllt ist. In diesem jedoch Falle kann ε_p verhältnismässig genau aus den bei verschiedenen b vorgenommen und im System $\ln b$, $1/T_m$ oder im System $\ln b, T^2$ verarbeiteten Messreihen laut der Gleichung

$$\varepsilon_p = kT_m \ln \frac{\nu\Omega_\infty \dfrac{kT_m^2}{\varepsilon_\infty}\left(1 + \dfrac{kT_m}{\varepsilon_p}\right)}{b} \tag{17}$$

ermittelt werden. ε_∞ dagegen kann aus der Verarbeitung des Anlaufteiles der Kurve (18) mit Hilfe der Richardsonschen Geraden bestimmt werden

$$\frac{N}{t} = n_0 \nu\Omega_\infty e^{-\frac{\varepsilon_\infty}{kT}} \tag{18}$$

Aus dieser Diskussion ist zu entnehmen, dass die aus dem Anlaufteil des Maximum bestimmte Energie (Gleichung (11) oder (18)) in der Regel der Austrittsarbeit der Elek-

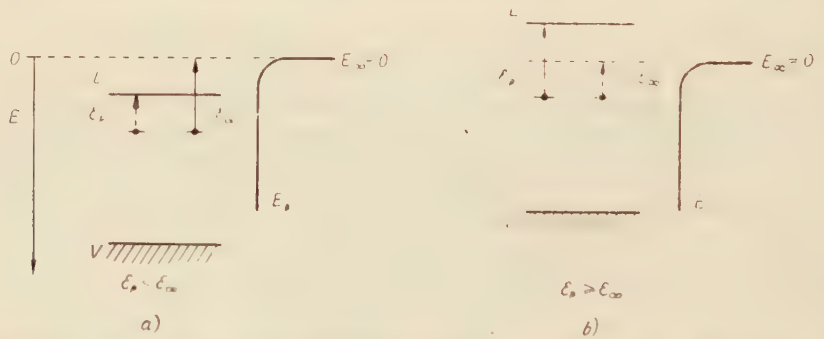

Fig. 3. Energetische Schemen der Emissionsmechanisme wobei: L — Boden des Leitfähigkeitsbandes, E_B — Verlauf der Energiebarriere für das Elektron, E_∞ — gleich Null gesetztes Energieniveau des Elektrons in Ruhezustand ist.
a) Emission wird durch die Austrittsarbeit bedingt. b) Emission wird durch die Aktivierungsenergie des inneren Prozesses bedingt (nach Seidl 1960).

tronen entspricht. Die Aktivationsenergie des inneren Prozesses entspricht dem Wert von ε_p, der mit Hilfe der Gleichungen (9), (10), (12), (13), (15) oder (17) ermittelt wird.

Für die Na- und K-Halogenide mit F-Zentren scheint die Emission durch den inneren Prozess bedingt zu sein, wie die Messergebnisse zeigen.

Um die Diskussion von Seidl besser vorfolgen zu können wurden in Fig. 3 die energetischen Schemata der Mechanisme wiedergegeben.

Photostimulierte Coelektronenemission

Eine Möglichkeit der Haftstellenanalyse mit Hilfe der photostimulierten Coelektronenemission wird an Hand der Abklingkurven während einer Beleuchtung mit Licht, sowie der Messungen von spektraler Quantenausbeute der zur Exoelektronenemission erregten Schichten von KCl zu diskuttieren versucht.

Im Falle einer KCl-Schicht kann das auf der Fig. 12 angeführte vereinfachte Bandmodell betrachtet werden (Arsenjewa-Geil 1957). Dabei sind die folgenden Bezeichnungen zu berücksichtigen:

ε_F — energetische Tiefe der *F*-Zentren,
ε_E — energetische Tiefe der erregten Zustände,
$\Delta\varepsilon$ — Breite des verbotenen Bandes,
$\varkappa$ — Austrittsarbeit vom Boden des Leitfähigkeitsbandes gemessen.[1]

Wenn die *F*-Zentren in einem wirksamen Oberflächenvolumen (Oberflächenschicht) von einer wirksamen Dicke generiert werden, so ist zu erwarten, dass ein Teil der Zentren nach der Beendigung der Generierung sich in einem erregten Zustand von der Tiefe ε_E

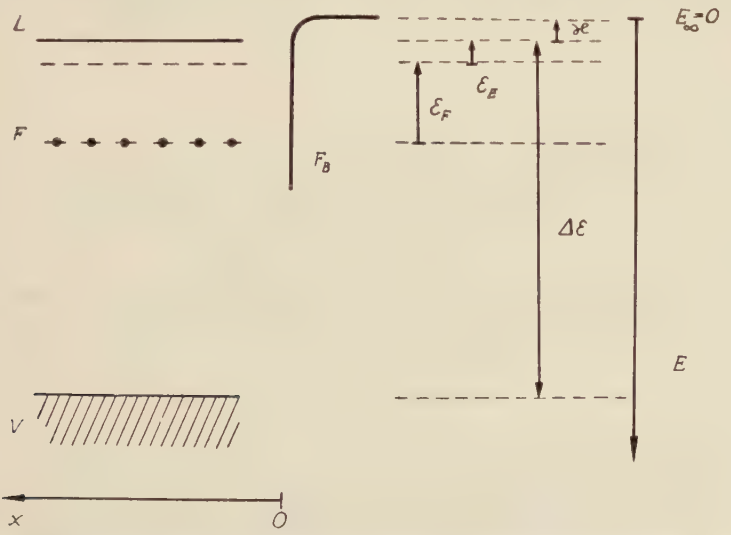

Fig. 4. Schema der energetischen Niveaus im Falle der verfärbten Alkalihalogenidkristallen. *V* — obere Valenzbankante, *L* — Boden des Leitfähigkeitsbandes. Über weiter Einzelheiten siehe Text.

befindet. Dank der Warmeenergie des Kristallgitters ($T \sim 300°K$) werden einige der erregten Zentren von den Elektronen entleert und die mit der Zeit abfallende Postelektronenemission in Dunkelheit beobachtet, wenn während der Messung kein Nachfüllen der Chlor-Vakanzen mit Elektronen stattfindet. Wenn die thermische Energie des Gitters zur Emission der Elektronen beitragen sollte, so müsste der dem einzelnen Elektron gelieferte Anteil etwa dem Wert der Austrittsarbeit $\varkappa$ entsprechen, da die erregten Zustände sehr flach unter dem Boden des Leitungsbandes liegen. Der Wert von $\varkappa$ wird für die Alkalihalogenide etwa

[1] Auch Elektronenaffinität bezeichnet

0,5 bis 0,8 eV angenommen (Wright 1957, Mott und Gurney 1950, Seitz 1940. Die Schätzung der thermischen Aktivationsenergie zur Emission auf Grund der Abhändigkeit (9) ergibt für $T_m = 300°K$

$$\varepsilon \sim 0{,}6 \text{ eV}$$

Dieses ist unter Voraussetzung geschätzt worden, dass eine Glow-Kurve des KCl, wenn bei tiefen Temperaturen zur Emission erregt, ein Maximum in der Umgebung von Zimmertemperatur aufweist. Die, auf diese Weise geschätzte, thermische Aktivationsenergie zur Emission von Exoelektronen bei Zimmertemperatur ist tatsächlich von der Grösse des angenommenen Wertes der Austrittsarbeit $\varkappa$.

Die Kurve A in Fig. 5, die in doppelogarithmischer Auffassung dargelegt wurde, zeigt das Abfallen der Dunkelemission einer vorher durch Gasentladung erregten Postelektronenemission aus einer KCl-Schicht, die an der Wand eines G. M.-Zählers niedergeschlagen wurde (Sujak 1956).

Die Kurve B in Fig. 5 zeigt die Abklingkurve der photostimulierten Coelektronenemission, die nach dem Abklingen der Dunkelemission (Kurve A) von der gleichen Schicht gemessen wurde. Das eingestrahlte Licht war von etwa 5700 Å Wellenlänge.

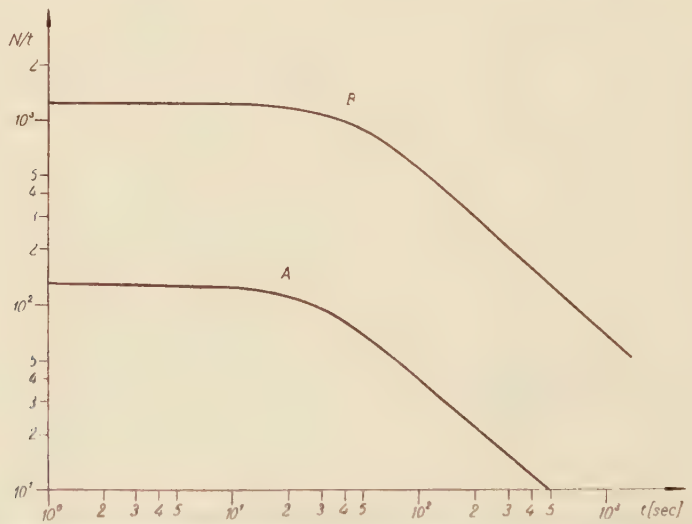

Fig. 5. Abklingkurven der Exoelektronenemission von einer KCl-Schicht (eigene Messungen). A — Abklingkurve der Postelektronenemission (im Dunkeln), B — Abklingkurve der photostimulierten Coelektronenemission unter Beleuchtung mit Licht von etwa 5700 Å Wellenlänge. Kurve B wurde aufgenommen nachdem die Aufnahme der Kurve A beendigt wurde.

Aus dem Übereinstimmen der Gestalten der Abklingkurven A und B in Fig. 5 ist zu erwarten, dass, wenn der Erregungszustand der F-Zentren (mit Elektronen gefüllten Elektronenhaftstellen) z. B. durch eine Beleuchtung mit Lichtquanten aus dem Bereich des Lichtabsorptionsbandes der F-Zentren erzeugt wird, das Afballen der photostimulierten Coelektronenemission auf die gleiche Art wie die in Dunkeln gemessene Postelektronenemission verlaufen wird. Der Unterschied wird sich lediglich in den Intensitäten der Emission

zeigen. Dieses wird nur in dem Falle gelten, wenn die gleichen Haftstellenarten in beiden Fällen zur Auswirkung kommen.

Wenn das eingestrahlte Licht Quanten enthält, die — wie das in Fig. 6 gedeutet wurde — nur ein diskretes Haftstellenniveau bedecken, so müsste eine Abklingkurve von der Art erwartet werden, die bei den Erwärgungen nach Nassenstein (1955) durch eine Gleichung von dem Typus (1) beschrieben wäre. Es wäre dabei vorauszusetzen, dass kein Nachfüllen mit Elektronen und Generieren der Haftstellen während der Messung stattfindet. Wenn

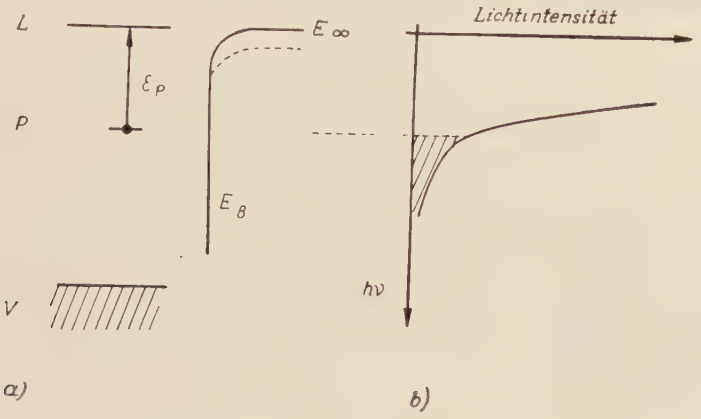

Fig. 6. Links: Energetisches Schema der mit Elektronen besetzten Haftstelle. Rechts: Intensitätsverteilung des eingestrahlten, weissen Lichtes der Quantenenergie nach. Wirkungsvoll für die Emission können also nur die Lichtquanten sein, für welche $h_\nu \geqslant \varepsilon_p$ ist.

dagegen mehrere diskrete Haftstellenniveaus durch das eingestrahlte Licht bedeckt werden, so wird eine Abklingkurve von der Art einer Summe

$$\frac{N}{t} = \sum_i A_i e^{-a_i t} \tag{19}$$

zu erwarten, die sich im Falle grösserer Unterschiede in der energetischen Tiefe der Haftstellenniveaus sehr leicht bei der halblogarithmischen Darstellung ln N/t, t auf die einzelnen Abklingkurven trennen lässt.

Im Falle, wenn die Haftstellenniveauss nicht diskret liegen, aber eine Verteilung der energetischen Tiefe nach zeigen, wird vielmehr eine Abklingkurve der photostimulierten Coelektronenemission von der Art

$$\frac{N}{t} = t^{-b} \tag{20}$$

zu erwarten sein.

Auf diese Weise kann eine Haftstellenanalyse der Abklingkurven bei festgelegter Temperatur auch unter Beleuchtung durchgeführt werden. Dadurch werden grössere Intensitäten als im Falle der Postelektronenemission in Dunkelheit erziehlt. Wenn das eingestrahlte Licht tatsächlich nur einzelne Haftstellenniveaus bedeckt, wird sogar kein

monochromatisches Licht dazu gebraucht. Die Voraussetzung ist, dass es Quanten in genügender Anzahl enthält, deren Energie $h\nu$ gleich oder grösser als die optische Aktivierungsenergie für eine Überführung des F-Zentrum in den angeregten Zustand ist

$$h\nu \geqslant \varepsilon_F + \varepsilon_E \tag{21}$$

Da das Energieniveau des angeregten Zustandes angeblich 0,1 bis 0,2 eV unter dem Boden des Leitfähigkeitsbandes liegt (siehe auch Bohun und Dolejsi 1959), kann folgendes angenommen werden (für Raumtemperaturen des Kristalles):

$$\varepsilon_F + \varepsilon_E \sim \varepsilon_F \tag{22}$$

Aus diesem Grunde kann bei vielen Untersuchungen weisses Licht benutzt werden, unter der Voraussetzung, dass energetisch erforderliche Quanten enthalten sind.

Eine Analyse der Abklingkurven unter Beleuchtung gibt also auch die Möglichkeit, die energetische Struktur der Elektronenhaftstellen zu untersuchen. Die Ergebnisse einer solchen Analyse müssen jedoch sehr kritisch betrachtet werden und immer nur bei denselben Versuchsverhältnissen untereinander verglichen werden. Die Änderungen der Austrittsarbeit für das Elektron sind nämlich sehr von den Zustandsänderungen der Oberfläche abhängig (Wolkenstein 1960, Simon und Suhrmann 1958). Dabei ist auch zu berücksichtigen, dass die Austrittsarbeit für die Halbleiter, je nach dem ob optisch oder thermisch ermittelt, folgend definiert wird:

$$\varphi_{\text{optisch}} = \varepsilon_p + \varkappa \tag{23}$$

$$\varphi_{\text{thermisch}} = \tfrac{1}{2}\varepsilon_p + \varkappa \tag{24}$$

Wenn weiterhin für $\varkappa$ positive wie auch negative Werte zugelassen werden, so kann die hier mit φ bezeichnete Austrittsarbeit mit der vom Seidl eingeführten Bezeichnung ε_∞ identifiziert werden.

Wenn die Wellenlänge des beleuchtenden Lichtes geändert und dabei die gemessene Elektronenintensität auf eine gleiche, auffallende Quantenzahl (oder Energie) reduziert wird, so ist im Falle einer selektiven Absorption des Lichtes K durch die mit Elektronen besetzen Elektronenhaftstellen (z. B. F-Zentren) eine dem entsprechende, selektive Kurve der photostimulierten Coelektronenemission zu erwarten:

$$\frac{N}{t \cdot E} = f(K, t) \tag{25}$$

wobei E — Energie des in der Zeiteinheit auffallenden Lichtes,
K — Absorptionskoeffizient,
t — Zeitdauer der Messung bedeuten.

Im Falle der Alkalihalogenide z. B. KCl oder NaCl, wurden unabhängig von Bohun (1960), (siehe auch Bohun und Mitarbeiter 1960) und mir (Sujak 1953, 1956, 1957) diesbezügliche Messungen durchgeführt. Der Verlauf der Kurven für NaCl und KCl ist in Fig. 7 und Fig. 8 zum Vergleich wiedergegeben werden.

Da die Analysentechnik der Absorptionsbänder der F-Zentren für Alkalihaloide sehr gut ausgearbeitet ist, können mit Hilfe des Vergleichens dieser mit dem Verlauf der auf das

auffallende Licht bezogenen Quantenausbeute weitere Erkenntnisse über die Rolle der Oberflächenzustande bei der Emission von Exoelektronen gewonnen werden.

Der Einfluss der Oberflächenzustände scheint sehr gross zu sein, da die genannten Selektivitäten bei NaCl und KCl bis jetzt nur im Falle der Emission in einer Gasatmosphäre gemessen werden, (Sujak, 1953, 1956, 1957, Bohun und Mitarbeiter 1960, Bohun 1957, Asmus 1936). Im Hochvakuum sind diese Selektivitäten nicht zu finden (Fleischmann 1933, Apker und Taft 1950, 1951, Klein, Schatz und Seeger 1960). Es ensteht also ein Problem und zugleich eine Möglichkeit, auf Grund dieser Unterschiede den Einfluss von Oberflächen-

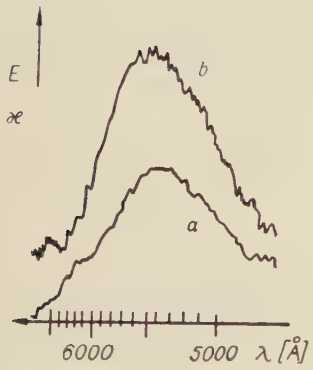

Fig. 7

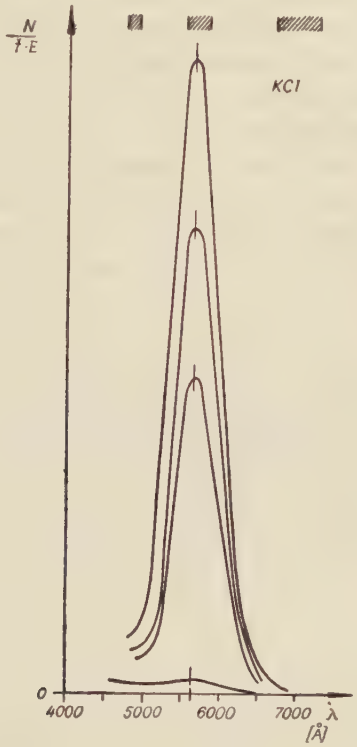

Fig. 8

Fig. 7. Verlauf der optischen Absorption (Kurve *a*) und der photostimulierten Coelektronenemission (Kurve *b*) für KCl-Kristall. (nach Bohun und Mitarbeitern 1960).

Fig. 8. Verlauf der photostimulierten Coelektronenemission für KCl-Schicht, die auf gleiche auffallende Lichtenergie normiert wurde (eigene Messungen 1957).

zuständen mit Hilfe der Exoelektronen-Methode näher zu studieren (Roubinek 1960). In diesem Falle muss aber auf die Untersuchungen der photoelektrischen Emission aus Nichtmetallen im allgemeinen hingewiesen werden (Arsenjewa-Geil 1957, Wright 1957, Mott und Gurney 1950, Seitz 1940, Joffe 1956). Ein grosser Teil der photostimulierten Exoelektronen-Emissionsphänomena kann nämlich als photoelektrische Emissionserscheinungen aus den Halbleitern oder Nichtmetallen anerkannt werden. Der grundlegende Unterschied

in diesen Fällen liegt vorwiegend in den gemessenen Stromdichten und den Versuchsverhältnissen.

An dieser Stelle muss noch darauf hingewiesen werden, dass die Potentiellschwelle (Energiebarriere) für Elektronen und die energetischen Bänder in den Oberflächenschichten eines nichtmetallischen Kristalles nicht so einfach verlaufen, wie das in der ersten Näherung z. B. vom Seidl (1959) und von mir in diesem Abschnitt diskuttiert wurde.

Es müssen weiterhin die Einwirkungen der Raumladung und der Oberflächenaufladung, die während einigen Erregungsprozessen der Exoelektronenemission zustande kommen, auf die Neigung des Leitfähigkeitsbandes berücksichtigt werden. Dieses wird nämlich eine Möglichkeit des Entweichens eines Elektrons aus den inneren Schichten der wirksamen Oberflächenschicht änderen. Dieser Einfluss der Raum- oder einer Oberflächenladung muss sich besonders bei den Messungen der photostimulierten Coelektronenemission bemerkbar machen.

Zu diesen Fragen wurden jedoch auf dem Gebiet der Exoelektronenemission bis jetzt wenige Versuchsergebnisse geschaffen, deswegen kann dieses Problem hier nur angedeutet werden (Matyás 1957; Hanle, Kanzler und Scharmann 1961).

Für die photoelektrisch gemessene Austrittsarbeit kann, wie bekannt geschrieben werden:

$$\varphi_{\text{optisch}} = \varepsilon_p + \varkappa \tag{26}$$

wobei diese für das Elektron aus einer Haftstelle von der energetischen Tiefe ε_p in einem Halbleiter deren Oberfläche elektrisch neutral ist, gemeint wird (siehe Fig. 9a). Wenn jedoch eine elektrische Überschussladungdichte auf der Oberfläche zugelassen wird, so werden

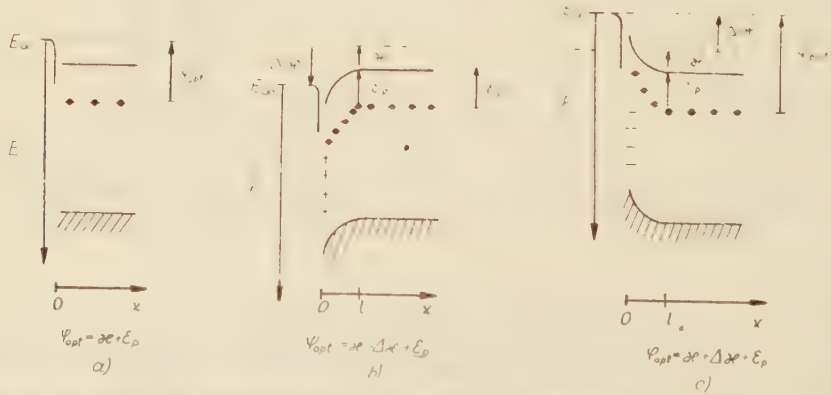

Fig. 9. Biegung der Bänder als Nachwirkung einer Aufladung der Oberfläche: *a*) Oberfläche neutral, *b*) Oberfläche positiv aufgeladen, *c*) Oberfläche negativ aufgeladen (Vergleiche Wolkenstein 1960).

die Energiebänder (Leitfähigkeits und Valzenband) je nach der Ladungsdichte und Zeichen nach oben oder nach unter in der Oberflächenschichtdicke von l gebogen. Dies ist in der Fig. 9b und 9c schematisch gezeigt. Die Biegung der Bänder ist also zu dem Fall nach Wolkenstein (1960) analog, wo die chemosorbierten Molekülen eine Überschussladungsdichte an der Oberfläche des Halbleiters bewirken.

Wenn also das emittierte Elektron aus einer Tiefe l heraustritt und die Oberfläche eine positive Überschussladung aufweist, so wird eine Herabsetzung der Austrittsarbeit φ um einen Wert $\Delta\varkappa$ erfolgen:

$$\varphi_{\text{optisch}} = \varepsilon_p + \varkappa - \Delta\varkappa \tag{27}$$

Die Tiefe l soll z. B. nach Wolkenstein (1960) um 10^{-4} bis 10^{-5} cm betragen. Dieser Wert entspricht merkwürdigerweise z. B. der optimalen Schichtdicke der Exoelektronenemittierende Oxyddeckschicht, die etwa 10^{-4} cm betragen soll (Müller 1957). Es kann also angenommen werden, dass im Falle der Emission von Exoelektronen die Tiefe von 10^{-4} bis 10^{-5} cm die optimale Emissionstiefe ist, dass heisst die Elektronen werden aus dieser Tiefe am leichtesten ausgesandt. Wenn aber das der Fall ist, so kann erwartet werden, dass wenn die Oberfläche mit einer, der Grösse nach, gleichen aber negativen Überschussladungsdichte belegt wird, erhöht sich die Austrittsarbeit um den gleichen Wert $\Delta\varkappa$ für jenes Elektron aus der Emissionstiefe l. Die Austrittsarbeit wird in diesem Falle also betragen:

$$\varphi_{\text{optisch}} = \varepsilon_p + \varkappa + \Delta\varkappa \tag{28}$$

Es wird auch verständlich, warum für die gleiche Lichtquelle und Oberflächengrösse öffters Photoelektronen aus den Staubkernen mit F-Zentren, die positive Oberflächenladung zeigen (nach der Theorie der Aufladung durch Brechen wird die Ladung an der Oberfläche lokaliesiert — Szaynok 1960), gemessen werden als aus denen, die negativ aufgeladen sind (Sujak und Szaynok 1961, Szaynok 1960, Sujak — Habilitationsschrift). Dies wird sich als grössere Emissionsintensität bei der photostimulierten Coelektronenemission auswirken, wenn die vorher durchgeführte Verfärbung der Ausgangskristalle eine positive Überschussladung in der Pulver-Wolke bewirkt. Es ist nämlich zu erwarten, dass die Lichtquanten von der Energie $h\nu$, wobei

$$\varepsilon_F \leqslant h\nu < \varepsilon_F + \varkappa \tag{29}$$

eine photostimulierte Coelektronenemission besonders von den Staubkernen die oberflächlich positiv aufgeladen sind, doch bewirken werden. Wenn die positive Aufladung der Oberfläche eine Herabsetzung der effektiven Austrittsarbeit um einen Betrag $\Delta\varkappa$ von der Grösse $|\Delta\varkappa| \geqslant |\varkappa|$ bewirkt, so kann für die Elektronen aus der optimalen Emissionstiefe l folgendes geschrieben werden:

$$\varphi_{\text{optisch}} \leqslant \varepsilon_p \tag{30}$$

oder wenn für φ_{optisch} die Bezeichnung ε_∞ gewählt wird:

$$\varepsilon_\infty \leqslant \varepsilon_p \tag{31}$$

Das bedeutet aber, dass die Exoelektronenemission lediglich durch den inneren Prozess — eine Überführung des Elektrons in das Leitfähigkeitsband — bedingt wird. In diesem Falle spielt also die Austrittsarbeit gar keine Rolle, wie das auch öfters beobachtet wurde (Bohun und Dolejsi 1959, Sujak 1956, 1957, 1959, Habilitationsschrift).

Aus der Ungleichheit (29) und aus der Fig. 9 kann auch verständlich sein warum für die gleiche Lichtquelle ein aus den mit β-Strahlen verfärbten KCl-Kristallen hergestellte Pulver fast keine Photoemission zeigte, solange die Pulver-Wolke eine grössere negative Überschussladung aufweiste (Sujak und Szaynok 1961, Szaynok 1960, Szaynok — Dissertation).

Vielleicht könnte dasgleiche auch die Glow-Kurven zutreffen. Dabei müsste aber die Gleichung (24) berücksichtigt werden. Eine Diskussion muss leider zur Zeit noch unterlassen bleiben, da zu dieser Frage auf dem Gebiet der Exoelektronen bis jetzt kaum Versuchsergebnisse geschaffen wurden.

LITERATURHINWEISE

Apker, L. und Taft, E., *Phys. Rev.*, **79,** 964 (1950); **81,** 698 (1951).

Arsenjewa-Geil, A. N., „*Vneshnyĭ Fotoéffekt s Poluprovodnikov i Diélektrykow*", Moskau 1957.

Asmus, E., *Ann. Phys.* (Leipzig), **26,** 723 (1936).

Bohun, A., *Czech. J. Phys.*, **4,** 139 (1954); *Acta phys. Hungarica*, **8,** 65 (1957).

Bohun, A. und Dolejsi J., *Czech. J. Phys.*, **9,** 578 (1959).

Bohun, A., Kanturek, J., Trnka, J. und Lebl, M., *Czech. J, Phys.*, **B10,** 349 (1960).

Fleischmann, R., *Z. Phys.* **84,** 717 (1933).

Hanle, W., Kanzler, G. und Scharmann, A., *Z. Phys.*, **162,** 483 (1961).

Joffe, A., F., „*Półprzewodniki w fizyce współczesnej*" Warszawa 1956, (Polnische Übersetzung aus dem Russischen).

Klein, W., Schatz, G. und Seeger, K., *Z. Phys.*, **160,** 443 (1960).

Matyás, M., *Czech. J. Phys.*, **7,** 277 (1957).

Mott, N. F. und Gurney, R. W., „*Electronic Processes in Ionic Crystals*", Oxford 1950.

Nassenstein, H., *Z. Naturforsch.*, **10a,** 944 (1955).

Randall, J. T. und Wilkins, M. H. F., *Proc. Roy. Soc.* (London), **A 184,** 366 (1945)a: **A 184,** 390 (1945) b.

Roubinek, F., *Czech. J. Phys.*, **B10,** 949 (1960).

Seidl, R., *Czech. J. Phys.*, **B 10,** 931 (1960).

Seitz, F. „*Modern Theory of Solids*" 1940.

Simon H. und Suhrmann R., „*Der Lichtelektrische Effekt und seine Anwendungen*", Berlin 1958.

Sujak, B., *Acta phys. Polon.*, **12,** 241 (1953); *Acta phys. Austriaca*, **10,** 353 (1957); *Zeszyty Naukowe Uniwersytetu Wrocławskiego*, **3 B,** 227 (1959); *Habilitationsschrift* — Universität zu Wrocław, 1961.

Sujak, B. und Szaynok, A., *Acta phys. Polon.*, **20,** 425 (1961).

Szaynok, A., *Dissertation* — Universität zu Wrocław, 1960.

Wolkenstein, F. F., „*Élektronnaya teoriya kataliza na poluprovodnikakh*", Moskau 1960.

Wright, D. A., „*Poluprovodniki*", Moskau 1957 (Übersetzung aus dem Englischen).

SPIN WAVE THEORY FOR CUBIC FERROMAGNETICS I. DYSON'S MODEL

By Jan Szaniecki (Śledzik)

Institute of Physics of the Polish Academy of Sciences, Department of Ferromagnetics in Poznań.

(Received May 31, 1961)

The principal features of the Dyson spin wave theory of a cubic crystalline isotropic ferromagnetic are presented.

In the subsequent part of the present paper a new spin wave approach is developed, based on Matsubara's technique.

1. Introduction

In his excellent analysis of the cubic ferromagnetic Dyson (1956a, b) formulated the strict theory of spin waves. As the spin wave states are non-orthogonal, Dyson developed a special formalism of interacting spin waves and proposed a method of obtaining the thermodynamical quantities within the framework of non-orthogonal states. There are two types of interactions in the Dyson model of a ferromagnetic. The one, termed kinematical interaction, is due to the fact that spin S (S — spin quantum number) of each atom can be located in space in $2S+1$ different ways only, so that the quantum numbers of the oscillator operators co-ordinated to the spin operators cannot exceed $2S$. The other type of spin wave interaction, termed dynamical interaction, results from the assumption of a special form of basic states independently of the Hamiltonian.

In the first part of the present paper Dyson's theory is outlined in general. The slight modifications introduced concern the generalization of the theory to any type of neighbourhood of lattice points and the derivation of correspondence between the oscillator operators and the spin operators directly from matrix elements for the indefinite metric operator.

As the kinematical interaction at low temperatures is small, as proved by Dyson (1956b), in the second part of the present paper we establish another form of the statistical function using the orthonormal set of basic states in the reciprocal lattice. We then apply the Matsubara (1955) representation. The ladder diagrams obtained thereafter enable us to compute any contribution to the magnetization.

In the third part, we derive formula for the mean magnetization for three types of cubic lattice. The formula obtained is identical with that given by Dyson (1956b). As to the correction to the magnetization proportional to T^4, we have computed only the one term

independent of S. Computation of the full coefficient requires consideration of higher order diagrams.

Our main aim was to give a method for computing various thermodynamical quantities easier than the strict but difficult formalism proposed by Dyson. The present modification of Dyson's theory satisfies this requirement.

2. *The Hamiltonian of a cubic ferromagnetic*

We assume the ferromagnetic to consist of a single species of atoms with any number of magnetic electrons. The atoms are located at regularly distributed cubic lattice points. We put $\hbar=1$. The vector to any translation lattice point is given by

$$\boldsymbol{j}=j^1\boldsymbol{a}_1+j^2\boldsymbol{a}_2+j^3\boldsymbol{a}_3\equiv j^i\boldsymbol{a}_i, \quad j^i\leqslant\left|\frac{N^{1/3}-1}{2}\right|, \tag{2.1}$$

where $\boldsymbol{a}_1, \boldsymbol{a}_2, \boldsymbol{a}_3$ are the principal vectors of the lattice and N — the number of lattice points. We apply the periodic boundary conditions. The reciprocal lattice is defined by

$$\vec{\lambda}=\frac{2\pi}{N^{1/3}}\ (\lambda_1\boldsymbol{b}^1+\lambda_2\boldsymbol{b}^2+\lambda_3\boldsymbol{b}^3)\equiv\frac{2\pi}{N^{1/3}}\lambda_i\boldsymbol{b}^i, \quad \lambda_i^1\leqslant\left|\frac{N^{1/3}-1}{2}\right|, \tag{2.2}$$

$$\boldsymbol{b}^i=\frac{1}{2v}\,\varepsilon^{ikl}\boldsymbol{a}_k\times\boldsymbol{a}_l, \quad v=\boldsymbol{a}_1\cdot(\boldsymbol{a}_2\times\boldsymbol{a}_3). \tag{2.3}$$

where ε^{ikl} is the permutation tensor.

To any lattice point $\boldsymbol{j}$ is attached the spin operator $\hat{\boldsymbol{S}}_j$ satisfying the commutation rules

$$[\hat{S}_j^x,\hat{S}_k^y]=i\delta_{j,k}\hat{S}_j^z, \quad [\hat{S}_j^y,\hat{S}_k^z]=i\delta_{j,k}\hat{S}_j^x, \quad [\hat{S}_j^z,\hat{S}_k^x]=i\delta_{j,k}\hat{S}_j^y, \tag{2.4}$$

$$\hat{S}_j^{\pm}=\hat{S}_j^x\pm i\hat{S}_j^y, \tag{2.5}$$

whence

$$[\hat{S}_j^z,\hat{S}_k^+]=\delta_{j,k}\hat{S}_j^+, \quad [\hat{S}_j^z,\hat{S}_k^-]=-\delta_{j,k}\hat{S}_j^-, \quad [\hat{S}_j^+,\hat{S}_k^-]=2\delta_{j,k}\hat{S}_j^z. \tag{2.6}$$

We write the Hamiltonian of the system as follows:

$$\hat{H}=L\sum_j\hat{S}_j^z-\tfrac{1}{2}\sum_{j\neq k}\mathcal{J}(|\boldsymbol{j}-\boldsymbol{k}|)\,\hat{\boldsymbol{S}}_j\cdot\hat{\boldsymbol{S}}_k=$$

$$=L\sum_j\hat{S}_j^z+\tfrac{1}{2}\mathcal{J}(0)\sum_j\hat{\boldsymbol{S}}_j^2-\tfrac{1}{2}\sum_{j,k}\mathcal{J}(|\boldsymbol{j}-\boldsymbol{k}|)\,\hat{\boldsymbol{S}}_j\cdot\hat{\boldsymbol{S}}_k,$$

$$L=\frac{mH}{S}, \tag{2.8}$$

wherein S is the spin quantum number of each atom, H — the magnetic field strength, $\mathcal{J}(|\boldsymbol{j}-\boldsymbol{k}|)$ — the exchange integral and m — the magnetic moment of each spin.

Since

$$\hat{\boldsymbol{S}}_j^2=S(S+1), \tag{2.9}$$

we have

$$\hat{H} = \tfrac{1}{2}\mathcal{J}(0)\,NS(S+1) + L\sum_j \hat{S}_j^z - \tfrac{1}{2}\sum_{j,k}\mathcal{J}(|\boldsymbol{j}-\boldsymbol{k}|)\,\hat{\mathbf{S}}_j\cdot\hat{\mathbf{S}}_k. \tag{2.10}$$

We can now expand the exchange integral in a series over the reciprocal lattice,

$$\mathcal{J}(|\boldsymbol{j}-\boldsymbol{k}|) = \frac{1}{N}\sum_\lambda \mathcal{J}_\lambda\, e^{i\vec{\lambda}\cdot(\boldsymbol{j}-\boldsymbol{k})},\quad \mathcal{J}_\lambda = \mathcal{J}_{-\lambda}, \tag{2.11}$$

whence

$$\mathcal{J}(0) = \frac{1}{N}\sum_\lambda \mathcal{J}_\lambda, \tag{2.12}$$

and, conversely,

$$\mathcal{J}_\lambda = \frac{1}{N}\sum_{j,k}\mathcal{J}(|\boldsymbol{j}-\boldsymbol{k}|)\,e^{-i\vec{\lambda}\cdot(\boldsymbol{j}-\boldsymbol{k})}. \tag{2.13}$$

In the special case of interaction only between nearest neighbours we denote by $\vec{\delta}$ the vector connecting the nearest lattice points and get

$$\boldsymbol{k} = \boldsymbol{j}+\vec{\delta},\quad \mathcal{J}(\delta)\equiv\mathcal{J},\quad \mathcal{J}(|\boldsymbol{j}-\boldsymbol{k}|) = \mathcal{J}\delta(\boldsymbol{k}-\boldsymbol{j}-\vec{\delta}),$$

$$\mathcal{J}_\lambda = \frac{1}{N}\sum_{j,k}\mathcal{J}\delta\,(\boldsymbol{k}-\boldsymbol{j}-\vec{\delta})\,e^{-i\vec{\lambda}\cdot(\boldsymbol{j}-\boldsymbol{k})} = \frac{\mathcal{J}}{N}\sum_{j,k} e^{-i\vec{\lambda}\cdot(\boldsymbol{j}-\boldsymbol{k})}\,\delta(\boldsymbol{k}-\boldsymbol{j}-\vec{\delta}) =$$

$$= \frac{\mathcal{J}}{N}\sum_{j,\delta} e^{i\vec{\lambda}\cdot\vec{\delta}} = \mathcal{J}\gamma_\lambda,\quad \gamma_\lambda = \sum_\delta e^{i\vec{\lambda}\cdot\vec{\delta}}. \tag{2.14}$$

The spin operator attached to a $\vec{\lambda}$ point in the reciprocal lattice can be given by the Fourier series

$$\hat{\mathbf{S}}_\lambda = N^{-1/2}\sum_j e^{-i\vec{\lambda}\cdot\boldsymbol{j}}\hat{\mathbf{S}}_j. \tag{2.15}$$

By the last equation we can rewrite Eq. (2.10) in the form

$$\hat{H} = \tfrac{1}{2}S(S+1)\sum_\lambda \mathcal{J}_\lambda + LN^{1/2}\hat{S}_0^z - \tfrac{1}{2}\sum_\lambda \mathcal{J}_\lambda\hat{\mathbf{S}}_\lambda\cdot\hat{\mathbf{S}}_{-\lambda}, \tag{2.16}$$

where we have used the Kroenecker delta

$$\delta(\boldsymbol{j}) = N^{-1}\sum_\lambda e^{i\vec{\lambda}\cdot\boldsymbol{j}}. \tag{2.17}$$

3. Spin wave states

Let us denote the ground state of the system as $|0\rangle$ and define it by the equation

$$\hat{S}_j^z|0\rangle = -S|0\rangle. \tag{3.1}$$

From the relation

$$\hat{S}_j^+ \hat{S}_j^- = (\hat{S}_j^x + i\hat{S}_j^y) \cdot (\hat{S}_j^x - i\hat{S}_j^y) = (\hat{S}_j^x)^2 - (\hat{S}_j^y)^2 - i[\hat{S}_j^x, \hat{S}_j^y] =$$
$$= \hat{\mathbf{S}}_j^2 - (\hat{S}_j^z)^2 + \hat{S}_j^z = S(S+1) - (\hat{S}_j^z)^2 + \hat{S}_j^z, \tag{3.2}$$

we conclude that

$$\hat{S}_j^+ \hat{S}_j^- |0\rangle = S(S+1)|0\rangle - (\hat{S}_j^z)^2 |0\rangle + \hat{S}_j^z |0\rangle = 0$$

or

$$\hat{S}_j^- |0\rangle = 0. \tag{3.3}$$

$\hat{S}_j^-$ is the spin deviation annihilation operator and $\hat{S}_j^+$ — the spin deviation creation operator.

Let the complete set of orthogonal but, not normal state vectors be determined as

$$|u\rangle = \prod_j [(2S)^{-\frac{1}{2}u_j} (u_j!)^{-\frac{1}{2}} (\hat{S}_j^+)^{u_j}] |0\rangle, \tag{3.4}$$

wherein u_j is the positive integer and $\prod_j$ denotes the product over all points of the lattice.

We now compute the norm of the vector of Eq. (3.4). For this purpose we notice that

$$\hat{S}_j^- (\hat{S}_j^+)^p = (\hat{S}_j^+)^p \hat{S}_j^- - 2(\hat{S}_j^+)^{p-1} [p\hat{S}_j^z + \binom{p}{2}], \quad p = 1, 2, 3, \ldots \tag{3.5}$$

The above relation can be proved by total induction on the ground of Eqs. (2.6). Eqs. (3.1), (3.3) and (3.5) now yield

$$\hat{S}_j^- (\hat{S}_j^+)^{u_j} |0\rangle = -2(\hat{S}_j^+)^{u_j - 1} \left[-Su_j + \binom{u_j}{2} \right] |0\rangle =$$

$$= 2S \cdot u_j \left(1 - \frac{u_j - 1}{2S}\right) (\hat{S}_j^+)^{u_j - 1} |0\rangle,$$

$$(\hat{S}_j^-)^2 (\hat{S}_j^+)^{u_j} |0\rangle = (2S)^2 u_j (u_j - 1) \left(1 - \frac{u_j - 1}{2S}\right) \left(1 - \frac{u_j - 2}{2S}\right) (\hat{S}_j^+)^{u_j - 2} |0\rangle,$$

and, quite generally,

$$\langle 0 | (\hat{S}_j^-)^{v_j} (\hat{S}_j^+)^{u_j} | 0 \rangle = (2S)^{u_j} \delta_{u_j, v_j} u_j!\, F(u_j), \tag{3.6}$$

with

$$F(u) = 1 \cdot \left(1 - \frac{1}{2S}\right) \left(1 - \frac{2}{2S}\right) \ldots \left(1 - \frac{u-1}{2S}\right). \tag{3.7}$$

We have, finally,

$$\langle v | u \rangle = F_u \delta_{u,v}, \qquad F_u = \prod_j F(u_j), \qquad \delta_{u,v} = \prod_j \delta_{u_j, v_j}. \tag{3.8}$$

We now introduce the complete set of orthonormal oscillator state vectors

$$|u) = \prod_j [(u_j!)^{-\frac{1}{2}} (\eta_j^*)^{u_j}] |0), \tag{3.9}$$

$$(v| = (0| \prod_j [\eta_j^{v_j} (v_j!)^{-\frac{1}{2}}], \tag{3.10}$$

$$[\eta_j, \eta_k] = [\eta_j^*, \eta_k^*] = 0, \qquad [\eta_j, \eta_k^*] = \delta_{j,k}. \tag{3.11}$$

Let $\hat{F}$ be the indefinite metric operator in the space of states (3.9). We require that

$$(v|\hat{F}|u) = \langle v|u\rangle \tag{3.12}$$

or

$$(v|\underset{\leftarrow}{\hat{F}} = (v|\hat{F}_v \equiv (0|\prod_j [\eta_j^{v_j}\hat{F}(v_j)\,(v_j!)^{-1/2}], \tag{3.13}$$

$$\hat{F}(v_j) = \prod_{l=1}^{v_j}\left[1 - \frac{1}{2S}\,(\eta_j^*\eta_j - l)\right]. \tag{3.14}$$

We shall prove that

$$(0|\,\eta_j^{v_j}\hat{F}(v_j) = (0|\left[\left(1 - \frac{1}{2S}\,\eta_j^*\eta_j\right)\,\eta_j\right]^{v_j}. \tag{3.15}$$

We have

$$\left[\eta_j, 1 - \frac{1}{2S}(\eta_j^*\eta_j - l)\right] = -\frac{1}{2S}\,[\eta_j, \eta_j^*\eta_j] = -\frac{1}{2S}\,\eta_j,$$

$$\eta_j\left[1 - \frac{1}{2S}(\eta_j^*\eta_j - l)\right] = \left[1 - \frac{1}{2S}\,(\eta_j^*\eta_j - l + 1)\right]\eta_j,$$

$$\eta_j^l\left[1 - \frac{1}{2S}(\eta_j^*\eta_j - l)\right] = \left[1 - \frac{1}{2S}\,\eta_j^*\eta_j\right]\eta_j^l,$$

yielding

$$\eta_j^{v_j}\hat{F}(v_j) = \eta_j^{v_j}\prod_{l=1}^{v_j}\left[1 - \frac{1}{2S}\,(\eta_j^*\eta_j - l)\right] = \eta_j^{v_j}\left[1 - \frac{1}{2S}(\eta_j^*\eta_j - v_j)\right]\times$$

$$\times\left[1 - \frac{1}{2S}\,(\eta_j^*\eta_j - v_j + 1)\right]\ldots\left[1 - \frac{1}{2S}(\eta_j^*\eta_j - 1)\right] = [1 - \frac{1}{2S}\eta_j^*\eta_j]\,\eta_j\cdot\eta_j^{v_j-1}\times$$

$$\times\left[1 - \frac{1}{2S}\,(\eta_j^*\eta_j - v_j + 1)\right]\ldots\left[1 - \frac{1}{2S}\,(\eta_j^*\eta_j - 1)\right] = [1 - \frac{1}{2S}\,\eta_j^*\eta_j]\,\eta_j\times$$

$$\times\left[1 - \frac{1}{2S}\,\eta_j^*\eta_j\right]\eta_j\cdot\eta_j^{v_j-2}\left[1 - \frac{1}{2S}\,(\eta_j^*\eta_j - v_j + 2)\right]\ldots\left[1 - \frac{1}{2S}(\eta_j^*\eta_j - 1)\right] =$$

$$= \left[\left(1 - \frac{1}{2S}\,\eta_j^*\eta_j\right)\eta_j\right]^{v_j-1}\cdot\eta_j\left[1 - \frac{1}{2S}\,(\eta_j^*\eta_j - 1)\right] = \left[\left(1 - \frac{1}{2S}\,\eta_j^*\eta_j\right)\eta_j\right]^{v_j}.$$

Thus Eq. (3.12) assumes the form

$$(0|\prod_j\left\{(v_j!\,u_j!)^{-1/2}\left[\left(1 - \frac{1}{2S}\,\eta_j^*\eta_j\right)\eta_j\right]^{v_j}(\eta_j^*)^{u_j}\right\}|0) =$$

$$= \langle 0\,|\prod_j[(2S)^{-\frac{1}{2}(v_j+u_j)}\,(v_j!\,u_j!)^{-1/2}\,(\hat{S}_j^-)^{v_j}\,(\hat{S}_j^+)^{u_j}]\,|\,0\rangle. \tag{3.16}$$

Thereby we have established the following correspondence, Morkowski (1959),

$$\hat{S}_j^- \to (2S)^{1/2}\left(1-\frac{1}{2S}\eta_j^*\eta_j\right)\eta_j, \tag{3.17a}$$

$$\hat{S}_j^+ \to (2S)^{1/2}\eta_j^*, \tag{3.17b}$$

$$\hat{S}_j^z \to -S+\eta_j^*\eta_j. \tag{3.17c}$$

The last equation (3.17c) results from Eq. (2.6),

$$[\hat{S}_j^+, \hat{S}_j^-] = 2\hat{S}_j^z.$$

In order to establish one to one correspondance between the space of physical states $|u\rangle$ and the space of ideal states $|u)$, we have still to add the condition

$$0 \leqslant u_j \leqslant 2S. \tag{3.18}$$

The Hamiltonian (2.10) in terms of the ideal operators η_j^*, η_j is now

$$\hat{\boldsymbol{S}}_j \cdot \hat{\boldsymbol{S}}_k = \tfrac{1}{2}(\hat{S}_j^-\hat{S}_k^+ + \hat{S}_j^+\hat{S}_k^-) + \hat{S}_j^z\hat{S}_k^z, \tag{3.19}$$

$$\hat{\mathcal{H}} = E_0 + L\sum_j \eta_j^*\eta_j + \tfrac{1}{2}S\sum_{j,k}\mathcal{J}(|\boldsymbol{j}-\boldsymbol{k}|)(\eta_j^*-\eta_k^*)(\eta_j-\eta_k) + \\ + \tfrac{1}{4}\sum_{j,k}\mathcal{J}(|\boldsymbol{j}-\boldsymbol{k}|)\eta_j^*\eta_k^*(\eta_j-\eta_k)^2, \tag{3.20}$$

$$E_0 = -LSN + \tfrac{1}{2}\mathcal{J}(0)NS(S+1) - \tfrac{1}{2}S^2\sum_{j,k}\mathcal{J}(|\boldsymbol{j}-\boldsymbol{k}|). \tag{3.21}$$

Taking into account the nearest neighbours only, we have by Eqs. (2.13) and (2.14)

$$\hat{\mathcal{H}} = E_0 + L\sum_j \eta_j^*\eta_j + \tfrac{1}{2}\mathcal{J}S\sum_{j,\delta}(\eta_j^*-\eta_{j+\delta}^*)(\eta_j-\eta_{j+\delta}) + \tfrac{1}{4}\mathcal{J}\sum_{j,\delta}\eta_j^*\eta_{j+\delta}^*(\eta_j-\eta_{j+\delta})^2. \tag{3.22}$$

$$E_0 = -LSN - \tfrac{1}{2}\mathcal{J}NS^2\gamma_0, \tag{3.23}$$

as

$$\mathcal{J}(0) = N^{-1}\sum_{\lambda}\mathcal{J}_\lambda = \mathcal{J}N^{-1}\sum_{\lambda}\gamma_\lambda = \mathcal{J}N^{-1}\sum_{\delta}\sum_{\lambda}e^{i\vec{\lambda}\cdot\vec{\delta}} = \mathcal{J}\sum_{\delta}\delta(\vec{\delta}) = 0,$$

where γ_0 is the number of nearest neighbours.

Obviously, we might also consider more highly complicated cases, *e.g.* including the exchange interactions between the nearest, next nearest, third, fourth and further neigbours, by putting

$$\mathcal{J}(|\boldsymbol{j}-\boldsymbol{k}|) = \mathcal{J}_1\delta(\boldsymbol{k}-\boldsymbol{j}-\vec{\delta}_1) + \mathcal{J}_2\delta(\boldsymbol{k}-\boldsymbol{j}-\vec{\delta}_2) + \mathcal{J}_3\delta[(\boldsymbol{k}-\boldsymbol{j}-\vec{\delta}_3) + \ldots, \tag{3.25}$$

$\vec{\delta}_i$ are the vectors from a given lattice point reaching to its nearest, next nearest *etc.* neighbours. $\mathcal{J}_i$, $i = 2, 3, \ldots$ can be treated as variational parameters; they can be deduced from the minimum condition for free energy.

We now introduce the Fourier transforms (ideal spin waves) of the ideal spin operators

$$\alpha_\lambda = N^{-\frac{1}{2}} \sum_j e^{-i\vec{\lambda}\cdot\vec{j}} \eta_j, \tag{3.25}$$

$$\alpha_\lambda^* = N^{-\frac{1}{2}} \sum_j e^{i\vec{\lambda}\cdot\vec{j}} \eta_j^*, \tag{3.26}$$

with the commutation rules

$$[\alpha_\lambda, \alpha_\mu] = [\alpha_\lambda^*, \alpha_\mu^*] = 0, \qquad [\alpha_\lambda, \alpha_\mu^*] = \delta_{\lambda,\mu}. \tag{3.27}$$

The Hamiltonian (3.20) transforms to the form

$$\hat{\mathcal{H}} = E_0 + \sum_\lambda (L + \varepsilon_\lambda)\alpha_\lambda^* \alpha_\lambda - \tfrac{1}{4}\mathcal{J}N^{-1} \sum_{\lambda\varrho\sigma} \Gamma^\lambda_{\varrho,\sigma} \alpha^*_{\sigma+\lambda}\alpha^*_{\varrho-\lambda}\alpha_\varrho\alpha_\sigma, \tag{3.28}$$

$$E_0 = -LSN + \tfrac{1}{2}S(S+1)\sum_\lambda \mathcal{J}_\lambda - \tfrac{1}{2}\mathcal{J}_0 S^2 N, \tag{3.29}$$

$$\Gamma^\lambda_{\varrho,\sigma} = \mathcal{J}^{-1}(\mathcal{J}_\lambda - \mathcal{J}_{\lambda-\varrho} - \mathcal{J}_{\lambda+\sigma} + \mathcal{J}_{\lambda+\sigma-\varrho}), \tag{3.30}$$

$$\varepsilon_\lambda = S(\mathcal{J}_0 - \mathcal{J}_\lambda). \tag{3.31}$$

The non-diagonal part of the Hamiltonian (3.28) describes the dynamical interaction between the spin waves. $\mathcal{J}\Gamma^\lambda_{\varrho,\sigma}$ are the coupling functions of spin wave interaction.

4. *The statistical function*

In full accordance with Eqs. (3.17a—c) and (3.18) we define the statistical function as

$$Z = \mathrm{Sp}\,\exp(-\beta\hat{\mathcal{H}}) \equiv \sum_u E_u(u|\exp(-\beta\hat{\mathcal{H}})|u), \tag{4.1}$$

wherein

$$\beta = \frac{1}{kT},\ E_u = \prod_j E_{u_j},\ E_{u_j} = \begin{cases} 1, & 0 \leqslant u_j \leqslant 2S, \\ 0, & u_j > 2S. \end{cases} \tag{4.2}$$

In formula (4.1) summation over u ranges over all numbers u_j of the state vector $|u)$.

Let us now introduce the set of orthonormal ideal spin wave state vectors

$$|a) = \prod_\lambda [(a_\lambda!)^{-\frac{1}{2}}(\alpha_\lambda^*)^{a_\lambda}]|0); \tag{4.3}$$

a_λ is a positive integer (zero included). The product $\prod_\lambda$ runs over the entire reciprocal lattice.

By Eq. (4.3), we have

$$Z = \sum_u E_u \sum_{a,b} (u|a)(a|e^{-\beta\hat{\mathcal{H}}}|b)(b|u). \tag{4.4}$$

Non-vanishing matrix elements in the above expression occur for

$$\sum_j u_j = \sum_\lambda a_\lambda = \sum_\lambda b_\lambda = q, \qquad q = 0, 1, 2, \ldots, 2SN. \tag{4.5}$$

We split the Hamiltonian (3.28) into three parts,

$$\hat{\mathcal{H}} = E_0 + \hat{\mathcal{H}}_0 + \hat{\mathcal{H}}_I, \tag{4.6a}$$

$$\hat{\mathcal{H}}_0 = \sum_{\lambda} (L + \varepsilon_\lambda) \alpha_\lambda^* \alpha_\lambda, \tag{4.6b}$$

$$\hat{\mathcal{H}}_I = -\tfrac{1}{4} \mathcal{J} N^{-1} \sum_{\lambda\varrho\sigma} \Gamma^{\lambda}_{\varrho,\sigma} \alpha^*_{\sigma+\lambda} \alpha^*_{\varrho-\lambda} \alpha_\varrho \alpha_\sigma. \tag{4.6c}$$

With respect to Eqs. (4.6b, c), we have

$$e^{-\beta(\hat{\mathcal{H}}_0 + \hat{\mathcal{H}}_I)} = e^{-\beta \hat{\mathcal{H}}_0} \hat{S}(\beta), \qquad \hat{S}(\beta) = e^{\beta \hat{\mathcal{H}}_0} \cdot e^{-\beta(\hat{\mathcal{H}}_0 + \hat{\mathcal{H}}_I)}. \tag{4.7}$$

The operator $\hat{S}(\beta)$ is given by, (Matsubara 1955),

$$\hat{S}(\beta) = \sum_{n=0}^{+\infty} \frac{(-1)^n}{n!} \int_0^\beta d\tau_1 \dots \int_0^\beta d\tau_n \hat{P} \left[\hat{\mathcal{H}}_I(\tau_1) \dots \hat{\mathcal{H}}_I(\tau_n) \right], \tag{4.8}$$

wherein the dynamical operator

$$\hat{\mathcal{H}}_I(\tau) = e^{\tau \hat{\mathcal{H}}_0} \hat{\mathcal{H}}_I e^{-\tau \hat{\mathcal{H}}_0} \tag{4.9}$$

is written in Matsubara's representation, and $\hat{P}$ is Dyson's ordering symbol

$$\hat{P}[\hat{\mathcal{H}}_I(\tau_1)\hat{\mathcal{H}}_I(\tau_2)\dots\hat{\mathcal{H}}_I(\tau_n)] = \hat{\mathcal{H}}_I(\tau_{i_1})\hat{\mathcal{H}}_I(\tau_{i_2})\dots\hat{\mathcal{H}}_I(\tau_{i_n}),$$

$$\tau_{i_1} \geqslant \tau_{i_2} \geqslant \dots \geqslant \tau_{i_n}. \tag{4.10}$$

The operator $\hat{P}$ may be replaced by Wicks's ordering symbol $\hat{T}$, since both are identical for the boson field.

The statistical function (4.4) is now

$$Z = e^{-\beta E_0} \sum_u E_u \sum_{a,b} (u|a)(a|e^{-\beta \hat{\mathcal{H}}_0} \hat{S}(\beta)|b)(b|u). \tag{4.11}$$

The state vector $(a|$ may be written in Matsubara's representation

$$U_{ab} = (a(\beta)|\hat{S}(\beta)|b), \tag{4.12}$$

wherein

$$(a(\beta)| = (0| \prod_\lambda [\alpha_\lambda^{a_\lambda}(\beta)(\alpha_\lambda!)^{-1/2}], \tag{4.13a}$$

$$|b) = \prod_\lambda [(b_\lambda!)^{-1/2} (\alpha_\lambda^*)^{b_\lambda}]|0) \tag{4.13b}$$

and

$$\alpha_\lambda(\tau) = e^{\tau \hat{\mathcal{H}}_0} \alpha_\lambda e^{-\tau \hat{\mathcal{H}}_0} = e^{-\tau(L+\varepsilon_\lambda)} \alpha_\lambda, \tag{4.13c}$$

$$\alpha_\lambda^*(\tau) = e^{\tau \hat{\mathcal{H}}_0} \alpha_\lambda^* e^{-\tau \hat{\mathcal{H}}_0} = e^{\tau(L+\varepsilon_\lambda)} \alpha_\lambda^*. \tag{4.13d}$$

We can now apply Wick's theorem to the expression $\alpha_\lambda^*(\tau_1)\alpha_\sigma(\tau_2)$. We have

$$\hat{T}[\alpha_\lambda^*(\tau_1)\alpha_\sigma(\tau_2)] = \hat{N}[\alpha_\lambda^*(\tau_1)\alpha_\sigma(\tau_2)] + \underline{\alpha_\lambda^*(\tau_1)\alpha_\sigma(\tau_2)}. \tag{4.14}$$

We shall term the last term in eq. (4.14) „τ-contraction". $\hat{N}$ is the symbol of the normal product. The arrangement of operators in the $\hat{N}$-product is the following: all annihilation operators stand to the right of the creation operators, *i.e.*

$$\hat{N}[(\alpha_\lambda^*(\tau_1)\,\alpha_\sigma(\tau_2)] = \alpha_\lambda^*(\tau_1)\,\alpha_\sigma(\tau_2). \tag{4.15}$$

The $\hat{T}$-product has the form

$$\hat{T}[\alpha_\lambda^*(\tau_1)\alpha_\sigma(\tau_2)] = \begin{cases} \alpha_\lambda^*(\tau_1)\,\alpha_\sigma(\tau_2), & \tau_1 > \tau_2, \\ \alpha_\sigma(\tau_2)\,\alpha_\lambda^*(\tau_1)], & \tau_1 < \tau_2. \end{cases} \tag{4.16}$$

whence

$$\alpha_\lambda^*(\tau_1)\alpha_\sigma(\tau_2) = \begin{cases} 0, & \tau_1 > \tau_2, \\ [\alpha_\sigma(\tau_2), \alpha_\lambda^*(\tau_1)] & \tau_1 < \tau_2. \end{cases}$$

Since, according to Eqs, (4.13c) and (4.13d), we have

$$[\alpha_\sigma(\tau_2),\, \alpha_\lambda^*(\tau_1)] = e^{(L+\varepsilon_\lambda)\tau_1} \cdot e^{-(L+\varepsilon_\sigma)\tau_2}[\alpha_\sigma,\, \delta_\lambda^*] = \delta_{\lambda,\sigma}\, e^{(L+\varepsilon_\lambda)(\tau_1-\tau_2)}, \tag{4.17}$$

the τ-contraction now becomes

$$\underline{\alpha_\lambda^*(\tau_1)\,\alpha_\sigma(\tau_2)} = \begin{cases} 0, & \tau_1 > \tau_2, \\ \delta_{\lambda,\sigma}\, e^{(L+\varepsilon_\lambda)(\tau_1-\tau_2)}, & \tau_1 < \tau_2, \end{cases} \tag{4.18}$$

or

$$\underline{\alpha_\lambda^*(\tau_1)\,\alpha_\sigma(\tau_2)} = \delta_{\lambda,\sigma}\,\theta(\tau_2 - \tau_1) e^{(L+\varepsilon_\lambda)(\tau_1-\tau_2)}, \tag{4.19}$$

wherein

$$\theta(\tau) = \begin{cases} 1, & \tau > 0, \\ 0, & \tau < 0, \end{cases} \tag{4.20}$$

$$\theta(\tau) = \frac{1}{2\pi i}\int d\alpha\, \frac{e^{i\alpha\cdot\tau}}{\alpha - i\varepsilon}, \quad 0 < \varepsilon \ll 1. \tag{4.21}$$

Quite similarly, we obtain

$$\underline{\alpha_\lambda(\tau_1)\,\alpha_\sigma^*(\tau_2)} = \delta_{\lambda,\sigma}\theta(\tau_1 - \tau_2)\, e^{-(L+\varepsilon_\lambda)(\tau_1-\tau_2)}. \tag{4.22}$$

We can now provide a graphical interpretation of the consecutive terms in the $\hat{S}(\beta)$ expansion. With respect to Eqs. (4.8) and (4.12), we have

$$U_{ab} = (a(\beta)|b) - \int_0^\beta d\tau (a(\beta)|\hat{\mathcal{H}}_{\mathrm{I}}(\tau)|b) + \frac{1}{2!}\int_0^\beta d\tau_1 \int_0^\beta d\tau_2\, (a(\beta)|\, \hat{T}[\hat{\mathcal{H}}_{\mathrm{I}}(\tau_1) \times$$

$$\times \hat{\mathcal{H}}_{\mathrm{I}}(\tau_2)]|b) - \frac{1}{3!}\int_0^\beta d\tau_1 \int_0^\beta d\tau_2 \int_0^\beta d\tau_3\, (a\,(\beta)|\hat{T}[\hat{\mathcal{H}}_{\mathrm{I}}(\tau_1)\hat{\mathcal{H}}_{\mathrm{I}}(\tau_2)\hat{\mathcal{H}}_{\mathrm{I}}(\tau_3)]|b) + \ldots \tag{4.23}$$

The first term in the foregoing series represents free motion of the $q = \sum_\lambda a_\lambda$ spin waves,

$$(a\,(\beta)|\,b) = e^{-\beta\sum_\lambda (L+\varepsilon_\lambda)a_\lambda} \cdot \delta_{a,b}$$

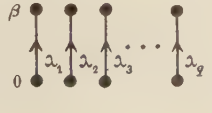

The second term in (4.23) can be written as follows:

$$[(a(\beta)|\hat{\mathscr{H}}_I(\tau)|b) = -\tfrac{1}{4}\mathscr{J}N^{-1}\sum_{\lambda\varrho\sigma}\Gamma^{\lambda}_{\varrho,\sigma}(0|\prod_{\varkappa}[(a_\varkappa!\ b_\varkappa!)^{-\frac{1}{2}}\alpha^{a_\varkappa}_{\varkappa}(\beta)\,\alpha^{*}_{\sigma+\lambda}(\tau)\times$$

$$\times\,\alpha^{*}_{\varrho-\lambda}(\tau)\,\alpha_{\varrho}(\tau)\,\alpha_{\sigma}(\tau)(\alpha^{*}_{\varkappa})^{b_\varkappa}]|0)\,. \tag{4.24}$$

The non-vanishing matrix elements satisfy the condition

$$\sum_{\lambda} a_\lambda = \sum_{\lambda} b_\lambda = q \geqslant 2 \tag{4.25}$$

and the Feynman diagram is of the form:

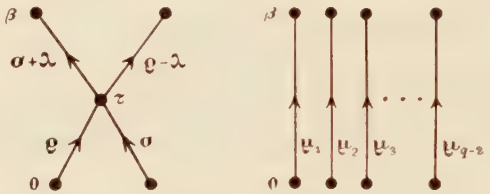

Fig. 1. Diagram illustrating the matrix element
$(a(\beta)|a^{*}_{\sigma+\lambda}(\tau)\,a^{*}_{\varrho-\lambda}(\tau)\,a_{\varrho}(\tau)\,a_{\sigma}(\tau)|b)$

We now apply the Wick theorem to the third term of (4.23), obtaining a single $\hat{N}$-product with all operators, eight terms with $\hat{N}$-products times one τ-contraction, and four terms with $\hat{N}$-products times two τ-contractions. The normal product with all operators yields two disconnected diagrams of the first order, as shown in Fig. 1, whereas *e.g.* a term with one τ-contraction yields the following graph:

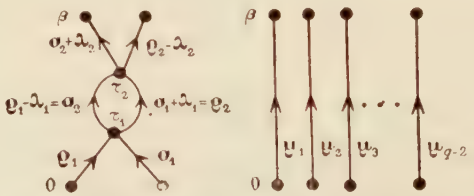

Fig. 2. Diagram illustrating the matrix element
$a^{*}_{\sigma_1+\lambda_1}(\tau_1)\,a_{\varrho_2}(\tau_2)\,(a(\beta)\,|a^{*}_{\varrho_1-\lambda_1}(\tau_1)\,a^{*}_{\sigma_2+\lambda_2}(\tau_2)\,a^{*}_{\varrho_2-\lambda_2}(\tau_2)\,a_{\varrho_1\tau_1}a_{\sigma_1}(\tau_1)\,a_{\sigma_2}(\tau_2)\,|b)$

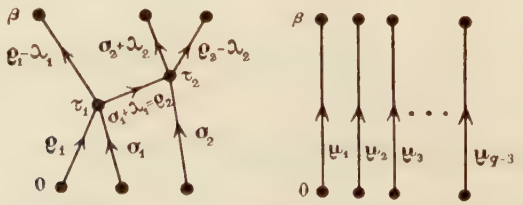

Fig. 3. Diagram illustrating the matrix element
$a^{*}_{\sigma_1+\lambda_1}(\tau_1)\,a_{\varrho_2}(\tau_2)\,a^{*}_{\varrho_1-\lambda_1}(\tau_1)\,a_{\sigma_2}(\tau_2)\,(a(\beta)|a^{*}_{\sigma_2+\lambda_2}(\tau_2)\,a^{*}_{\varrho_2-\lambda_2}(\tau_2)\,a_{\varrho_1}(\tau_1)\,a_{\sigma_1}(\tau_1)|b)$

The Feynman graph for two τ-contractions and the corresponding matrix element is represented in Fig. 3.

The technique of constructing an arbitrary diagram is presented in Dyson's paper (1956a).

REFERENCES

Dyson, F., *Phys. Rev.*, **102,** 1217 (1956a), *Ibid.* **102,** 1230 (1956b).
Matsubara, T., *Progr. theor. Phys.*, **14,** 351 (1955).
Morkowski, J., *Acta phys. Polon.*, **19,** 3 (1959).

SPIN WAVE THEORY FOR CUBIC FERROMAGNETICS II. NEW APPROACH

By Jan Szaniecki (Śledzik)

Institute of Physics of the Polish Academy of Sciences, Department of Ferromagnetics in Poznań.

(Received May 31, 1961)

A new spin wave approach to the theory of a cubic ferromagnetic is developed. The smallness of the spin wave kinematical interaction at low temperatures is taken into account, which enables us to compute the statistical function as the trace over the complete orthonormal set of ideal spin wave vectors. The Hamiltonian of the ferromagnetic is taken from Dyson's theory, but, owing to the new way of obtaining the statistical function and applying Matsubara's technique, the logarithm of the grand partition function is now virial expansion containing Bloch's term and the sum of connected ladder diagrams.

1. New definition of the statistical function

In the first part of the present paper we referred to Dyson's definition of the statistical unction for a ferromagnetic at low temperatures. In his second paper Dyson (1956b) estimated ne kinematical spin wave interaction to be proportional to $\exp(-aT_c/T)$, where $a(>0)$ a number of order unity, T — the absolute temperature, T_c — the Curie temperature. n this way, kinematical interaction obviously being a purely statistical effect is quite small t suitably low temperatures. This fact enables us to proceed to a new definition of the tatistical function which, following Bloch (1930), we define as

$$Z = Sp\ e^{-\beta\hat{\mathcal{H}}} \equiv \sum_{q=0}^{2SN} \sum_{a} \delta\left(\sum_{\lambda} a_\lambda - q\right)(a|e^{-\beta\hat{\mathcal{H}}}|a), \tag{1.1}$$

here, according to Eq. (I 3.28) (part I of the present paper will be henceforth referred o as I),

$$\hat{\mathcal{H}} = E_0 + \sum_{\lambda} (L + \varepsilon_\lambda)\alpha_\lambda^* \alpha_\lambda - \tfrac{1}{4}\mathcal{J}N^{-1} \sum_{\lambda\varrho\sigma} \Gamma^{\lambda}_{\varrho,\sigma} \alpha^*_{\sigma+\lambda}\alpha^*_{\varrho-\lambda}\alpha_\varrho\alpha_\sigma. \tag{1.2}$$

yson's definition of the statistical function

$$Z = \sum_{u} E_u (u|e^{-\beta\hat{\mathcal{H}}}|u) \tag{I4.1}$$

ıtroduces certain restrictions as to the localization of the ideal spin waves around a reciprocal ttice point. This becomes evident when we replace the oscillator operators η_j^*, η_j in $|u)$ Eq.

(I 4.1) by their Fourier transforms α_λ^*, α_λ by means of Eqs. (I 3.25—26). The sums of factors $\overrightarrow{\exp}\,(i\vec{\lambda}_i\vec{j}_s)$ appearing thereupon restrict the number of spin waves that can be localized in any $\vec{\lambda}$ point. Since, as stated above; the kinematical interaction is small, we may neglect these restrictions and assume $q \leqslant 2SN$ spin waves can propagate simultaneously through any $\vec{\lambda}$ point. It will be shown in Part III of the present paper that the new definition (1.1) of the statistical function leads to the same results as obtained by Dyson.

As in Part I, we expand the operator $\exp(-\beta\hat{\mathcal{H}})$,

$$\hat{\mathcal{H}} = E_0 + \hat{\mathcal{H}}_0 + \hat{\mathcal{H}}_I, \tag{1.3}$$

$$E_0 = -LSN + \tfrac{1}{2}S(S+1)\sum_\lambda \mathcal{J}_\lambda - \tfrac{1}{2}\mathcal{J}_0 S^2 N, \tag{1.4a}$$

$$\hat{\mathcal{H}}_0 = \sum_\lambda (L+\varepsilon_\lambda)\alpha_\lambda^*\alpha_\lambda, \tag{1.4b}$$

$$\hat{\mathcal{H}}_I = -\tfrac{1}{4}\mathcal{J}N^{-1}\sum_{\lambda\varrho\sigma} \Gamma^\lambda_{\varrho,\sigma}\alpha^*_{\sigma+\lambda}\alpha^*_{\varrho-\lambda}\alpha_\varrho\alpha_\sigma, \tag{1.4c}$$

in the perturbation series

$$e^{-\beta\hat{\mathcal{H}}} = e^{-\beta E_0}\cdot e^{-\beta\hat{\mathcal{H}}_0}\hat{S}(\beta),\quad \hat{S}(\beta) = \sum_{n=0}^{+\infty}\frac{(-1)^n}{n!}\int_0^\beta d\tau_1 \dots \int_0^\beta d\tau_n\, \hat{T}[\hat{\mathcal{H}}_I(\tau_1)\dots\hat{\mathcal{H}}_I(\tau_n)], \tag{1.5}$$

with

$$\hat{\mathcal{H}}(\tau) = e^{\tau\hat{\mathcal{H}}_0}\hat{\mathcal{H}}_I e^{-\tau\hat{\mathcal{H}}_0} \tag{1.6}$$

in Matsubara's representation.

Equation (1.1) now assumes the form

$$Z = e^{-\beta E_0}\sum_{q=0}^{2SN}\sum_a \delta\Big(\sum_\lambda a_\lambda - q\Big)(a|e^{-\beta\hat{\mathcal{H}}_0}\hat{S}(\beta)|a). \tag{1.7}$$

On expressing $\hat{S}(\beta)$ by its perturbation series and on retaining the first term only, we obtain Bloch's partition function

$$Z^{(0)} = e^{-\beta E_0}\sum_{q=0}^{2SN}\sum_a \delta\Big(\sum_\lambda a_\lambda - q\Big)(a|e^{-\beta\hat{\mathcal{H}}_0}|a). \tag{1.8}$$

We have further

$$(a|e^{-\beta\hat{\mathcal{H}}_0}| = (0|\prod_\lambda[\alpha_\lambda^{a_\lambda}e^{-\beta\hat{\mathcal{H}}_0}(a_\lambda!)^{-1/2}] = (0|\prod_\lambda[\alpha_\lambda^{a_\lambda}(\beta)(a_\lambda!)^{-1/2}] =$$

$$= \exp\Big[-\beta\sum_\lambda(L+\varepsilon_\lambda)a_\lambda\Big](0|\prod_\lambda[\alpha_a^{a_\lambda}(a_\lambda!)^{-1/2}] = \exp\Big[-\beta\sum_\lambda(L+\varepsilon_\lambda)a_\lambda\Big](a|. \tag{1.9a}$$

whence

$$Z^{(0)} = e^{-\beta E_0}\sum_{q=0}^{2SN}\sum_{a_{\lambda_1}=0}^{2SN}\dots\sum_{a_{\lambda_N}=0}^{2SN}\delta\Big(\sum_\lambda a_\lambda - q\Big)\prod_\lambda e^{-\beta(L+\varepsilon_\lambda)a_\lambda}. \tag{1.9b}$$

The difference between Eq. (1.9b) and the expression

$$Z^{(0)'} = e^{-\beta E_0} \sum_{a_{\lambda_1}=0}^{+\infty} \cdots \sum_{a_{\lambda_N}=0}^{+\infty} \prod_{\lambda} e^{-\beta(L+\varepsilon_\lambda)a_\lambda}. \tag{1.10}$$

is of the form

$$\begin{aligned} Z^{(0)'} - Z^{(0)} = e^{-\beta E_0} \sum_{q=2SN+1}^{+\infty} e^{-q\beta L} \{ \sum_{\lambda} e^{-q\beta\varepsilon_\lambda} + \sum_{\lambda_i<\lambda_j} [e^{-\beta((q-1)\varepsilon_{\lambda_i}+\varepsilon_{\lambda_j})} + \\ + e^{-\beta(\varepsilon_{\lambda_i}+(q-1)\varepsilon_{\lambda_j})} + e^{-\beta((q-2)\varepsilon_{\lambda_i}+2\varepsilon_{\lambda_j})} + e^{-\beta(2\varepsilon_{\lambda_i}+(q-2)\varepsilon_{\lambda_j})} + \\ + e^{-\beta((q-3)\varepsilon_{\lambda_i}+3\varepsilon_{\lambda_j})} + e^{-\beta(3\varepsilon_{\lambda_i}+(q-3)\varepsilon_{\lambda_j})} + \ldots] + \sum_{\lambda_i<\lambda_j<\lambda_k} [e^{-\beta((q-2)\varepsilon_{\lambda_i}+\varepsilon_{\lambda_j}+\varepsilon_{\lambda_k})} + \\ + e^{-\beta(\varepsilon_{\lambda_i}+(q-2)\varepsilon_{\lambda_j}+\varepsilon_{\lambda_k})} + e^{-\beta(\varepsilon_{\lambda_i}+\varepsilon_{\lambda_j}+(q-2)\varepsilon_{\lambda_k})} + e^{-\beta((q-3)\varepsilon_{\lambda_i}+2\varepsilon_{\lambda_j}+\varepsilon_{\lambda_k})} + \\ + e^{-\beta((q-3)\varepsilon_{\lambda_i}+\varepsilon_{\lambda_j}+2\varepsilon_{\lambda_k})} + e^{-\beta(2\varepsilon_{\lambda_i}+(q-3)\varepsilon_{\lambda_j}+\varepsilon_{\lambda_k})} + e^{-\beta(\varepsilon_{\lambda_i}+(q-3)\varepsilon_{\lambda_j}+2\varepsilon_{\lambda_k})} + \\ + e^{-\beta(2\varepsilon_{\lambda_i}+\varepsilon_{\lambda_j}+(q-3)\varepsilon_{\lambda_k})} + e^{-\beta(\varepsilon_{\lambda_i}+2\varepsilon_{\lambda_j}+(q-3)\varepsilon_{\lambda_k})} + \ldots] + \ldots \} \end{aligned} \tag{1.11}$$

Even at zero magnetic field strength, the condition $\beta \gg 1$ (low temperatures) and the presence of at least $(2SN+1)\varepsilon_{\lambda_1}$, $(\lambda_1 < \ldots < \lambda_N)$, terms in exponents guarantee that the difference is negligible.

We can now write

$$\frac{Z}{Z^{(0)}} = \langle \hat{S}(\beta) \rangle = \frac{\sum_a (a|e^{-\beta\hat{\mathcal{H}}_0}\hat{S}(\beta)|a)}{\sum_a (a|e^{-\beta\hat{\mathcal{H}}_0}|a)}, \tag{1.12}$$

$$Z^{(0)} = e^{-\beta E_0} \sum_a (a|e^{-\beta\hat{\mathcal{H}}_0}|a). \tag{1.13}$$

Summation over a ranges over all positive integers $a_\lambda = 0, 1, 2, \ldots, +\infty$.

2. *Matsubara's representation*

In order to compute the average $\langle \hat{S}(\beta) \rangle$, we introduce the formalism developed by Matsubara (1955). We have

$$\alpha_\lambda(\tau) = e^{\tau\hat{\mathcal{H}}_0}\alpha_\lambda e^{-\tau\hat{\mathcal{H}}_0} = \alpha_\lambda e^{-(L+\varepsilon_\lambda)\tau}, \tag{2.1a}$$

$$\alpha_\lambda^*(\tau) = e^{\tau\hat{\mathcal{H}}_0}\alpha_\lambda^* e^{-\tau\hat{\mathcal{H}}_0} = \alpha_\lambda^* e^{(L+\varepsilon_\lambda)\tau}. \tag{2.1b}$$

We now split the operators $\alpha_\lambda(\tau)$, $\alpha_\lambda^*(\tau)$ into positive and negative parts,

$$\alpha_\lambda(\tau) = \alpha_\lambda^{(+)}(\tau) + \alpha_\lambda^{(-)}(\tau), \qquad \alpha_\lambda^*(\tau) = \alpha_\lambda^{*(+)}(\tau) + \alpha_\lambda^{*(-)}(\tau), \tag{2.2}$$

$$\left.\begin{aligned} \alpha_\lambda^{(-)}(\tau) &= q_\lambda \alpha_\lambda e^{-(L+\varepsilon_\lambda)\tau}, & \alpha_\lambda^{*(-)}(\tau) &= \omega_\lambda \alpha_\lambda^* e^{(L+\varepsilon_\lambda)\tau}, \\ \alpha_\lambda^{(+)}(\tau) &= (1-q_\lambda)\alpha_\lambda e^{-(L+\varepsilon_\lambda)\tau}, & \alpha_\lambda^{*(+)}(\tau) &= (1-\omega_\lambda)\alpha_\lambda^* e^{(L+\varepsilon_\lambda)\tau}. \end{aligned}\right\} \tag{2.3}$$

The coefficients q_λ and ω_λ will be determined later on. As usual, we define the normal product

of a certain number of field operators as a product in which all negative operator parts stand to the right of the positive ones, *e.g.*

$$\hat{N}[\alpha_\lambda(\tau_1)\alpha_\sigma^*(\tau_2)] = \hat{N}\{[\alpha_\lambda^{(+)}(\tau_1) + \alpha_\lambda^{(-)}(\tau_1)][\alpha_\sigma^{*(+)}(\tau_2) + \alpha_\sigma^{*(-)}(\tau_2)]\} -$$
$$= \hat{N}[\alpha_\lambda^{(+)}(\tau_1)\alpha_\sigma^{*(+)}(\tau_2) + \alpha_\lambda^{(+)}(\tau_1)\alpha_\sigma^{*(-)}(\tau_2) + \alpha_\lambda^{(-)}(\tau_1)\alpha_\sigma^{*(+)}(\tau_2) + \alpha_\lambda^{(-)}(\tau_1)\alpha_\sigma^{*(-)}(\tau_2)] =$$
$$= \alpha_\lambda^{(+)}(\tau_1)\alpha_\sigma^{*(+)}(\tau_2) + \alpha_\lambda^{(+)}(\tau_1)\alpha_\sigma^{*(-)}(\tau_2) + \alpha_\sigma^{*(+)}(\tau_2)\alpha_\lambda^{(-)}(\tau_1) + \alpha_\lambda^{(-)}(\tau_1)\alpha_\sigma^{*(-)}(\tau_2) =$$
$$= \alpha_\lambda(\tau_1)\alpha_\sigma^*(\tau_2) + [\alpha_\lambda^{(-)}(\tau_1), \alpha_\sigma^{*(+)}(\tau_2)] = \alpha_\sigma^*(\tau_2)\alpha_\lambda(\tau_1) + [\alpha_\lambda(\tau_1), \alpha_\sigma^*(\tau_2)] +$$
$$+ [\alpha_\lambda^{(-)}(\tau_1), \alpha_\sigma^{*(+)}(\tau_2)]. \tag{2.4}$$

The $\hat{T}$-product of $\alpha_\lambda(\tau_1)\alpha_\sigma^*(\tau_2)$ is

$$\hat{T}[\alpha_\lambda(\tau_1)\alpha_\sigma^*(\tau_2)] = \begin{cases} \alpha_\lambda(\tau_1)\alpha_\sigma^*(\tau_2), & \tau_1 > \tau_2, \\ \alpha_\sigma^*(\tau_2)\alpha_\lambda(\tau_1), & \tau_1 < \tau_2. \end{cases} \tag{2.5}$$

The τ-contraction is now

$$\hat{T}[\alpha_\lambda(\tau_1)\alpha_\sigma^*(\tau_2)] = \hat{N}[\alpha_\lambda(\tau_1)\alpha_\sigma^*(\tau_2)] + \underbrace{\alpha_\lambda(\tau_1)\alpha_\sigma^*(\tau_2)}, \tag{2.6}$$

$$\underbrace{\alpha_\lambda(\tau_1)\alpha_\sigma^*(\tau_2)} = \begin{cases} [\alpha_\lambda^{(-)}(\tau_1), \alpha_\sigma^{*(+)}(\tau_2)], & \tau_1 > \tau_2, \\ [\alpha_\lambda^{(-)}(\tau_1), \alpha_\sigma^{*(+)}(\tau_2)] - [\alpha_\lambda(\tau_1), \alpha_\sigma^*(\tau_2)], & \tau_1 < \tau_2 \end{cases} \tag{2.7}$$

or, with respect to Eqs. (2.1a, b) and (2.3)

$$\underbrace{\alpha_\lambda(\tau_1)\alpha_\sigma^*(\tau_2)} = \begin{cases} \delta_{\lambda,\sigma} q_\lambda (1-\omega_\lambda)\, e^{-(L+\varepsilon_\lambda)(\tau_1-\tau_2)}, & \tau_1 > \tau_2 \\ \delta_{\lambda,\sigma}[q_\lambda(1-\omega_\lambda)-1]\, e^{-(L+\varepsilon_\lambda)(\tau_1-\tau_2)}. & \tau_1 < \tau_2. \end{cases} \tag{2.8}$$

We now require that the average of the $\hat{N}$-product shall vanish:

$$\langle \hat{N}[\alpha_\lambda(\tau_1)\alpha_\sigma^*(\tau_2)] \rangle = \frac{\sum_a (a|e^{-\beta\hat{\mathscr{H}}_0}\hat{N}[\alpha_\lambda(\tau_1)\alpha_\sigma^*(\tau_2)]|a)}{\sum_a (a|e^{-\beta\hat{\mathscr{H}}_0}|a)} = 0.$$

This yields

$$\langle \alpha_\lambda(\tau_1)\alpha_\sigma^*(\tau_2) - [\alpha_\lambda^{(-)}(\tau_1), \alpha_\sigma^{*(+)}(\tau_2)] \rangle = e^{-(L+\varepsilon_\lambda)\tau_1} \cdot e^{(L+\varepsilon_\sigma)\tau_2} \times$$
$$\times [\langle \alpha_\lambda \alpha_\sigma^* \rangle - \delta_{\lambda,\sigma} q_\lambda (1-\omega_\lambda)] = \delta_{\lambda,\sigma} e^{-(L+\varepsilon_\lambda)(\tau_1-\tau_2)} \times$$
$$\times [\langle \alpha_\lambda \alpha_\lambda^* \rangle - q_\lambda(1-\omega_\lambda)] = 0.$$
$$\langle \alpha_\lambda \alpha_\lambda^* \rangle = \langle \alpha_\lambda^* \alpha_\lambda \rangle + 1 = n_\lambda + 1 = q_\lambda(1-\omega_\lambda), \tag{2.9}$$
$$n_\lambda = [e^{\beta(L+\varepsilon_\lambda)} - 1]^{-1} \tag{2.10}$$

and

$$\underbrace{\alpha_\lambda(\tau_1)\alpha_\sigma^*(\tau_2)} = \delta_{\lambda,\sigma} e^{-(L+\varepsilon_\lambda)(\tau_1-\tau_2)}[\theta(\tau_1-\tau_2)(n_\lambda+1) + \theta(\tau_2-\tau_1)n_\lambda], \tag{2.11}$$

$$\theta(x) = \begin{cases} 1, & x > 0, \\ 0, & x < 0. \end{cases} \tag{2.12}$$

Similar computation yields

$$\underbrace{\alpha_\lambda^*(\tau_1)\alpha_\sigma(\tau_2)} = \delta_{\lambda,\sigma} e^{(L+\varepsilon_\lambda)(\tau_1-\tau_2)}[\theta(\tau_1-\tau_2)n_\lambda + \theta(\tau_2-\tau_1)(n_\lambda+1)] \tag{2.13}$$

and

$$-\omega_\lambda(1-q_\lambda)=n_\lambda. \tag{2.14}$$

By Eqs. (2.9) and (2.14), we have

$$q_\lambda=n_\lambda+1+\varepsilon[n_\lambda(n_\lambda+1)]^{1/2},\quad \omega_\lambda=-n_\lambda+\varepsilon[n_\lambda(n_\lambda+1)]^{1/2},\quad \varepsilon=\pm 1. \tag{2.15}$$

In the special case of coinciding variables τ, we obtain

$$\underline{\alpha_\lambda(\tau)\alpha^*_\sigma(\tau)}=\delta_{\lambda,\sigma}(n_\lambda+1), \tag{2.16a}$$

$$\underline{\alpha^*_\lambda(\tau)\alpha_\sigma(\tau)}=\delta_{\lambda,\sigma}n_\lambda. \tag{2.16b}$$

Direct computation also yields

$$\langle \hat{N}[\alpha^*_\lambda(\tau_1)\,\alpha^*_\sigma(\tau_2)\,\alpha_\varrho(\tau_3)\,\alpha_\mu(\tau_4)]\rangle=0 \tag{2.17}$$

and, quite generally,

$$\langle \hat{N}[\alpha^*_{\lambda_1}(\tau_1)\alpha^*_{\lambda_2}(\tau_2)\dots\alpha^*_{\lambda_n}(\tau_n)\,\alpha_{\sigma_1}(\tau_{n+1})\,\alpha_{\sigma_2}(\tau_{n+2})\dots\alpha_{\sigma_n}(\tau_{2n})]\rangle=0,$$
$$n=1,2,3,\dots,+\infty, \tag{2.18}$$

as was proved by Thouless (1957). Thus, the $\hat{T}$-product may be written directly as the sum of products of suitable number of τ-contractions, which, being c-numbers, can be put outside the symbol of averaging.

3. *Graphical interpretation*

By (1.12), we have

$$Z=Z^{(0)}\langle \hat{S}(\beta)\rangle=Z^{(0)}\sum_{n=0}^{+\infty}\frac{(-1)^n}{n!}\int_0^\beta d\tau_1\dots\int_0^\beta d\tau_n\langle \hat{T}[\hat{\mathcal{H}}_I(\tau_1)\dots\hat{\mathcal{H}}_I(\tau_n)]\rangle=$$

$$=Z^{(0)}\Big\{1-\int_0^\beta d\tau\langle \hat{T}[\hat{\mathcal{H}}_I(\tau)]\rangle+\frac{1}{2!}\int_0^\beta d\tau_1\int_0^\beta d\tau_2\langle \hat{T}[\hat{\mathcal{H}}_I(\tau_1)\hat{\mathcal{H}}_I(\tau_2)]\rangle-$$

$$-\frac{1}{3!}\int_0^\beta d\tau_1\int_0^\beta d\tau_2\int_0^\beta d\tau_3\langle \hat{T}[\hat{\mathcal{H}}_I(\tau_1)\hat{\mathcal{H}}_I(\tau_2)\hat{\mathcal{H}}_I(\tau_3)]\rangle+\dots\Big\}, \tag{3.1}$$

with

$$\hat{\mathcal{H}}_I(\tau)=-\tfrac{1}{4}\mathcal{J}N^{-1}\sum_{\lambda\varrho\sigma}\Gamma^\lambda_{\varrho,\sigma}\alpha^*_{\sigma+\lambda}(\tau)\,\alpha^*_{\varrho-\lambda}(\tau)\,\alpha_\varrho(\tau)\,\alpha_\sigma(\tau). \tag{3.2}$$

The first term in the expansion (3.1) now assumes the form

$$\Gamma_1=-\int_0^\beta d\tau\langle \hat{T}[\hat{\mathcal{H}}_I(\tau)]\rangle=\tfrac{1}{4}\mathcal{J}N^{-1}\sum_{\lambda\varrho\sigma}\Gamma^\lambda_{\varrho,\sigma}\int_0^\beta d\tau\langle \hat{T}[\alpha^*_{\sigma+\lambda}(\tau)\,\alpha^*_{\varrho-\lambda}(\tau)\,\alpha_\varrho(\tau)\,\alpha_\sigma(\tau)]\rangle=$$

$$=\tfrac{1}{4}\mathcal{J}N^{-1}\sum_{\lambda\varrho\sigma}\Gamma^\lambda_{\varrho,\sigma}\int_0^\beta d\tau\,[\langle \underline{\alpha^*_{\sigma+\lambda}(\tau)\,\alpha^*_{\varrho-\lambda}(\tau)\,\alpha_\varrho(\tau)\,\alpha_\sigma(\tau)}\rangle+\langle \underline{\alpha^*_{\sigma+\lambda}(\tau)\,\alpha^*_{\varrho-\lambda}(\tau)\,\alpha_\varrho(\tau)\,\alpha_\sigma(\tau)}\rangle]=$$

$$= \tfrac{1}{4}\mathcal{J}N^{-1}\sum_{\lambda\varrho\sigma}\Gamma^{\lambda}_{\varrho,\sigma}\int\limits_0^\beta d\tau\, e^{(\varepsilon_{\sigma+\lambda}+\varepsilon_{\varrho-\lambda}-\varepsilon_\varrho-\varepsilon_\sigma)\tau}(\delta_{\sigma+\lambda,\varrho}\delta_{\varrho-\lambda,\sigma}n_\varrho n_\sigma+\delta_{\sigma+\lambda,\sigma}\delta_{\varrho-\lambda,\varrho}n_\varrho n_\sigma) =$$

$$= \tfrac{1}{4}\mathcal{J}N^{-1}\beta\sum_{\lambda\varrho}\Gamma^{\lambda}_{\varrho,\varrho-\lambda}n_\varrho n_{\varrho-\lambda}+\tfrac{1}{4}\mathcal{J}N^{-1}\beta\sum_{\varrho,\sigma}\Gamma^{0}_{\varrho,\sigma}n_\varrho n_\sigma . \tag{3.3}$$

The Feynman graphs for both cases are illustrated below:

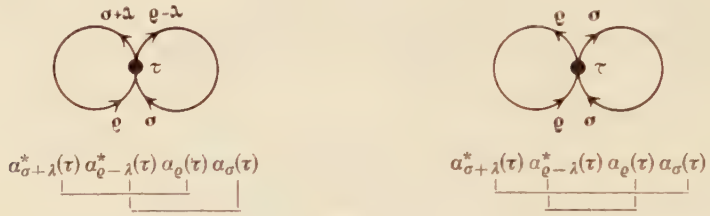

Fig. 1.

Let us now analyse the second order term in eq. (3.1):

$$\frac{1}{2!}\int\limits_0^\beta d\tau_1\int\limits_0^\beta d\tau_2\langle\hat{T}[\hat{\mathscr{H}}_\mathrm{I}(\tau_1)\hat{\mathscr{H}}_\mathrm{I}(\tau_2)]\rangle=\frac{1}{2!}\left(\frac{1}{4}\mathcal{J}N^{-1}\right)^2\sum_{\substack{\lambda\varrho\sigma\\ \varkappa\mu\nu}}\Gamma^{\lambda}_{\sigma,\varrho}\Gamma^{\varkappa}_{\mu,\nu}\times$$

$$\times\int\limits_0^\beta d\tau_1\int\limits_0^\beta d\tau_2\langle\hat{T}[\alpha^*_{\sigma+\lambda}(\tau_1)\,\alpha^*_{\varrho-\lambda}(\tau_1)\,\alpha_\varrho(\tau_1)\,\alpha_\sigma(\tau_1)\,\alpha^*_{\nu+\varkappa}(\tau_2)\,\alpha^*_{\mu-\varkappa}(\tau_2)\,\alpha_\mu(\tau_2)\,\alpha_\nu(\tau_2)]\rangle .$$

τ-contractions between the same τ-variables yields the disconnected diagram of the first order equal to $1/2!\,\Gamma_1^2$. We consider therefore the graph with contractions between different τ. We have

$$\Gamma_2=\frac{1}{2!}\left(\frac{1}{4}\mathcal{J}N^{-1}\right)^2\sum_{\substack{\lambda\varrho\sigma\\ \varkappa\mu\nu}}\Gamma^{\lambda}_{\varrho,\sigma}\Gamma^{\varkappa}_{\mu,\nu}\times$$

$$\times\int\limits_0^\beta d\tau_1\int\limits_0^\beta d\tau_2\,[\alpha^*_{\sigma+\lambda}(\tau_1)\,\alpha^*_{\varrho-\lambda}(\tau_1)\,\alpha_\varrho(\tau_1)\,\alpha_\sigma(\tau_1)\,\alpha^*_{\nu+\varkappa}(\tau_2)\,\alpha^*_{\mu-\varkappa}(\tau_2)\,\alpha_\mu(\tau_2)\,\alpha_\nu(\tau_2)+$$

$$+\alpha^*_{\sigma+\lambda}(\tau_1)\,\alpha^*_{\varrho-\lambda}(\tau_1)\,\alpha_\varrho(\tau_1)\,\alpha_\sigma(\tau_1)\,\alpha^*_{\nu+\varkappa}(\tau_2)\,\alpha^*_{\mu-\varkappa}(\tau_2)\,\alpha_\mu(\tau_2)\,\alpha_\nu(\tau_2)+$$

$$+\alpha^*_{\sigma+\lambda}(\tau_1)\,\alpha^*_{\varrho-\lambda}(\tau_1)\,\alpha_\varrho(\tau_1)\,\alpha_\sigma(\tau_1)\,\alpha^*_{\nu+\varkappa}(\tau_2)\,\alpha^*_{\mu-\varkappa}(\tau_2)\,\alpha_\mu(\tau_2)\,\alpha_\nu(\tau_2)+$$

$$+\alpha^*_{\sigma+\lambda}(\tau_1)\,\alpha^*_{\varrho-\lambda}(\tau_1)\,\alpha_\varrho(\tau_1)\,\alpha_\sigma(\tau_1)\,\alpha^*_{\nu+\varkappa}(\tau_2)\,\alpha^*_{\mu-\varkappa}(\tau_2)\,\alpha_\mu(\tau_2)\,\alpha_\nu(\tau_2)].$$

By Eqs. (2.11) and (2.13) we get

$$\Gamma_2 = \frac{1}{2!}\left(\frac{1}{4}\mathcal{J}N^{-1}\right)^2 \sum_{\substack{\lambda\varrho\sigma\\ \varkappa\mu\nu}} \Gamma^{\varkappa}_{\varrho,\sigma}\Gamma^{\varkappa}_{\mu,\nu}\int_0^\beta d\tau_1 \int_0^\beta d\tau_2\, e^{(\varepsilon_\mu+\varepsilon_\nu-\varepsilon_\varrho-\varepsilon_\sigma)(\tau_1-\tau_2}\times$$

$$\times[\theta(\tau_1-\tau_2)\,n_\mu n_\nu(n_\varrho+1)\,(n_\sigma+1)+\theta(\tau_2-\tau_1)\,(n_\mu+1)\,(n_\nu+1)\,n_\varrho n_\sigma]\,.\,[\delta(\vec{\sigma}+\vec{\lambda}-\vec{\nu})\delta(\vec{\varrho}-\vec{\lambda}-\vec{\mu})\times$$

$$\times\,\delta(\vec{\nu}+\vec{\varkappa}-\vec{\sigma})\,\delta(\vec{\mu}-\vec{\varkappa}-\vec{\varrho})+\delta(\vec{\sigma}+\vec{\lambda}-\vec{\mu})\,\delta(\vec{\varrho}-\vec{\lambda}-\vec{\nu})\,\delta(\vec{\nu}+\vec{\varkappa}-\vec{\sigma})\,\delta(\vec{\mu}-\vec{\varkappa}-\vec{\varrho})+\delta(\vec{\sigma}+\lambda-\vec{\nu})\times$$

$$\times\,\delta(\vec{\varrho}-\vec{\lambda}-\vec{\mu})\,\delta(\vec{\nu}+\vec{\varkappa}-\vec{\varrho})\,\delta(\vec{\mu}-\vec{\varkappa}-\vec{\sigma})+\delta(\vec{\sigma}+\vec{\lambda}-\vec{\mu})\,\delta(\vec{\varrho}-\vec{\lambda}-\vec{\nu})\,\delta(\vec{\nu}+\vec{\varkappa}-\vec{\varrho})\,\delta(\vec{\mu}-\vec{\varkappa}-\vec{\sigma})].$$

(3.4a)

Integration over τ_1 and τ_2 yields

$$\int_0^\beta d\tau_1\int_0^\beta d\tau_2\, e^{(\varepsilon_\mu+\varepsilon_\nu-\varepsilon_\varrho-\xi_\sigma)(\tau_1-\tau_2)}\,[\theta(\tau_1-\tau_2)\,n_\mu n_\nu(n_\varrho+1)\,(n_\sigma+1)+\theta(\tau_2-\tau_1)\,(n_\mu+1)\,(n_\nu+1)\times$$

$$\times\, n_\varrho n_\sigma] = \int_0^\beta d\tau_1\, e^{\alpha\tau_1}\int_0^{\tau_1} d\tau_2\, e^{-\alpha\tau_2}\, n_\mu n_\nu(n_\varrho+1)\,(n_\sigma+1)+\int_0^\beta d\tau_2\, e^{-\alpha\tau_2}\int_0^{\tau_2} d\tau_1\, e^{\alpha\tau_1}\times$$

$$\times\,(n_\mu+1)\,(n_\nu+1)\,n_\varrho n_\sigma = \frac{\beta}{\alpha}\,[(n_\mu+1)\,(n_\nu+1)\,n_\varrho n_\sigma - n_\mu n_\nu(n_\varrho+1)\,(n_\sigma+1)]+\frac{1}{\alpha^2}\,[(e^{\alpha\beta}-1)\times$$

$$\times\, n_\mu n_\nu(n_\varrho+1)\,(n_\nu+1)+(e^{-\alpha\beta}-1)\,(n_\mu+1)\,(n_\nu+1)\,n_\varrho n_\sigma], \qquad \alpha=\varepsilon_\mu+\varepsilon_\nu-\varepsilon_\varrho-\varepsilon_\sigma. \tag{3.4b}$$

Albeit, from Eq. (2.9) we know that

$$n_\lambda = [e^{\beta(L+\varepsilon_\lambda)}-1]^{-1},\ e^{\beta\varepsilon_\lambda} = e^{-\beta L}\,\frac{n_\lambda+1}{n_\lambda},\ e^{\beta\alpha} = \frac{(n_\mu+1)\,(n_\nu+1)\,n_\varrho n_\sigma}{n_\mu n_\nu(n_\varrho+1)\,(n_\sigma+1)},$$

whence

$$(e^{\alpha\beta}-1)\,n_\mu n_\nu(n_\varrho+1)\,(n_\sigma+1)+(e^{-\alpha\beta}-1)\,(n_\mu+1\,(n_\nu+1)\,n_\varrho n_\sigma = (n_\mu+1)(n_\nu+1)\,n_\varrho n_\sigma -$$

$$-\,n_\mu n_\nu(n_\varrho+1)\,(n_\sigma+1)+n_\mu n_\nu(n_\varrho+1)\,(n_\sigma+1)-(n_\mu+1)\,(n_\nu+1)\,n_\varrho n_\sigma = 0. \tag{3.4c}$$

Making use of the Eqs. (3.4a, b, c), doing some interchangements with vector indexes $\vec{\mu}, \vec{\nu}$ and taking advantage of the symmetry property $\Gamma^{\lambda}_{\varrho,\sigma} = \Gamma^{-\lambda}_{\sigma,\varrho}$, $\Gamma^{\lambda}_{\varrho,\sigma} = \Gamma^{\lambda+\sigma-\varrho}_{\sigma,\varrho}$, we get finally,

$$\Gamma_2 = \frac{1}{8}\,(\mathcal{J}N^{-1})^2\,\beta\sum_{\lambda\mu\nu}\Gamma^{\lambda}_{\nu+\lambda,\,\mu-\lambda}\,\Gamma^{\lambda}_{\mu,\nu}\,\frac{1}{\varepsilon_\mu+\varepsilon_\nu-\varepsilon_{\nu+\lambda}-\varepsilon_{\mu-\lambda}}\,[(n_\mu+1)\,(n_\nu+1)\times$$

$$\times\, n_{\nu+\lambda}\,n_{\mu-\lambda}-n_\mu n_\nu\,(n_{\nu+\lambda}+1)\,(n_{\mu-\lambda}+1)]. \tag{3.5}$$

One part of the ladder diagram of Eq. (3.4a) has the graphical shape represented below:

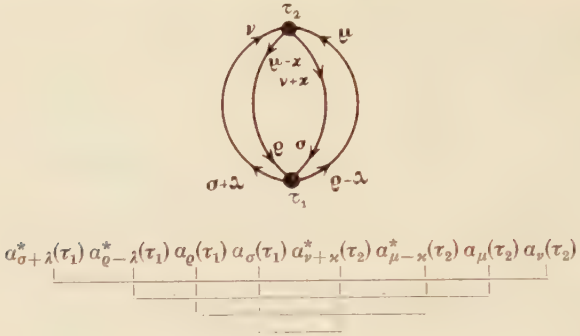

Fig. 2.

One part of the connected third order diagram is exemplified as follows:

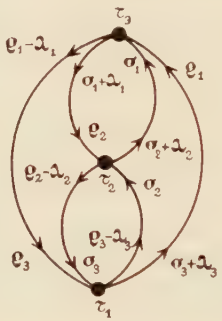

$$a^*_{\sigma_1+\lambda_1}(\tau_1)\, a^*_{\varrho_1-\lambda_1}(\tau_1)\, a_{\varrho_1}(\tau_1)\, a_{\sigma_1}(\tau_1)\, a^*_{\sigma_2}\ \lambda_2(\tau_2)\, a^*_{\varrho_2}\ \lambda_2(\tau_2)\, a_{\varrho_2}(\tau_2)\, a_{\sigma_2}(\tau_2)\, a^*_{\sigma_3}\ \lambda_3(\tau_3)\, a^*_{\varrho_3}\ \lambda_3(\tau_3)\, a^*_{\varrho_3}(\tau_3)\, a_{\sigma_3}(\tau_3)$$

Fig. 3*

We denote the connected diagram, which in general consists of several parts, by Γ_i, wherin i points to the order of the diagram. We include in Γ_i only those part of the connected diagram that are distinct as to their physical meaning; thus we obtain

$$\langle \hat{S}(\beta) \rangle = e^{\Gamma_1+\Gamma_2+\Gamma_3+\cdots} = \exp\Big(\sum_{i=1}^{+\infty} \Gamma_i\Big). \tag{3.6}$$

The grand partition function is now

$$Z = Z^{(0)} \exp\Big(\sum_{i=1}^{+\infty} \Gamma_i\Big). \tag{3.7}$$

* In Fig. 3 τ_1 should be in place of τ_3 and inversely.

By Eqs. (I 4.3), (1.4b) and (1.13), we have

$$Z^{(0)} = e^{-\beta E_0} \sum_a (a|e^{-\beta \hat{\mathscr{H}}_0}|a) = e^{-\beta E_0} \prod_\lambda \sum_{a_\lambda=0}^{+\infty} (a_\lambda!)^{-1} (0| \prod_\mu [\alpha_\mu^{a_\mu} \times$$

$$\times e^{-\beta \hat{\mathscr{H}}_0} (\alpha_\mu^*)^{a_\mu}]|0) = e^{-\beta E_0} \prod_\lambda \sum_{a_\lambda=0}^{+\infty} (a_\lambda!)^{-1} (0| \prod_\mu [\alpha_\mu^{a_\mu}(\beta) (\alpha_\mu^*)^{a_\mu}]|0) =$$

$$= e^{-\beta E_0} \prod_\lambda \sum_{a_\lambda=0}^{+\infty} e^{-\beta(L+\varepsilon_\lambda) a_\lambda} = e^{-\beta E_0} \prod_\lambda [1 - e^{-\beta(L+\varepsilon_\lambda)}]^{-1}. \tag{3.8}$$

We used the well-known relations

$$\alpha_\lambda|0), \qquad (0|\alpha_\lambda^* = 0, \qquad (0|e^{\beta \hat{\mathscr{H}}_0} = (0|. \tag{3.9}$$

Thus, the function Z finally assumes the form

$$Z = e^{-\beta E_0} \prod_\lambda [1 - e^{-\beta(L+\varepsilon_\lambda)}]^{-1} \exp\left(\sum_{i=1}^{+\infty} \Gamma_i\right). \tag{3.10}$$

REFERENCES

Bloch, F., *Z. Phys.*, **61,** 206 (1930).
Dyson, F., *Phys. Rev.*, **102,** 1217 (1956a), *Ibid.* **102,** 1230 (1956b).
Keffer, F. and Loudon, R., *J. appl. Phys.*, **32,** Suppl. No 3, 2 (1961).
Matsubara, T., *Progr. theor. Phys.*, **14,** 351 (1955).
Oguchi, T., *Phys. Rev.*, **117,** 117 (1960).
Thouless, D. J., *Phys. Rev.*, **107,** 1162 (1957).

EFFECT OF pH ON THE FLUORESCENCE OF FLUORESCEIN SOLUTIONS

By M. Rozwadowski

Physics Department, N. Copernicus University, Toruń

(Received June 14, 1961)

The absorption and emission spectra, mean decay time, relative yield and anisotropy of fluorescence emission of a fluorescein solution of the constant concentration of 10^{-5} g/cm^3 were investigated as to their dependence on the pH of the medium. The absorption and emission spectra were found to vary according to the pH value. This effect of pH can be explained by the molecule in the excited state giving off a proton.

Introduction

Owing to its intense fluorescence in the visible region, fluorescein is one of the dyes whose photoluminescence has been most often investigated. However, the fact that different ions of the dye, presenting different optical properties, are present simultaneously in the solutions throughout a wide range of pH values has not been taken into account in all cases. This is of especial importance in the investigation of the photoluminescence as dependent on the dye concentration, the temperature and the solvent. As these parameters are changed, the relative concentrations of the different ionic forms of the dye molecule can vary. In strongly acid solutions, the green-blue fluorescence of fluorescein is ascribed to positive ions, whereas the green-yellow fluorescence exhibited in basic solutions is considered to be due to bi-negative ions (Batscha 1926, Levshin 1951, Pringsheim 1949, Förster 1951). In certain neutral solutions fluorescein fails to exhibit fluorescence (Howe 1916). Zanker and Peter (1958) carried out a systematic investigation of the effect of the hydrogen ion concentration on the absorption spectrum. In order to obtain solutions of different pH, they added water, ammonia, or sulfuric acid to solutions of fluorescein in dioxane. They considered the spectrum obtained from a solution in a mixture of dioxane and water to be due to univalent negative ions, that of a solution in dioxane and ammonia to bivalent negative ions, and that of a solution in dioxane and sulfuric acid to univalent positive ions. Fluorescein in pure dioxane possesses no absorption band in the visible range; this points to the presence of the colourless, neutral form in the solution (lacton form). Grigorian *et al.* (1960) obtained the emission spectra of similarly prepared solutions. By adding 0.1 *n* sulfuric acid to dioxane, they observed

the appearance of a maximum shifted towards longer waves with respect to the band corresponding to bivalent negative ions, whereas when 12 *n* nitric acid was added the maximum appeared on the short-wave side. The authors considered these differences to be due to the effect of sulfuric or nitric acid. Like Zanker and Peter, they correlated the different maxima in the emission spectrum to the respective ions of the dye.

As the solutions used by the foregoing authors in their investigations of the absorption and emission spectra were prepared in different conditions, the necessity was felt of a more detailed investigation of the effect of pH on the fluorescence of fluorescein by measuring the different parameters for one and the same solution.

Preparation of the solutions, and methods of measurement applied

Chromatographically pure fluorescein of the red variety was used. All solutions were prepared as follows: fluorescein was dissolved in twice distilled water with an admixture of ammonia (required for full dissolving of the dye); then in order to produce the required pH, NH_3 or H_2SO_4 or HNO_3 was added. Nitric and sulfuric acids were chosen as the ions SO_4^{--} and NO_3^- are very weak quenchers of fluorescence (Pringsheim 1949). The effect of reabsorption and secondary fluorescence did not exceed the accuracy of the measurements. For all solutions investigated, the dye concentration was 10^{-5} g cm^3. The solutions were stored in dark.

The pH values were measured with a battery pH-meter made by "Ridan", Warsaw. A glass electrode was used. The measurements accuracy was about 0.05 units of the pH scale. As the hydrogen ion concentration changes with storage (especially in weakly acid and weakly basic solutions), the pH values were checked before each measurement. Fig. 1 shows the absorption spectra of the same solution measured after different periods of storage.

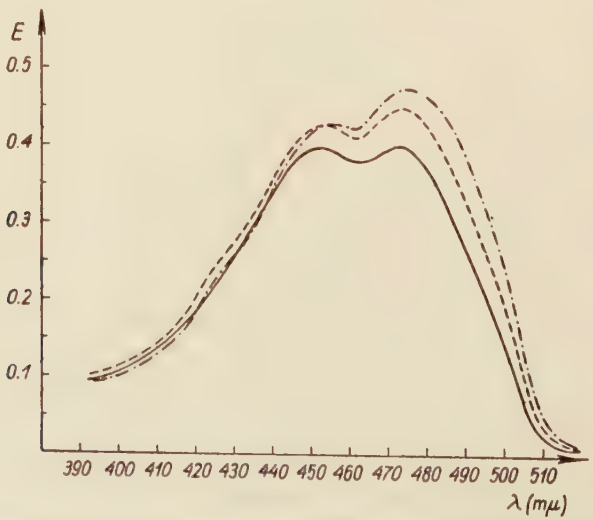

Fig. 1. Absorption spectra from one and the same solution, measured after different times of storage: ——— after 20 minutes (pH = 5.10) — — — — after an hour (pH = 5.42) —.—.— after 12 hours (pH = 5.77)

The absorption and emission spectra were measured by the photoelectric method, using a Zeiss mirror monochromator and *EMI* 6294 photomultiplier in connection with a galvanometer ("Skalengalvanometer" Zeiss-Jena). When the temperature dependence of the absorption was measured, the standard and the one investigated solutions were placed in a thermostatized vessel yielding stability up to 0.1° C.

The measurements of the mean decay times of luminescence were carried out by means of a fluorometer built together with R. Bauer (R. Bauer and M. Rozwadowski 1959). The accuracy of the measurements depended on the intensity of fluorescence and exceeded 10^{-10} sec. In this fluorometer, an ultrasonic birefringence modulator of higher luminosity and greater simplicity than the diffraction modulators was successfully applied for the first time.

The device for measuring the emission anisotropy[1] was also built in collaboration with R. Bauer (Bauer and Rozwadowski 1961). It makes possible the measurement of small values of the anisotropy of weak fluorescence. Values of the emission anisotropy of the order of 1% were determined to within 5% of the value measured.

The relative fluorescence yields were measured by the method proposed by D. Frąckowiak and T. Marszałek (1960, 1961).

The light source consisted throughout of a 12 V 50 W bulb supplied from a battery of accumulators.

Results of the measurements, and their interpretation

Fig. 2 shows the absorption and emission spectra of an aqueous solution of fluorescein in their dependence on the pH of the medium, at constant concentration of the dye. For the absorption spectra, the extinction coefficients are plotted on the axis of ordinates (all vessels had the same thickness), whereas the emission spectra are normalized to the same height of the maximum. No differences were found to occur in the position of the emission and absorption bands at the same pH values obtained by adding H_2SO_4 or HNO_3. However, the value of the coefficient of extinction, at identical values of pH, is

---

[1] Emission anisotropy (Jabłoński 1960) on excitation with polarized light is defined as follows:

$$r_p = \frac{I_{||} - I_{\perp}}{I_{||} + 2I_{\perp}} = \frac{1-\varrho}{1+2\varrho} = \frac{2P}{3-P},$$

wherein $I_{||}$ and $I_{\perp}$ are the intensity components parallel and perpendicular to the electric vector of the exciting light respectively, $\varrho = \frac{I_{\perp}}{I_{||}}$ is the degree of depolarization, and $P = \frac{I_{||} - I_{\perp}}{I_{||} + I_{\perp}}$ — the degree of polarization. On the other hand, on excitation with natural light, we have

$$r_n = \frac{I' - I''}{2I' + I''} = \frac{1-\varrho_n}{2+\varrho_n} = \frac{2P_n}{3+P_n},$$

wherein I' and I'' are the components perpendicular and parallel to the direction of the exciting light beam and ϱ_n and P_n are the rates of depolarization and polarization at excitation with natural light, respectively.

slightly higher in sulfuric than in nitric acid. The temperature effect of the absorption spectrum of fluorescein is more marked in HNO_3 than in H_2SO_4 (Fig. 5). It seems probable that Grigorian *et al.* (1960) would have obtained identical changes in the emission spectra

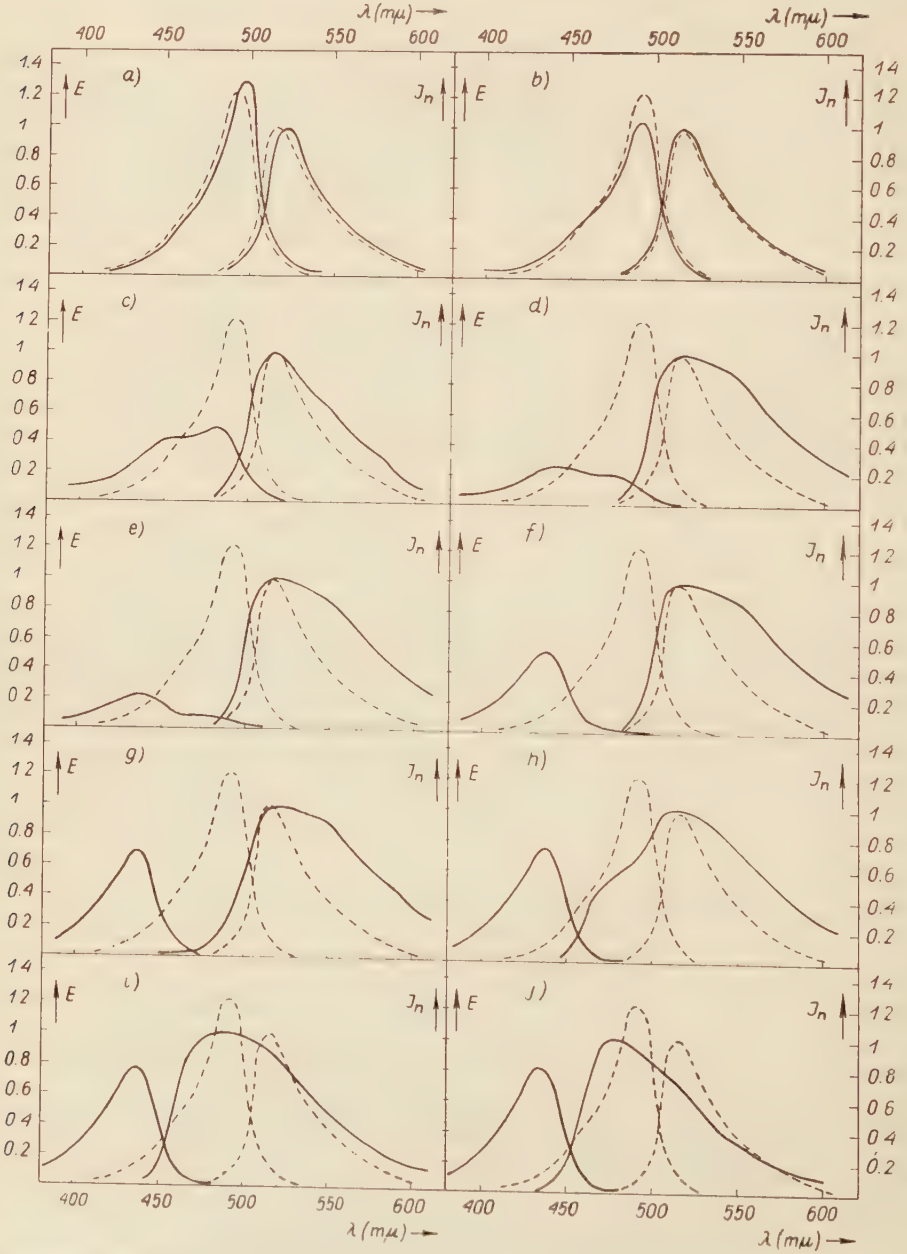

Fig. 2. Absorption and emission spectra of fluorescein solutions, for different values of pH (against the standard spectra at pH=10.5, shown by the dashed line): *a*) 12 n NH_3, *b*) pH=7.57 (NH_3), *c*) pH=6.3 (HNO_3), *d*) pH=1.15 (HNO_3), *e*) pH=3.21(HNO_3), *f*) pH=1.92(HNO_3), *g*) 0.1 n H_2SO_4, *h*) 2 n H_2SO_4, *i*) 5 n H_2SO_4, *j*) 10 n H_2SO_4

from sulfuric acid and nitric acid if they had applied higher H_2SO_4 concentrations. The appearance of new bands in the absorption or emission spectrum points to the existence of different kinds of ions at different values of pH. Zanker and Peter (1958) proposed seven distinct possible forms of the fluorescein molecule (Fig. 3).

It is a well-established fact that, in strongly basic solutions, bivalent negative ions are present (VI), whereas strongly acid solutions contain univalent positive ions (I). Hence the absorption band presenting $\lambda_{max} \approx 495$ mμ should be attributed to modification VI, and the

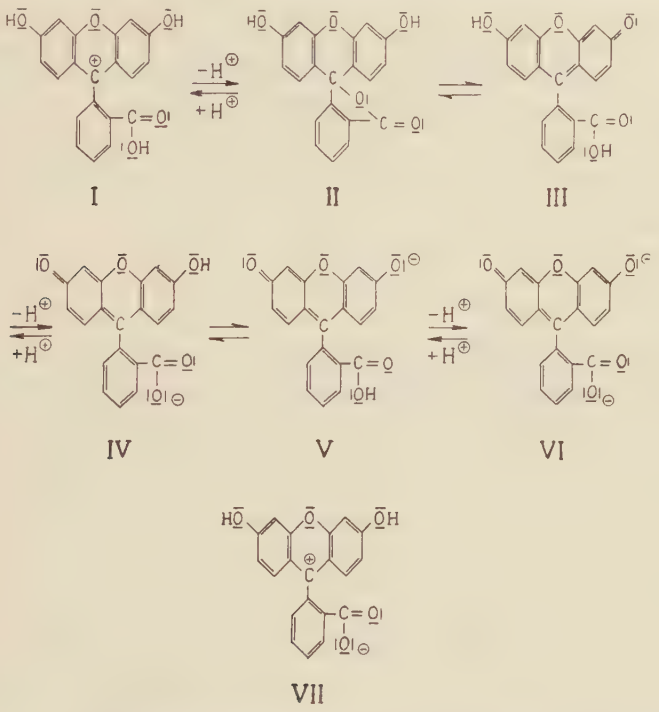

Fig. 3. Ionic modifications of fluorescein, according to Zanker. I — univalent positive ion, II and III — neutral molecule, IV and V — univalent negative ion, VI — bivalent negative ion, VII — modification being a transition between I and II

band with $\lambda_{max} \approx 434$ mμ — to modification I. Modification II is colourless because of the oxygen bridge at the lower benzene ring. Modification VII is a transition between I and II. As modifications VI and V present a similar structure of the upper part, their spectra are undistinguishable. The spectral position of the 0,0 transitions for modifications I and VI (or V) is in very good agreement with the results obtained by the FEMO method[2]. The band with $\lambda_{max} \approx 460$ mμ appearing in acid solutions (from pH=7 to pH=2) should be attributed to univalent negative ions (IV) or neutral molecules (III). Nevertheless, the fact that on adding acid to the solution an absorption band appears at first at the long-wave

[2] The calculations were carried out by Mr. A. Zieliński in the Chair of Theoretical Physics of the N. Copernicus University at Toruń.

side remains incomprehensible. It is only in very acid solutions that a band corresponding to cations appears to the short-wave side (the spectrum becomes similar to the one obtained in vitrous boric acid). Grigorian, Kantardjian and Chirkinian failed to notice that the changes in the emission spectrum do not occur simultaneously with the changes in the absorption spectrum. This results clearly from Fig. 2. The short-wave absorption maximum relating to cations appears in solutions of considerably lower acidity than for emission. Even in 10 n H_2SO_4 solutions emission still exhibits the maxima dominating in slightly acid and basic solutions, whereas already at pH=2 the long-wave absorption bands vanish completely.

Weber (1931) observed a similar effect in 1-naphtylamin-4-sulphonate, later and Förster (1950, 1950a), Weller (1952, 1954, 1955, 1956, 1957), Kokubun (1958) and Derkacheva (1960) for a number of other compounds. Förster, moreover, proposed an explanation of the effect. He assumed that the molecule in the excited state can give off or capture a proton (protolytic reactions) and emit radiation as a different ion or neutral molecule. Such a reaction is greatly facilitated if the H^+ is given off by O or N. Quite generally, the protolytic reaction can be written as follows:

$$(AH)^n + B^m \rightleftarrows A^{n-1} + (HB)^{m+1},$$

wherein n and m denote the number of positive elementary charges. The energy diagram of the reaction is shown on Fig. 4. ΔE is the excitation energy of a molecule in the non-dissociated form, $\Delta E'$ — that of the dissociated molecule, whereas E_D and E_{D^*} are the energy of dissociation in the ground state and excited state, respectively.

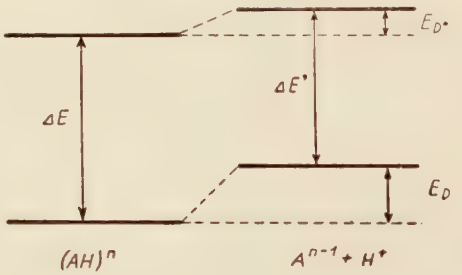

Fig. 4. Energy levels of molecule previous and subsequent to giving off a proton

According to whether $\Delta E'$ is smaller or larger than ΔE, the emission spectrum shifts towards longer or shorter wavelengths. However, the effect of protolytic reactions on the emission spectra becomes accessible to observation only if the mean lifetime (τ) of the molecule in the excited state is longer than the mean time required by the molecule in the excited state for giving off the proton. As proved by investigations on proton mobility (Ackermann 1961, Samoylov 1957), the mean time during which a proton remains with a water molecule in acid media is of the order of 10^{-13} sec, which is by over four orders shorter than τ. The decisive factor here is the value of the energy of dissociation in the excited state which, however, should not be estimated to be much larger in fluorescein than in water, since even in the ground state the cations are not stable, as proved by the effect of the

temperature on the absorption spectra (Fig. 5). The area under the absorption curve of the cations diminishes strongly with increase of temperature, whereas the absorption band of the bivalent negative ions only undergoes a displacement towards longer wavelengths owing to the change in population of the vibrational levels. The value of E_{D^*} decreases as the value of pH at which protolytic reactions cease to occur rises. From Fig. 2 anions are seen to exist even in 10 n H_2SO_4 in the excited state, which points to a considerable difference between E_{D^*} and E_D. Although it is not possible to determine the dissociation constants for the excited

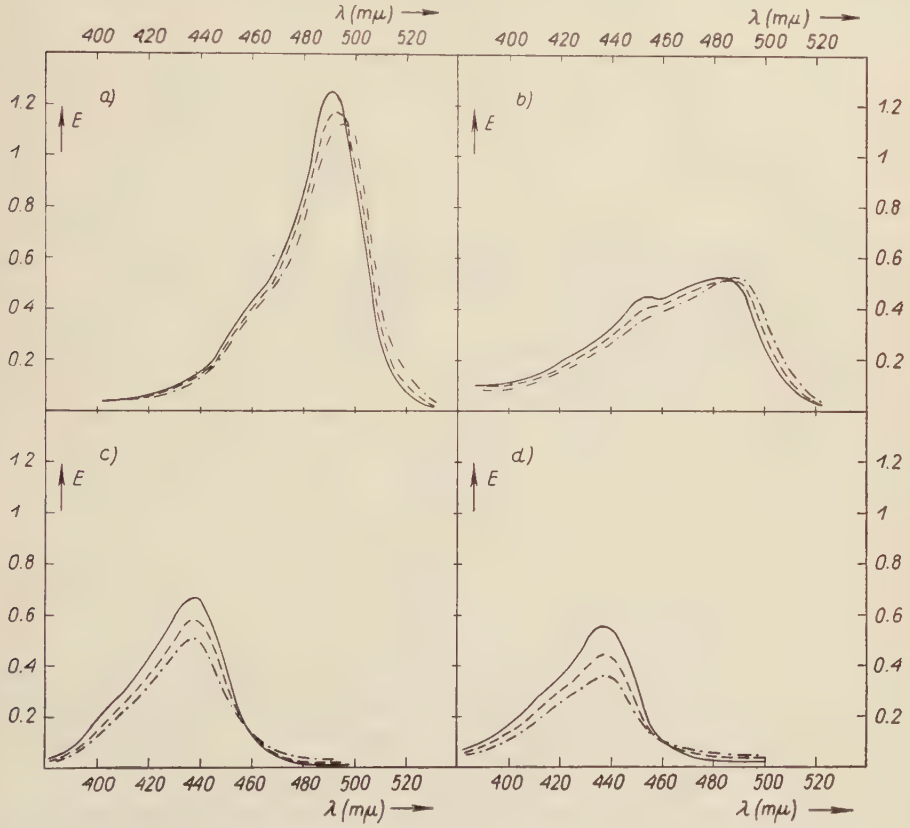

Fig. 5. Effect of the temperature on the absorption spectrum: ———— coefficients of extinction at $t = 15°C$ — — — — coefficients of extinction at $t = 40°C$ — . — . — . coefficients of extinction at 70°C *a*) pH = 11.85 (NH_3), *b*) pH = 6.48 (HNO_3), *c*) pH = 1.9 (H_2SO_4), *d*) pH = 1.88 (HNO_3) pH was measured at $t = 20°C$ in the solutions

state in fluorescein because of the lacton form occupying an intermediate position between the cations and anions, the occurrence of protolytic reactions would seem to be beyond doubt also in the case of fluorescein. Dissociation constants were found in simpler cases only (Weller 1952, 1957, Derkacheva 1960).

Figs. 6 and 7 and Tables I and II contain the values of τ and those of the relative quantum yields η_r *versus* the pH of the medium. In the Tables I and II, the values

TABLE I

NH_3		HNO_3		H_2SO_4		
pH	$\tau\times10^2$ sec	pH	$\tau\times10^2$ sec	pH	$c_{H_2SO_4}$	$\tau\times10^2$ sec
11.92	4.53	6.70	3.60	5.33		3.40
10.50	4.54	6.30	3.49	3.05		3.43
9.90	4.52	4.62	3.43	2.13		3.21
7.57	4.40	3.40	3.16	<1.00		3.10
		1.94	3.24		0.5 n	3.65
		<1.00	3.11		2 n	3.75
					5 n	3.92
					10 n	4.41

TABLE II

NH_3			HNO_3			H_2SO_4		
	η_r			η_r			η_r	
pH	λ_{excit}= =437 mμ	λ_{excit}= =490 mμ	pH	λ_{excit}= =437 mμ	λ_{excit}= =490 mμ	pH	λ_{excit}= =437 mμ	λ_{excit}= =490 mμ
11.85	1.01	0.99	7.30	0.93	1.00	6.12	0.42	0.78
11.23	1.01	0.99	6.74	0.68	0.96	6.02	0.40	0.74
10.15	1.02	1.00	5.56	0.39	0.59	5.70	0.37	0.59
8.50	0.98	1.00	4.95	0.32	0.35	3.05	0.29	0.30
			3.10	0.29	0.30	2.10	0.28	0.28
			1.90	0.28	—	1.95	0.28	—
			<1(0.7)	0.28	—	<1(0.8)	0.28	—

of τ and η_r have been placed in separate columns for the different admixtures added to the initial slightly basic solution ($7<$pH<8) of fluorescein. We assumed $\eta_r=1$ for the solution pH$=10$ and excitation in the absorption band of bivalent negative ions. The considerable differences in yield on excitation with wavelengths $\lambda=490$ mμ and $\lambda=437$ mμ in the case of solutions containing simultaneously anions and cations in the ground state is due to the fact that, on excitaion in the absorption band of the cations, fluorescence of the cations undergoing dissociation prevails, whereas at excitation in the absorption band of the anions, fluorescence of the anions not participating in protolytic reactions is prevalent. τ was measured at excitation through a *BG* 12 Schott filter, *i.e.* at simultaneous excitation of both bands. On the other hand, yield measurements were carried out on excitation through a monochromator. From either graph, the choice of the acid is seen to have little effect on τ and η_r. It is only at pH≈3 that τ differs somewhat for different acids. This is probably due to the effect of the difference in mobility of the hydrogen ions from HNO_3 and H_2SO_4. Unfortunately there was no possibility of measuring τ and η_r for each modification separately because of superposition of the emission bands, except for the case of bivalent negative ions. This is why the interpretation of the results becomes

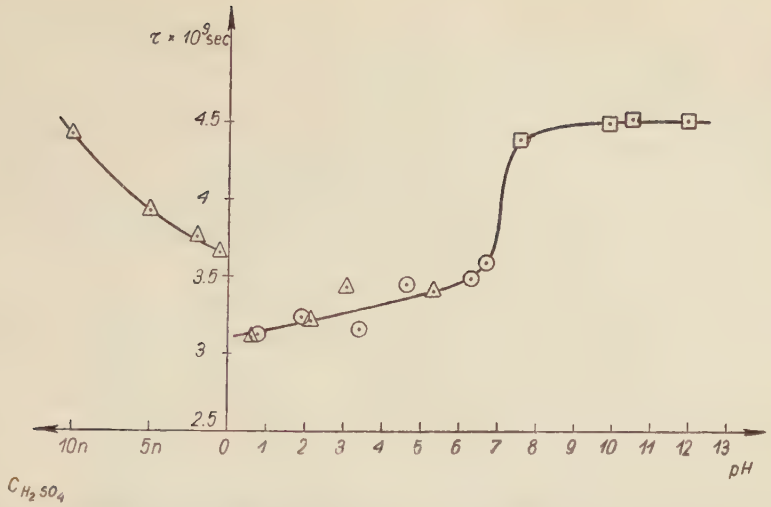

Fig. 6. Mean decay times of fluorescence *versus* pH of the solutions: ⊡ — in solutions containing NH_3 ⊙ — in solutions containing HNO_3, △ — in solutions containing H_2SO_4

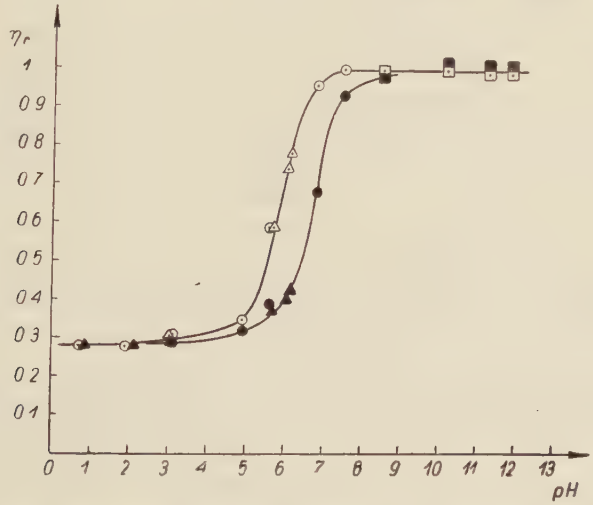

Fig. 7. Relative fluorescence yield *versus* pH of the solutions: ⊡ — solutions with NH_3, excitation with $\lambda = 490$ mμ, ■ — solutions with NH_3, excitation with $\lambda = 437$ mμ, ⊙ — solutions with HNO_3, excitation with $\lambda = 490$ mμ, ● — solutions with HNO_3, excitation with $\lambda = 437$ mμ, △ — solutions with H_2SO_4, excitation with $\lambda = 490$ mμ, ▲ — solutions with H_2SO_4, excitation with $\lambda = 437$ mμ

difficult. If, indeed, the different modifications of fluorescein possess intrinsically different τ and η [3], the experimental results are a superposition of two independent effects, namely, of the intrinsically different τ and η and of the effect of the protolytic reactions.

In the case of 3-aminopyren-5,8,10-trisulphonate, Hanle and Scharmann (1952) found that when the molecule gives off a proton no change intrinsic in τ and η occurs. Hence, on the

[3] η denotes the absolute quantum yield, and η_r — the relative quantum yield.

assumption of equal τ and η for all modifications of the fluorescein ion also, the protolytic reactions alone suffice for explaining the observed changes in τ and η_τ. Changes of τ and η_τ set in simultaneously when short-wave bands corresponding to positive and univalent negative ions appear in the absorption spectrum. As further changes towards lower pH values occur, the variations of τ and η_τ diminish, and it is only towards higher concentrations of H_2SO_4 that τ again increases, although the yield does not exhibit variations exceeding experimental errors (in strongly acid solutions, the error in measuring η_τ increases owing to the considerable changes in the emission spectrum).

Let us consider what can happen to a positive or univalent negative ion after excitation. In a time of the order of 10^{-13} sec it gives off one or several protons. By giving off a single proton, the cation passes into a nonfluorescent lacton form. This process does not affect the mean decay time of the fluorescence, but solely the yield. If two or three protons are given off, a fluorescent negative ion arises. However, owing to reversibility of the protolytic reactions, there exists a certain probability (per unit time) of capture of a proton by the negative ion, which can lead to a non-fluorescent neutral molecule. Thus, inverse reactions tend to shorten the lifetime of the molecule in the excited state. However, at high values of the hydrogen ion concentration, a short-wave band appears in the emission spectrum, indicating to emission by fluorescein in the form of positive ions. The reactions, however, have not yet ceased completely, as the maxima corresponding to emission by negative ions have as yet not disappeared at the long-wave side. The lack of an appreciable increase in the yield also points to continued formation of the lacton form. It is noteworthy that the shortening of τ amounts to about one third of its value for bivalent negative ions, whereas the yield falls to one third. This is explained by the greater probability for the formation of neutral molecules than for that of negative ions, as the latter involve giving off more than one proton by the cations.

The measurements also covered the dependence of the emission anisotropy of fluorescence r_p on the pH of the medium at excitation in the cation absorption band (through a HgM-D filter) and in that of bivalent negative ions (through an interference filter of $\lambda_{max}=473$ mμ). The experimental results are shown in Fig. 8 and Table III. For basic solutions, r_p is seen not to depend on the wavelength of the exciting light, to within experimental

TABLE III

NH_3			HNO_3			H_2SO_4		
pH	r_p(%)		pH	r_p(%)		pH	r_p(%)	
	$\lambda_{excit}=410$ mμ	$\lambda_{excit}=473$ mμ		$\lambda_{excit}=410$ mμ	$\lambda_{excit}=473$ mμ		$\lambda_{excit}=410$ mμ	$\lambda_{excit}=473$ mμ
11.88	—	1.04	6.72	1.11	1.10	6.27	—	1.11
10.73	1.03	1.01	6.58	1.08	1.12	3.16	1.14	1.39
10.00	—	1.02	4.36	1.27	1.34	2.21	1.19	—
9.23	1.03	1.02	4.25	1.27	1.38	1.75	1.23	—
7.43	1.03	1.09	3.33	1.29	1.45	1.30	1.27	—
			1.30	1.24	—	—		
			1.00	1.15	—	—		

error, in accordance with the polarization spectrum for fluorescein at dye concentration $c=10^{-5}$ g/cm³ (Feofilov 1959). On the other hand, at pH<7, an increase in the hydrogen ion concentration produces an increase in the value of r_p. This is due essentially to the shortening of τ. Protolytic reactions involve a change in sign of the charge carried by the fluorescein ions, thus affecting the hydratation envelope. Thus, the molecule obtains a transient enhanced freedom of motion; this, in turn, tends to reduce r_p. This effect manifests itself by the distinct dependence of r_p on the exciting wavelength for acid solutions, and is dependent on the properties of the acid utilized. According to Hanle and Scharmann (1952), the process

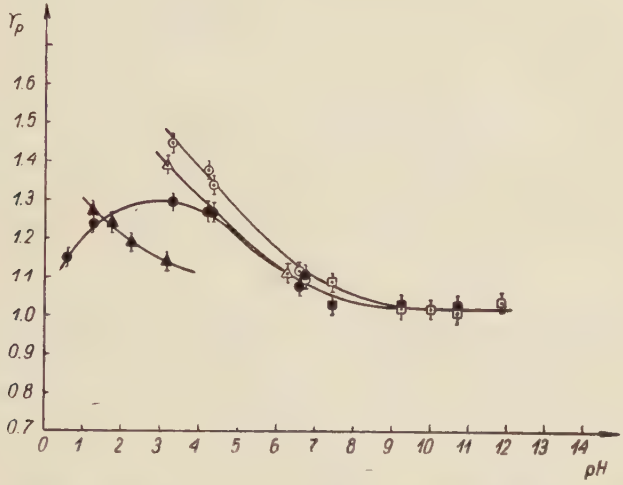

Fig. 8. Anisotropy of emission *versus* pH of solution: ⊡ — in solution with NH_3 excited with $\lambda=473$ mμ, ■ — in solutions with NH_3 excited with $\lambda=410$ mμ, ○ — in solutions with HNO_3 excited with $\lambda=473$ mμ, ● — in solutions with HNO_3 excited with $\lambda=410$ mμ, △ — in solutions with H_2SO_4 excited with $\lambda=473$ mμ, ▲ — in solutions with H_2SO_4 excited with $\lambda=410$ mμ

of giving off a proton does not affect the orientation of the molecule. The decrease in the degree of polarization by 3% of the measured value, as found by these authors, was attributed to experimental error.

In solutions containing nitric acid, r_p is maximum at pH≈3, which is not the case with sulfuric acid. This is no doubt due to the effect of the NO_3^- ions, which tend to enhance the mobility of the water molecules (Samoylov 1957, Andrussov 1958) and, at higher concentrations, disrupt the hydratation envelope of the fluorescein ions. Yet in sulfuric acid the strongly hydratated SO_4^{--} ions gradually diminish the mobility of the dye molecules. It is noteworthy that, at pH≈3 when the greatest difference in r_p occurs as between sulfuric and nitric acid, differences in the mean decay times are also observed to occur (Fig. 5). Fig. 4 shows that the effect of the temperature on the absorption spectrum is greater in nitric than in sulfuric acid, too. Also, the area of the absorption curve for cations is smaller in nitric acid, at equal values of pH. This points to a lesser relative concentration of the fluorescein cations in HNO_3 and, thus, toa greater number of the univalent negative ions, which are excited through the two filters used in the measurements of r_p and contribute to the rise in r_p

in solutions of pH<7. This explains the fact that higher values of r_p are obtained in solutions with nitric acid than in those with sulfuric acid at pH ranging from 7 to 2.

The exceedingly low value of r_p of the aqueous solution is primarily due to Brownian rotations and torsioned vibrations of luminescent molecules. whose effect greatly exceeds that of the remaining depolarizing factors.

Results

1. Simultaneous existence of different ions and the lacton form of fluorescein in solution throughout a wide interval of pH values is confirmed.

2. Protolytic reactions were found involving the loss of more than one proton by the excited molecule.

3. The assumption of protolytic reactions made possible the explanation of the experimental effect of pH on the emission spectrum, mean decay time, and fluorescence yield.

4. The effect of NO_3^- ions on the mobility of water molecules found in direct measurements of the viscosity manifests itself also in the results obtained in measuring the emission anisotropy.

5. The change in the charge of the dye ion in the excited state leads to smaller values of r_p.

The author wishes to express his great indebtedness to Professor A. Jabłoński for drawing his attention to the present subject and for his guidance throughout the investigation. The author is also indebted to Dr W. Woźnicki and Dr S. Poczopko for their valuable discussions.

REFERENCES

Batscha, B., *Chem. Ber.*, **59,** 311 (1926).
Lewshin, W. L., *Fotoluminestsentsija zhidkikh i tviordykh vyeshchestv.* Gos. Izd. Tekh.-Teoret. Lit. Moskva (1951).
Pringsheim, P., *Fluorescence and Phosphorescence.* Interscience Publishers Inc. New York (1949).
Förster, Th., *Lumineszenz Organischer Verbindungen.* Göttingen (1951).
Howe, E., *Phys. Rev.*, **8,** 684 (1916).
Zanker, V. and Peter W., *Chem. Ber.*, **1,** 572 (1958).
Grigorian, E. V., Kantardjian, L. T., Chirkinian, S. S., *Izv. Akad. Nauk SSSR, Ser. fiz.*, **24,** 771 (1960).
Bauer, R. and Rozwadowski, M., *Bull. Acad. Polon. Sci. Cl. III.*, **7,** 365 (1959).
Jabłoński, A., *Bull. Acad. Polon. Sci. Cl. III.*, **8,** 259 (1960).
Bauer, R. and Rozwadowski, M., *Optik*, **18,** 37 (1961).
Frąckowiak, D. and Marszałek, T., *Bull. Acad. Polon. Sci. Cl. III.*, **8,** 713 (1960).
Frąckowiak, D. and Marszałek, T., *Bull. Acad. Polon. Sci. Cl. III.*, **9,** 53 (1961).
Weber, K., *Z. phys. Chem.* (*B*) [Leipzig], **15,** 18 (1931).
Förster, Th., *Z. Elektrochem.*, **54,** 42 (1950).
Förster, Th., *Z. Elektrochem.*, **54,** 531 (1950a).
Weller, A., *Z. Elektrochem.*, **56,** 662 (1952).
Weller, A., *Z. Elektrochem.*, **58,** 849 (1954).
Weller, A., *Z. phys. Chem. N. F.*, **3,** 238 (1955).
Weller, A., *Z. Elektrochem.*, **60,** 1144 (1956).
Weller, A., *Z. Elektrochem.*, **61,** 956 (1957).
Kokubun, H., *Z. Elektrochem.*, **62,** 599 (1958).
Derkacheva, L. D., *Optika i Spektrosk.*, **9,** 209 (1960).

Ackermann, Th., *Z. phys. Chem. N. F.*, **27,** 253 (1961).
Samoylov, O. J., *Struktura vodnykh rastvorov elektrolitov i gidratatsija ionov*, Izd. Ak. Nauk SSSR, Moskva (1957).
Hanle, W. and Scharmann, A., *Z. Naturforsch.*, **7a,** 635 (1952).
Feofilov, P. P., *Polarizovannaya luminestsentsiya atomov, molekul i kristallov*, Gos. Izd. Fiz.-Mat. Lit., Moskva (1958).
Andrussow, L., *Z. Elektrochem.*, **62,** 608 (1958).

LETTERS TO THE EDITOR

SOME REMARKS ON THE THEORY OF PHOTODISINTEGRATION OF Be^9 AND Li^7

By A. Kowalska

Institute of Theoretical Physics, Jagellonian University, Cracow

(Received September 6, 1961)

Some corrections in the theory of the reactions $Be^9(\gamma, n)Be^8$ and $Li^7(\gamma, H^3)He^4$ are introduced.

In the paper of E. Guth and J. Mullin [1] on photodisintegration of Be^9 the following formula is used in order to describe the cross section for the $P \to D$ transition:

$$\sigma_{PD} = (128/729)(\pi^2 e^2/\hbar c)\hbar\omega |R_{PD}|^2$$

where

$$R_{PD} = \frac{B_1[(2/\pi)(\mu k/\hbar^2)]^{1/2}}{\{k^2 r_0^2(3QP + k^2 r_0^2)^2 + (3QP + k^2 r_0^2 \xi r_0 \cot \xi r_0)^2\}^{1/2}} \times$$

$$\times \left\{ k^2 r_0^2 \left[\frac{2k^2(1+\alpha r_0) - \alpha^2 r_0^2(\alpha^2+k^2)}{(\alpha^2+k^2)^2} - \frac{2\xi^2(1+\alpha r_0) - \alpha^2 r_0^2(\xi^2-\beta^2)}{(\xi^2-\beta^2)^2} \right] + \right.$$

$$+ k^2 r_0^2 Q \left[\frac{(\alpha^2+k^2)(1+\alpha r_0 + 3(\alpha^2/k^2)) + 2\alpha^2}{(\alpha^2+k^2)^2} - \frac{(\xi^2-\beta^2)(1+\alpha r_0 + (\alpha^2/\xi^2)) + 2\alpha^2}{(\xi^2-\beta^2)^2} \right] +$$

$$\left. + 3QP \left[\frac{2k^2(1+\alpha r_0) - \alpha^2 r_0^2(\alpha^2+k^2)}{(\alpha^2+k^2)^2} \right] \right\},$$

where $Q = 1 - \xi r_0 \cot \xi r_0$ and $P = 1 - \xi^2/k^2$.

This expression becomes infinite for $\xi \to \beta$. In order to obtain a correct formula changes must be made in two points. First P must be equal to $1 - (k^2/\xi^2)$ instead of $1 - (\xi^2/k^2)$ second, one of the ingredients, namely

$$- k^2 r_0^2 Q \left[\frac{(\xi^2-\beta^2)(1+\alpha r_0 + (\alpha^2/\xi^2)) + 2\alpha^2}{(\xi^2-\beta^2)^2} \right]$$

must be changed into

$$-k^2 r_0^2 Q\left[\frac{(\xi^2-\beta^2)(1-\alpha r_0+(3\alpha^2/\xi^2))+2\alpha^2}{(\xi^2-\beta^2)^2}\right].$$

In the new R_{PD} the part containing $(\xi^2-\beta^2)$ in the denominator (which forms an expression of the type $\frac{0}{0}$ for $\xi=\beta$) stays finite for $\xi\to\beta$ and equals:

$$\frac{3(1+\alpha r_0)^2(\beta^2/\alpha^2)+15(1+\alpha r_0)+5\alpha^2 r_0^2}{4\beta^2}$$

The last formula may be obtained either by putting $\xi=\beta$ into the integral expression $R_{PD}=\int_0^\infty R_2^* R_{1,3/2}^* r^3 dr$, or by passing to the limit $\xi\to\beta$ in the corrected expression for R_{PD}.

These corrections change the graph on figure 3. in the cited paper [1]. The maximum of the curve is at a photon energy of about 7 MeV instead of about 5 MeV and the maximum value of σ_{PD} is *ca* 20×10^{-28} cm^2, instead of *ca* 15×10^{-28} cm^2

For the same reason the conclusions about the potential well depth in the paper of W. Czyż [2] on photodisintegration of Li^7 must be changed. The author suggests the existence of repulsive forces between the triton and α particle in the D state. The corrections given above show rather that the attracting forces are more suitable for fitting the theoretical curve to the experimental one.

REFERENCES

(1) Guth, E. and Mullin, C. J., *Phys. Rev.*, **76**, 234 (1949).
(2) Czyż, W., *Acta phys. Polon.*, **15**, 129 (1956).

NOTE ON POSITRON RADIATION FROM Pr^{140}

By S. Chojnacki, J. Kopystyński

Institute of Experimental Physics, Warsaw University, Warsaw,

Z. Preibisz, R. Sosnowski, J. Żylicz

Institute for Nuclear Research, Polish Academy of Sciences, Warsaw,

I. Yutlandov

Joint Institute for Nuclear Research, Dubna, USSR

(Received June 1, 1961)

The positron spectrum of Pr^{140} was investigated with a magnetic long lens spectrometer It was established that the Kurie plot is a straight line from 350 keV up to the maximum energy of 2366±24 keV.

In a decay scheme of Pr^{140} proposed by Dzhelepov *et al.* (1959a) there are three positron transitions β_1, β_2, β_3 corresponding respectively to the ground state (0^+), to the first excited state (2^+) with energy 1597 keV, and to the second excited state (0^+) with energy 1902 keV of Ce^{140}. As it results from measurements of the intensities of the 1597 keV and 1902 keV transitions (Dzhelepov *et al.* 1959b) the components β_2 and β_3 are so weak that they cannot cause distortion in the Kurie plot of the β_1 transition. However, in the works as far published some non-linearity was observed which might suggest the existence of a positron component, but there is no place for such a transition in the decay scheme of Dzhelepov *et al.* (1959a). Moreover the discrepancies in the maximum energy determinations of different authors reach 10%. For these reasons it was decided to investigate the positron spectrum of Pr^{140} once again.

The measurements were carried out with a long lens spectrometer in which helical baffles were applied in order to separate the positron and electron radiation (Chojnacki *et al.* 1960). The investigated isotope was obtained from a neodymium fraction separated from a tantalum target by the chromatographic method. The target was irradiated with 660 MeV protons (synchrocyclotron of the Joint Institute for Nuclear Research at Dubna). This fraction contains Nd^{140} which decays into Pr^{140} by electron capture. The source was prepared by evaporating the drops of the neodymium fraction on a thin (1.36 mg/cm^2) aluminium foil moistened with insulin solution. The figure presents the Kurie plot for one of the measurements. The deviations from a straight line below 350 keV seem to be caused

by apparatus effects. The final results of this work together with the results of other authors as well as the results predicted by semiempirical equations of Cameron (1957) and Levy (1957) are collected in the following table.

Authors	Maximum energy of β_1 component E_{max} in keV	Method of measurement	Linearity of Kurie plot from E_{max} to (in keV)
1. Browne *et al.* (1952)	2230±20	magnetic spectrometer	1000
2. Gromov *et al.* (1958)	2470	magnetic spectrometer	750
3. Dzhelepov *et al.* (1959b)	2380±10	magnetic spectrometer	500
4. Brabec *et al.* (1960)	2318±10	magnetic spectrometer	?
5. Boley (1953)	2400	scintillation spectrometer	—
6. Gorodinsky *et al.* (1957)	2300	scintillation spectrometer	—
7. Cameron (1957)	2109	—	—
8. Levy (1957)	2810	—	—
9. Present work[1]	2366±24	magnetic spectrometer	350

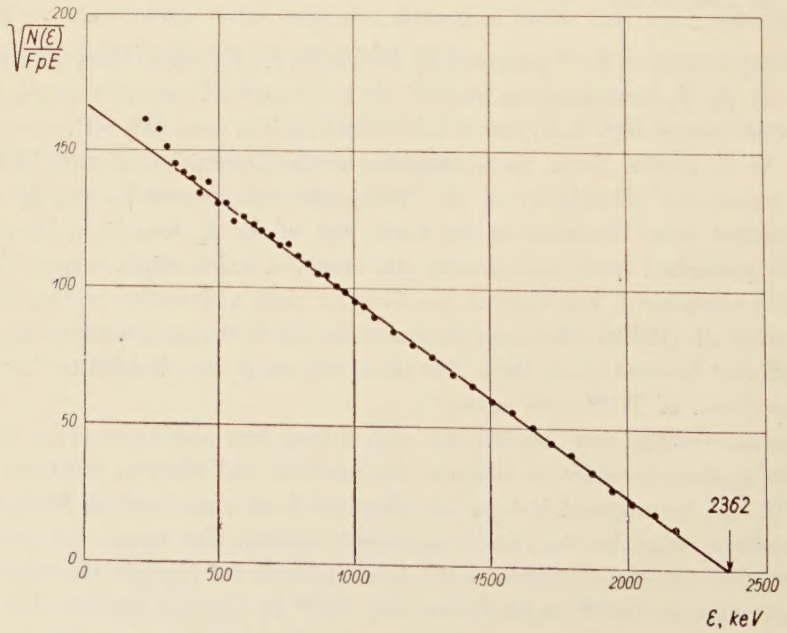

Kurie plot of positron radiation from Pr^{140}

[1] See also Chojnacki *et al.* (1960).

REFERENCES

Boley, F., *NSA*, **7,** No 24B (1953).

Brabec, V., Kracik, B., Vobecky, M., *Czech. J. Phys.*, **10,** 855 (1960).

Browne, C. J., Rasmussen, J. O., Surls, J. P. and Martin, D. F., *Phys. Rev.*, **85,** 146 (1952).

Cameron, A. G. W., *Canad. J. Phys.*, **35,** 1021 (1957).

Chojnacki, S., Kopystyński, J., Preibisz, Z., Sosnowski, R., Yutlandov, I., Żylicz, J., *Pol. Acad. of Sci., Inst. of Nuclear Research*, Report No 148/I-A Warsaw, April (1960).

Dzhelepov, B. S., Utchevatkin, J. F. and Shestopalova, S. A., *Zh. eksper. teor. Fiz.*, **37,** 857 (1959a).

Dzhelepov, B. S., Utchevatkin, J. F. and Shestopalova, S. A., *Papers presented at the second conference on neutron deficient isotopes of the rare earth elements*, Joint Inst. of Nuclear Research, Dubna (1959b)

Gorodinsky, G., Murin, A., Pokrovsky, V., Preobrazhensky, B., *Izv. Akad. Nauk SSSR Ser fiz.*, **21,** No 12 (1957).

Gromov, K. J., Dzhelepov, B. S., Dmitriev, A. G. and Preobrazhensky, B. K., *Izv. Akad. Nauk SSSR. Ser. fiz.*, **22,** 153 (1958).

Levy, H. B., *Phys. Rev.*, **106,** 1265 (1957).